FUNCTIONAL MRI AS A TOOL TO ASSESS VISION IN DOGS

A Thesis

Presented to

The Faculty of Graduate Studies

of

The University of Guelph

by

CRAIG K R WILLIS

In partial fulfillment of requirements

for the degree of

Master of Science

August, 1999

ABSTRACT

FUNCTIONAL MRI AS A TOOL TO ASSESS VISION IN DOGS

Craig K R Willis
University of Guelph 1999

Advisors:
R Quinn, D.V.M., D.V.Sc.
W McDonell, D.V.M., Ph.D.

This thesis is an investigation of brain responses to visual stimuli in anesthetized dogs. Current tests for canine vision are subjective and poorly standardized and this complicates evaluation of treatments for visual disease. Functional magnetic resonance imaging is a new technique in neuroimaging which has been enormously productive for human vision research and has potential for veterinary use as well.

As the first step in the development of fMRI as a technique for evaluating canine vision six anesthetized dogs were presented with a vertical grating visual stimulus and scanned under each of three anesthetic protocols: isoflurane, propofol and fentanyl / midazolam. This was done to determine if different anesthetic agents have different impacts on fMR signal. The size of activated areas, and the mean percentage signal change in response to visual stimuli were determined in the lateral geniculate nucleus (LGN) of the thalamus and the occipital cortex. No significant differences were observed between anesthetic protocols and no anesthetic dose dependence was observed. Images tended to be less variable under isoflurane anesthesia, possibly due to the relative difficulty of controlling intravenous anesthetic depth in a high magnetic field environment.

Functional MR images of the same six dogs were assessed as above to compare brain activity between monocular and binocular stimulation and between left and right LGN and occipital cortex during monocular stimulation. A larger area of LGN

was activated during monocular stimulation than binocular. There was no significant difference in percentage signal change or the size of activated areas between LGN and occipital cortex ipsilateral and contralateral to the stimulus, suggesting that previous estimates of axon decussation at the optic chiasm in dogs may be excessive.

ACKNOWLEDGEMENTS

I am grateful to my co-advisors, Dr. Rick Quinn who initiated this work and provided exceptional advice and support; and to Dr. Wayne McDonell, whose experience as an anesthetist, researcher and graduate student advisor was essential to the project.

I thank my advisory committee for their assistance. Dr. Joanne Parent and Dr. Gary Partlow provided first rate neuroanatomical, and thesis advice, while Dr. Tutis Vilis, Dr. Ravi Menon and Dr. David Nicolle helped with technical fMRI considerations. Drs. Nicolle and Vilis also provided helpful comments on drafts of the thesis. I am extremely grateful to Joe Gati, imaging coordinator at the Robart's Research Institute in London, Ontario, for running the MR scanner during all experiments and for explaining fMRI biophysics in small words. Dr Mohamed Shoukri and Dr. William Matthes-Sears provided excellent statistical support. Dr. N. R. Willis also provided very helpful comments on a draft of the thesis.

Veterinary technical support for this project was excellent, as well. Sarah Henderson's skill, experience and constant patience was an enormous benefit. Kathy Cavenaugh, Kim Thomaes and Christine Torres were a pleasure to work with and made sure the dogs were very safe in spite of my assistance.

Funding support for this research was generously provided by Pet Trust; OVC Department of Clinical Studies; London Health Sciences Centre, Department of Ophthalmology; and by an Ontario Graduate Scholarship in Science and Technology.

TABLE OF CONTENTS

DECLARATION OF WORK PERFORMED

I declare that I performed all of the work in the preparation of this thesis with the following exceptions. Rick Quinn, D.V.M., D.V.Sc. performed the ophthalmic examinations on each dog prior to scanning, and Joe Gati ran the 4T Whole Body MRI scanner during acquisition of all fMR data. Dr. William Matthes-Sears wrote the SAS programs used to analyse quantitative measures of fMR image quality. Finally, for all experiments catheterization was performed, and anesthesia induced by, one of Sarah Henderson R.V.T., Kim Thomaes, R.V.T., Christine Torres R.V.T., or Cathy Cavenaugh, R.V.T.

LIST OF TABLES

LIST OF FIGURES

CHAPTER ONE

LITERATURE REVIEW

1.1 INTRODUCTION

Human ophthalmologists employ the Snellen chart as an inexpensive and accurate tool to assess visual acuity and provide an objective measure of visual perception. Unfortunately, this tool is impractical for veterinary use because of our inability to communicate verbally with animals. When examining canine patients, for example, the veterinary ophthalmologist must rely on techniques such as poorly controlled behavioural tests (eg. using a rapid hand movement to elicit a flinching response). These can be subjective and vary widely in application and response.[1] Particularly vexing to both pet owners and clinicians is the uncertainty of tests for visual perception following costly surgery or drug treatment. How can we justify this expense if we cannot assess visual perception, accurately and objectively, as a follow up to treatment?

Functional Magnetic Resonance Imaging (fMRI), a recent development in neuroimaging, has yielded considerable gains in the study of human vision. The technique may provide veterinary ophthalmologists with a much needed objective test of animal vision. Due to the sensitivity of fMRI to movement, however, animals must be anesthetized during the procedure. As this is unnecessary for human patients, few direct data addressing anesthetic effects on fMRI are available. This chapter will first outline some of the theory behind fMRI followed by general aspects of mammalian vision and specifics of the canine visual system. Finally, fMRI's potential as a tool to assess canine vision and the considerations this requires, particularly regarding anesthesia, will be discussed.

1.2 FUNCTIONAL MAGNETIC RESONANCE IMAGING

1.2.1 Physics and Physiology of Magnetic Resonance Imaging

Nuclear Magnetic Resonance (NMR), of which magnetic resonance imaging (MRI) is an example, exploits the inherent magnetic fields of atomic nuclei which have "spin" or free rotation and have an odd number of protons and neutrons.[2] Spin is characteristic of many elements found in animals but hydrogen (^{1}H) atoms (i.e. protons),[3, 4] specifically those found in water molecules, are the basis for the MRI signal.[5]

Magnetization

Protons with spin have a bipolar magnetic field with a strength and direction described by a vector: the "magnetic moment".[4] Magnetic moments are usually randomly aligned in animal tissue. When an external magnetic field is applied, protons align with the field producing net magnetization,[2] expressed as the magnetization vector,[6] the strength of which correlates with the external magnetic field strength.[3] Alignment is not precise, however, and instead protons precess (rotate with a motion analogous to a wobbling top)[7] around the magnetization vector at a specific frequency. This means that individual vectors have both a longitudinal and a transverse component.[7] Precession frequency is constant, though, so the orthogonal transverse component is canceled leaving longitudinal net magnetization.[7]

To produce a signal, proton magnetic fields are made to resonate by exposure to a new magnetic field,[3] the oscillation frequency of which must match proton precession frequency.[7] For NMR this falls in the radiofrequency range so the field is called an RF pulse and when applied causes protons to resonate through some angle (usually 90° or 180°) determined by pulse amplitude and duration. Protons "relax", or realign themselves, with the external field when the pulse is terminated[4] and a receiver coil surrounding the sample detects the resulting change in current.[3] Images cannot be obtained from single RF pulses and instead sequences are required which include

saturation recovery, which relies on variations in the time between pulses (i.e. repetition time (TR)),[8] echo imaging sequences,[9] high speed sequences,[10] and other sequences.[7]

Relaxation, Image Weighting and Spatial Encoding

Longitudinal, or T_1, relaxation equals the time required for 63% of the magnetization vector to return to the longitudinal direction, usually between 200 to 2000 ms.[6,8] Transverse, or T_2, relaxation describes proton dephasing and has a greater impact on the MR signal than longitudinal relaxation.[8] Some protons experience greater magnetization from the external field than others because of energy exchange between protons. Those that experience less magnetization precess more slowly during relaxation causing exponentially growing phase dispersion. This, in turn, causes increasing signal loss, the rate of which is defined as T_2: the time required for 63% of this signal decay to occur. It is usually between 20 to 300 ms and is always shorter than T_1 for a given tissue type.[3,4,7] Pulse sequence adjustments can be used to enhance contrast between tissue properties and create, for example, T_1-weighted images, particularly suited to revealing anatomic detail, or T_2- weighted images, often used to show pathological details.[11]

Most important to functional imaging are the effects of flow on MR signals. Flowing blood can cause artifacts in MRI which depend, in part, on the speed, direction and turbulence of flow.[6] Flow related enhancement occurs when inflowing blood has not been exposed to an RF pulse and therefore exhibits greater signal intensity than surrounding tissue,[12] while outflowing blood and turbulence, on the other hand, can "wash-out" the MR signal.[6] Techniques exist to minimize flow artifacts, but flow can also be accentuated and was exploited by early functional imaging researchers.

Variation in the properties of different types of tissue is the basis o contrast in MRI, but equally important is the transcription of different sample regions into an image.

Spatial encoding requires that proton frequencies and phase properties vary with respect to position.[4] First, a plane of interest is chosen by application of a magnetic field gradient perpendicular to the chosen plane. This causes protons within the plane to precess at an identical frequency depending on distance along the gradient.[3,4] Following plane selection, another gradient causes similar precession frequency differences across the plane. Finally, 2-dimensional Fourier transform (2DFT) is used to resolve the second dimension of the image plane via a third orthogonal magnetic field gradient which induces phase, instead of frequency, differences.[8]

Only in the last ten years has the potential for functional mapping using MRI been appreciated. Functional MRI can be used to record high resolution, real time images of brain function using several approaches. All of these approaches involve either direct or indirect effects of flowing blood on the MR signal.

1.2.2 Functional Magnetic Resonance Imaging: Physics and Physiology

Properties of Blood and Blood Flow Relevant to fMRI

The circulatory system of the mammalian brain is more specialized than that of other tissues, especially with respect to flow regulation. Control of blood flow is vital to brain function because tissue damage from hypoxia can occur rapidly.[13] Large arterial vessel size and rapid vasoconstrictive responses to factors ranging from arterial pressure to chemical stimuli all serve to maintain pressure and flow.[14] Although blood flow in the brain is kept relatively constant, some variation does occur with changing metabolic needs.[14] This is the basis for currently popular fMRI techniques.

The fundamental principle of all fMRI methods is that increased neuronal activity leads to localized increases in metabolic activity,[15,16] blood volume,[17,18] and especially blood flow.[19,20] Despite considerable attention in the literature, the direct mechanisms underlying these changes remain speculative. Products of tissue metabolism like nitric

oxide, CO_2, adenosine, and $[H^+]$ (i.e. pH) have been proposed as potential regulatory cues,[20,21] while some evidence suggests that direct neuronal connections to vessel musculature are responsible.[22] This latter possibility is less likely, however, due to the potential for regulatory interference by neurotransmitters, which are particularly concentrated and diverse in brain tissue.[14]

Better characterized, and particularly relevant to current fMRI techniques, are blood's magnetic properties. Oxygenated hemoglobin (oxyhemoglobin) is diamagnetic, while deoxygenated hemoglobin (deoxyhemoglobin) is paramagnetic and possesses a permanent dipole.[23] The latter, therefore, aligns readily with an external magnetic field which, in brain tissue, causes localized field gradients between vasculature and surrounding tissue resulting in spin dephasing and signal loss in regions with high capillary density.[24] Deoxyhemoglobin is referred to as having greater magnetic susceptibility than its oxygenated counterpart, and this difference is an important factor in the most widely used fMRI approach.[14]

Until the potential of hemoglobin's magnetic properties for fMRI was realized, the effects of other paramagnetic chemicals on MR contrast were examined. Magnetic resonance signal changes accompanying the flow of gadolinium-DTPA (diethylenetriamine pentacetic acid) through cerebral vasculature can reveal areas of increased blood volume indicative of neural activity.[18, 25] Limitations of this method are numerous and include the minor toxic risk posed by gadolinium, especially after repeated injections,[26] and the time required between experiments to allow for contrast agent elimination.[5] Perfusion imaging, another early form of fMRI, identifies areas of elevated blood flow using signal from magnetically labeled, inflowing blood. Accentuating T_1 properties of blood already in the imaging volume reduces its signal strength so "new blood" appears bright. Therefore, comparisons of rest and task state images reveal

areas of increased blood flow.[27,28,29] Problems with flow based inversion recovery fMRI techniques include the relatively rapid decay of the magnetic label, and the fact that generally only single slices can be obtained in a session.[5]

Physics and Physiology of BOLD Contrast

Blood oxygenation level dependent (BOLD) contrast fMRI is by far the most widely used and successful fMRI method, and it has all but replaced contrast agent and perfusion imaging.[30,31] BOLD contrast is based on two characteristics of blood and cerebral blood flow: 1) increases in neural activity lead to localized increases in blood flow which exceed corresponding changes in blood volume and metabolic activity; and 2) deoxyhemoglobin is paramagnetic. Numerous authors have demonstrated changes in the MR relaxation properties of human and animal brain tissue as a result of blood volume,[32,33,34] and tissue perfusion changes.[27,28,31] It is blood flow changes, however, when combined with changes in blood oxygenation that give rise to the BOLD signal.[35,29]

Before outlining the specifics of BOLD, the concept of tissue relaxation in MRI needs to be re-addressed. Recall that T_2 describes the decay of phase coherence resulting from interactions between neighboring magnetic fields, and causes signal loss. Phase dispersion independent of T_2, however, can also occur at the onset of image acquisition, due to microscopic applied field heterogeneity, and contribute to further signal loss.[7] The time course of combined signal loss caused by both T_2 and this second phenomenon is described by the time constant T_2^*. By adjustment of TR and other factors, T_2^*-weighted images can be acquired.[7]

Figure 1.1 outlines the current understanding of BOLD. A specific task leads to a localized increase in neural activity (e.g. seeing causes neural activity in visual cortex) which leads to a localized increase in metabolic rate,[15,16] cerebral blood volume,[17,18] and cerebral blood flow,[20,21] though the increase in flow far outweighs both the metabolic and volume increases.[17] Fick's principle relates cerebral blood flow (CBF) with oxygen

extraction (OE) using the difference between arterial and venous blood oxygenation (O_a and O_v respectively):

$$OE = CBF(O_a - O_v) \quad (1)$$

The flow increase associated with neuronal activity outweighs the metabolic rate increase, so according to Fick's principle there is an increase in the oxygen content (and therefore oxyhemoglobin content) of the venous microvascular blood supply, the basis for BOLD signal.[33,36,37] As venous oxygen accumulates with no change in OE, the ratio of deoxy : oxyhemoglobin decreases.[29,38]

Unlike exogenous paramagnetic agents, which are injected into the extracellular plasma environment of blood, deoxyhemoglobin is localized intracellularly in erythrocytes. Deoxyhemoglobin's high magnetic susceptibility creates a gradient between erythrocytes and surrounding plasma and tissue.[14] This leads to considerable magnetic field heterogeneity and essentially amplifies T_2^* signal loss. Blood vessels in T_2^*-weighted images, therefore, appear as dark lines with radii considerably greater than those of the vessels themselves.[33] When neuronal activity leads to an increased oxyhemoglobin : deoxyhemoglobin ratio an increase in signal occurs because the susceptibility gradient and subsequent T_2^* spin dephasing are reduced. This signal increase is known as BOLD contrast.[33]

Applying BOLD fMRI

The experimental principle behind functional imaging is to compare brain activity during a task state and a control state, and then to superimpose the functional results onto a precisely corresponding anatomical image.[39,40] A "sequential task activation paradigm" is normally used for BOLD fMRI because fMRI is very sensitive to even slight movement,[14] and because signal changes from individual experiments are generally insufficient to provide the statistical power required for analysis.[29] The sequential task activation paradigm involves a repeating pattern of task and control states imaged in

rapid succession. The successive images are averaged so the task and control states can be compared on a voxel (discrete volume element) by voxel basis.

Parametric and non-parametric analyses have been employed for fMRI.[5] Traditionally Student's t-test has been used to compare control and task state signal intensities for each voxel in an image.[7,30] Changes in the variance of signal intensity can occur without changes in the mean, however, and more recently the non-parametric Kolmogorov-Smirnov statistic has been utilized because of its sensitivity to differences in variance as well as mean.[26] Once voxels with a significant signal change are identified, they can be superimposed on an anatomic image.

BOLD fMRI was originally described on hardware with field strengths far above those of most available imaging equipment. For example, Ogawa and Lee used 7 Tesla (T) while standard clinical machines often reach only 1.5 T.[33] This has inspired some work to determine the importance of field strength to detection of BOLD contrast. Higher field strengths result in greater magnetization, so the use of powerful hardware seems intuitively advantageous. A number of reports confirm that the BOLD effect at 1.5 - 2 T yields signal changes of 1 - 6 %,[34,38] while 4 T affords a 5 - 20 % signal change.[34,35] The design of pulse sequences best suited to fMRI has also received considerable attention as a means of fine tuning the BOLD approach and many possible sequences exist.[14]

One of the benefits of BOLD fMRI over other imaging techniques, such as positron emission tomography (PET), is its excellent spatial resolution. The spatial resolution of PET (7-10 mm)[19] is often insufficient to resolve boundaries between distinct brain regions, which can be as small as 1-2 mm.[41] Another advantage of fMRI over PET is the high signal to noise ratio (SNR), which allows for detection of activity differences within single subjects.[26] PET usually requires the averaging of responses from a group of subjects,[42] which in turn requires transformation to a standard coordinate system, like that devised by Talairach and Tournoux.[43] This is not necessarily required for fMRI.

Advances in the use of Talairach coordinates have permitted detailed inter - subject comparison of human cortex, however, and fMR image data are now also routinely projected into Talairach 3-D space.[44]

One limitation of the BOLD approach is that task and resting state images taken in rapid succession are often treated as independent samples. There is some evidence that a "hemodynamic memory" exists causing subsequent changes in signal to be influenced by activity underlying data already acquired. Sufficient time (several seconds) between image acquisitions may help alleviate this concern.[26] BOLD fMRI, like all MRI techniques, is also limited by artifacts related to movement which means only a limited number of sensory, cognitive and especially motor functions can be examined. Even movement associated with respiration and circulation can be problematic so investigating motor control of speech or complex body movements is clearly not feasible.[26] Concern also exists about the accuracy of the relationship between neural activity and blood flow, because of the possibility that the strong signals associated with large vessels may overshadow microvascular signals closer to areas of activation.[39,40,45] This means that brain vasculature anatomy must be considered during fMRI analysis and also that especially strong signals (i.e. >5% at 4T) must be filtered out during data processing.[40] Despite these limitations, fMRI has enormous potential as a result of the BOLD method, and considerable advances in our understanding of the human brain have already been achieved.

Experimental, Auditory and Motor Advances

One characteristic feature of fMRI has been the rapidity with which advances in its underlying technology and methodology occur. In fact, progress in the understanding of brain function is often accompanied by modifications in fMRI methods,[45,46] which has led to consistent improvement in data quality, sometimes at the cost of studies addressing concerns such as statistical analysis and experimental design.[47]

Several authors have addressed concerns with fMRI experimental design. As mentioned above, the sequential or blocked task paradigm treats repeated stimuli as independent samples even though, occasionally, this may be inappropriate. Buckner et al. report a method of data acquisition which allows images to be obtained from single tasks without the use of a blocked task paradigm.[48] This is not a replacement for the existing method, which is productive if sufficient time between stimuli is allowed, but instead complements it by offering more flexibility in experimental design and by permitting exploitation of fMRI's high temporal resolution.[48] This method is now used quite often, especially at high magnetic fields where signal averaging may not be required.[40] Another experimental advance in fMRI was achieved by Boynton et al. who demonstrated that a quantitative, non-linear relationship between stimulus properties (duration and contrast) and fMRI signal intensity exists in primary visual cortex (V1).[49] This is an important early step in understanding the link between neural activity and the fMRI signal.

The majority of fMRI studies to date have focused on the visual system but auditory and motor cortices have also received attention. Early auditory work demonstrated that significant, stimulus-dependant BOLD activity could be obtained despite constant background scanning noise, and that results were consistent with previous lesion, EEG, and PET studies.[50] Following these preliminary steps, investigating the effects of word presentation rate on activation in various cortical regions has been an important focus. Both Binder et al. and Dhankar et al. report significant word presentation rate-dependant signal increase in primary and secondary auditory cortex. As for V1, the signal increase / stimulus intensity relationship is non-linear.[51,52]

Although the study of motor activity using fMRI is limited, progress has been made particularly using small finger movements as a task of interest.[45,46,53,54] Kim et al. observed a large activation of primary motor cortex (M1) contralateral to the movement

hand, as well as a smaller ipsilateral signal.[46] This led to their proposal that size of activated areas may be as important as signal strength when interpreting fMRI results.

Continuing improvement in experimental design and analysis of fMRI, and in our understanding of the relationship between neural activity and BOLD contrast should lend further credibility to the technique. As methods are refined on human patients and equipment costs continue to decrease, the fine spatial resolution and single subject capability of fMRI suggest considerable potential for use in veterinary research.

1.3 CANINE VISION

1.3.1 Mammalian Visual System

Anatomy of the Early Visual Pathway

The anatomy of the early visual system is similar throughout the Mammalia (Figure 1.2), with differences becoming more pronounced as one advances through successive regions of visual cortex.[55] The visual receptor cells (rods and cones) are spread over the retinal surface and contain photopigments which facilitate transduction of light energy into voltage across a cell membrane. In contrast to the majority of receptor cells, exposure of rods and cones to relevant stimuli results in a hyperpolarizing membrane current (i.e. depolarization and neurotransmitter release occur in the dark and stop when light is absorbed).[56]

Rods and cones synapse with retinal bipolar cells which, in turn, synapse primarily with ganglion cells, axons of which comprise the optic nerve. Processing of visual information is already occurring at this level, in part due to amacrine and horizontal cells which synapse with all three retinal cell layers and influence lateral interactions between cells to enhance contrast and movement perception.[56] An important feature of visual processing, first evident at the retinal level, is retinotopic organization, or the conservation of spatial relationships between the visual field and the

receptive fields of retinal and cortical neurons. Neighboring cells have receptive fields which represent neighboring regions of the visual field.[56] Spatial relationships become increasingly important as the optic nerves of the left and right eyes meet at the optic chiasm. Here the visual field is divided in two, as cells responsive to the left halves of both retinas project to the left side of the brain, and vice versa. When combined with the eye's optical characteristics this arrangement means that objects appearing to our left are processed in our right brain and objects to our right in the left brain[55]. In humans we know that roughly 50% of optic nerve fibres decussate at the optic chiasm and widely accepted estimates suggest that about 75% decussate in dogs.[57]

Downstream of the optic chiasm, the majority of visual signals travel the optic tract to the lateral geniculate nucleus (LGN) in the thalamus, though some ganglion cells innervate the superior colliculus directly to help coordinate head and eye movement.[55] The LGN has a layered structure which helps segregate information based on the side of origin. Each layer receives input from the contralateral visual field, but exclusively from either the ipsilateral or contralateral retina.[58] Neurons from LGN synapse with those of the visual cortex, many areas of which have been identified by histological and cytoarchitectural characteristics.[59] It is at this level where the similarity across mammalian orders begins to decrease. Non-human primate and cat visual cortices are the best studied due to single cell recording and other relatively invasive techniques.[60,61,62] The development of fMRI, however, has allowed for direct non-invasive investigation of human visual cortex.

Striate and Extrastriate Cortex

The first stage of visual processing in cerebral cortex, and by far the best studied visual area, is primary visual cortex (V1), or striate cortex, named "striate" for the series of myelinated stripes in its layer IV. This area is located at the occipital poles of both hemispheres.[59] Its columnar, or modular arrangement is an important model in

neuroscience, first described by Hubel and Weisel based on their work using cats and old world monkeys.[60,63,64] Ocular dominance is one aspect of this region. Cells are arranged in alternating columns such that left eye and right eye sensitive cells are grouped separately,[60] a phenomenon recently confirmed using fMRI.[39] Cells in V1 are also arranged based on the shapes to which they are responsive so that cells with receptive fields of similar shape and orientation are grouped more closely than those with diverse receptive fields.[60,65,66]

Neurons from V1 synapse with higher visual cortical areas, (e.g. V2, V3, etc.), which are referred to collectively as extrastriate cortex. Extrastriate cortex occupies much of the occipital cortex, and parts of the temporal cortex. These visual areas are retinotopically organized and include V2, V3, VP (ventral posterior area), V3a, and V4v (ventral), where the spatial relationships of the visual field are well maintained in cortical anatomy. Other areas, specific to each of two parallel processing streams, can be identified wherein spatial relationships of cells depend more on stimulus characteristics (e.g. colour, form, movement) than visual field position.[62] Functional MRI has been important in confirming boundaries of striate and extrastriate areas in humans (Figure 1.3).[67,68,69]

Retinotopy of the Human Visual Pathway Revealed by fMRI

Prior to fMRI development, many of our assumptions of the human visual pathway arose from invasive procedures in macaques (*Macaca* spp.),[62] in whom over 30 functional cortical units have been identified.[70,71] Humans and macaques were traditionally assumed to share many homologous cortical areas, especially in the early visual pathway, because of our evolutionary proximity.[62] Due to the limited spatial resolution of the existing imaging methods, like PET (7-10 mm),[41] this homology has only recently been tested experimentally. Indeed, one focus of visual fMRI to date has been to confirm or refute existing assumptions of cortical retinotopy in humans.[42]

Mapping of the human visual cortex using fMRI has revealed that humans and monkeys share a very similar retinotopic organization of V1, V2, and V3a,[41,66,72] and that a similar reduction of retinotopy in the medial temporal area (MT) also exists.[73] Also confirmed is the general property that retinotopic organization is strict early in the pathway, but that neurons become increasingly "stimulus specific", and much less "position specific", in later areas.[71] For example, V1 neurons fire in response to simple stimuli like lines and edges depending on their position and orientation in the visual field. Neurons in the inferior temporal cortex (IT), which receive extrastriate input, fire in response to specific objects, like faces, irrespective of position.[70,74] Controversy does remain, however, as to differences between even early visual areas in macaques and humans.[62,72,75] This justifies the use of fMRI to confirm the borders of brain regions instead of relying on evidence from evolutionary relatives.

Motion Processing in the Human Visual Pathway Revealed by fMRI

Defining retinotopic borders is crucial to studies of function within distinct regions of extrastriate cortex, another focus of fMRI vision research. Functional specialization is evident in the two processing streams identified in the macaque visual cortex, both of which originate in V1 but diverge in later areas.[71] In macaques, the parietal or dorsal stream processes components of stimuli related to movement, while the temporal or ventral stream processes shape, form, and colour information.[76,77,78]

Processing of object motion via the proposed human dorsal stream is thought to project through V1, V2, and V3 to the middle temporal area (MT), or V5,[79] now a relatively well established homologue of MT in macaque brain based in part on fMRI evidence. Tootell et al. were among the first to record a fMRI signal from human MT while patients observed moving stimuli followed by stationary controls.[73] They also demonstrated that MT is more sensitive to contrast than is V1. This, combined with their retinotopic evidence mentioned above, supports the notion of species similarities in

motion processing and the existence of a human dorsal stream. Other evidence suggests that motion attributes of stimuli are further processed in the medial superior temporal area (MST),[62] and an MT-MST complex has been the focus of studies on the effects of attention on the visual system.[80,81]

Particularly exciting fMRI contributions to our understanding of dorsal stream function have involved recognition of the importance of MT to reading and language skills. Eden et al. revealed that MT in dyslexic men showed virtually no activation in response to moving stimuli which elicited MT activation in control subjects, even though stationary stimuli resulted in identical activation in V1 and V2 of both groups.[82] With behavioural testing, they also detected reduced motion sensitivity in dyslexic men which was so subtle that it had previously gone unnoticed even by the dyslexic patients themselves.[82] Howard et al. provided further evidence for a link between motion processing and language when they observed firing in response to motion in MT as well as in an area of the superior temporal gyrus known to be activated by listening to words.[79]

Object Processing in the Human Visual Pathway Revealed by fMRI

The ventral stream for object processing projects through V1, V2, and V4 to the inferior temporal cortex (IT) in monkeys and it is thought to follow a similar arrangement in humans.[76] Investigations of areas specifically responsive to facial images have been one fMRI focus. Evidence suggests that a face specific area does exist within the proposed ventral stream.[83,84] Courtney et al. performed particularly elegant fMRI experiments on both visual perception and working memory to demonstrate activation of occipitotemporal cortical areas in response to face presentation, as well as prefrontal cortical activation in response to a memory activity.[84] The face selective region of occipitotemporal cortex is not exclusively activated by facial images, however, and it overlaps functionally with areas sensitive to letter sequences and words.[83] This may

have implications for our understanding of the trade-off between determinism and plasticity in cortical development. Evolution is unlikely to have resulted in areas specifically tuned to groups of letters because written language is relatively new, on an evolutionary time scale. Such cortical units are likely the result of modeling and remodeling in the brain as we learn and continue to read.[71] Functional MRI experiments addressing changes in the functional brain anatomy of subjects over the course of a learning experience could help resolve this issue.[71]

Some neural areas, like those sensitive to letterstrings and faces, are dedicated exclusively to specific stimuli. We encounter so many different objects visually, however, that, due to space limitations alone, it would be impossible for a different cortical unit to be set aside for each possible stimulus.[71] Functional MRI has helped identify a region of lateral occipitotemporal cortex (LO) which responds to all objects, and produces a larger fMRI signal during object presentation than during the presentation of textured space or object fragments.[85] Positron emission tomography evidence suggests that LO is involved in processing form to determine whether or not a pattern in the visual field represents an object, not in recognizing and differentiating specific objects.[86]

Colour processing is a ventral stream function, as well, and a colour selective area in human occipitotemporal cortex has been identified by PET,[87] lesion,[88] and fMRI studies.[89] Although this area has been compared to the colour selective monkey area V4, there remains some controversy as to their homology based on conflicting evidence from a different human V4 identified retinotopically.[71] A recent fMRI study supported previous results suggesting that colour processing may begin very early in the ventral stream, in areas V1 and V2,[90] and it seems likely that colour is processed in a range of occipital and cortical areas.

Cortical Design: "Top Down" Processing

Since our visual system absorbs far more information that we can actively use at any given time, some filter must allow us to focus on stimuli of immediate importance.[81] Attention is the main mechanism by which this is achieved and can occur via "bottom up" influences based on stimulus attributes (e.g. a fast moving object in the peripheral field), or by "top down" influences, where voluntary choice determines attention (e.g. concentrating on a computer screen).[81] "Bottom up" processing involves retinotopy as well as ventral and dorsal processing but "top down" processing involves the influence of our own cerebrum on visual experience.

The parietal and prefrontal cortices, downstream of the visual cortex, have been associated with visual attention and "top-down" influences using traditional techniques[80,91,92] and fMRI.[93,94] Courtney et al. used fMRI to examine prefrontal cortices during prolonged working memory tasks where subjects visualized faces they had previously been shown.[84] While occipitotemporal areas selective for activation by faces showed only transient activity during the memory task, regions of prefrontal cortex showed consistent, prolonged activation, suggesting their importance in maintaining perception of an image. Positron emission tomography evidence suggests that attention and prefrontal cortex can also influence the earliest visual areas. Kosslyn et al., for example, observed activity in V1 when subjects visualized objects, demonstrating that stored information can activate the early pathway via descending inputs.[94] Le Bihan et al. obtained similar results in an early functional imaging study.[95] "Top down" influences have also been observed for motion processing, particularly in the MT-MST complex. O'Craven et al. found significantly greater MT-MST activation when subjects focused on the moving component of a stimulus (i.e. a moving dot on a computer screen), than when they focused on the stationary component (a non-moving dot on the same screen).[81]

The results cited above confirm that not only do stimulus components and ascending neuronal inputs influence the visual cortex, but also that higher visual and cognitive centres exert considerable influence through descending connections. This raises challenging questions about visual perception, and how to identify cortical areas of visual awareness in a noncommunicative animal like a dog. Where does perception of a visual stimulus actually occur? Clearly, areas throughout the neocortex are involved in various aspects of visual processing, so in the future a fMRI test of visual perception may need to address, not just V1 or occipital cortex, but a range of cortical areas.

1.3.2 Specifics of the Canine Visual System

The Early Visual Pathway

Compared with cats and primates, we know relatively little about the canine visual cortex but there are differences early in the pathway which are well described. A dog's ability to see in much lower light than humans is one of these, facilitated by aspects of canine ocular anatomy.[96] In contrast to the fovea of humans, the central region of a dog's retina consists mainly of low-light sensitive rods,[97] and the reflective tapetum lucidum is well developed allowing the eye to re-use light already detected by the retina.[96] Canine vision is flexible, however, as dogs also see well in bright light. As in humans, pupillary dilation and constriction, recruitment of rods or cones where necessary, and changes in rod sensitivity contribute to this flexibility.[96]

A second specialization of the canine visual system is the distinct lack of a fovea in favor of an oval shaped visual streak, the central area of the retina in dogs.[98] As in the primate fovea, ganglion cell density is higher in the visual streak, which corresponds with enhanced visual acuity. Wolves have a more pronounced and elongate visual streak than do domestic dogs, which some propose is an adaptation for improved vision when scanning the horizon. This variation is also apparent between dog breeds (e.g. German Shepherds have a wolf-like streak and beagles a more oval streak,[98] which suggests

that other aspects of vision could vary between breeds, as well. To address this issue, inter-breed fMRI studies of vision will be worthwhile.

Colour sensitivity is a third difference between the early visual pathways of dogs and primates. Contrary to widely held opinion, dogs are not colour blind, and instead posses dichromatic colour vision,[99] which differs from primate trichromatic colour vision in that it affords dogs a level of sensitivity similar to that of a deuteranopic (red-green colour blind) human.[96,99] The two types of cones in the canine retina occur in much lower numbers than the three types found in primates, allowing for the trade-off of improved low light vision, but still permitting considerable colour sensitivity.[96] Behavioural testing suggests that postretinal processing of colour occurs in dogs, based on the ease with which they can be trained to distinguish between colours, compared with other animals.[99]

Cortical Areas of Vision in Dogs

Although cats have provided an important neuroscientific model of cerebral cortex for many years,[63] canine cerebral cortex has been largely ignored. Ofri et al. used electrode recordings to provide precise coordinates for the central area of vision in canine cortex and confirmed that, as in other mammals, V1 is found in the occipital lobes.[100] More precise localization of V1 in dogs has not been presented. In dogs, research on areas beyond V1 remains conspicuously absent from the literature.

Early work describing mammalian striate cortex is based largely on cats[63,64,101] and many striate cortex properties are similar in primates[60,64,100] and other mammals.[59] Some aspects of V1 do vary between mammals, such as the amount of cortex devoted to central vision[59] and the retinotopic differences between monkeys and humans, mentioned above. Motion processing, especially important for predators like dogs and cats, whom we know are highly sensitive to movement,[96] also illustrates species differences. Several areas of cat visual cortex have been proposed and rejected as

homologues to primate MT,[102,103] which suggests that motion may be processed somewhat differently in cats and primates. This lends support to the possibility that differences also exist between dogs and primates because canine precortical visual anatomy is more similar to that of cats than of primates.[96] Feline cortical anatomy may be a preferable reference for generating hypotheses regarding locations and connectivity of processing areas in dogs since there is little direct information on canine visual cortices in the literature, and because of the differences between motion processing in cats and primates.

1.3.3 Current Tests for Canine Vision

Evaluating canine vision remains an inexact science because methods of testing vary considerably.[96] Behavioural testing,[1] optokinetic devices,[104] electroretinography (ERG),[105,106] and visually evoked potentials (VEP)[105,107] have all been employed.

The use of innate behaviours in animals is an inexpensive and rapid method of sensory assessment.[1] The menace response test is based on a blinking response to a threatening hand gesture toward the dog's face. Optokinetic devices provide a more controlled visual test and exploit a dog's optokinetic reflex, which involves the animal following movement with the eyes and head. By gradually decreasing the size of presented objects a threshold of visual acuity can be determined.[104] Electroretinograms have also been widely used in small animals to assess retinal function. The ERG relies on a "contact lens electrode" to record retinal cell activity during stimulus presentation.[105] Flash ERGs involve a stroboscopic flash as a stimulus and are thought to record activity elicited by luminance, in the photoreceptor layer of the retina.[108] Pattern ERGs, developed more recently, use alternating patterns as stimuli to record information about luminance and spatial contrast indirectly, representative of cones near the retinal centre.[108] Neither ERG type addresses postretinal processing.[105]

Obvious problems are intrinsic to behavioural methods and ERG recording. The former is limited in part by the fact that no environment is devoid of distracting stimuli so observed behaviours may be elicited by distraction,[1] or even by air currents caused by the clinician's hand movement. Optokinetic devices also require that patients remain focused on the stimulus which means responses may depend as much on attention span as visual acuity. These problems can be controlled to an extent, however, and do not represent the most striking limitations. A fundamental problem with both behavioural and ERG methods involves the difference between a reflex response and one indicative of perception. Pet owners often feel that visual perception is important to the quality of life of their pets.[104] If possible, then, it is visual perception for which a veterinary ophthalmologist should be testing. Unfortunately, by using a reflex response test, or recording activity in the retina, we ignore the areas of the visual pathway responsible for perception, and therefore the priority of pet owners: that their dogs experience the world visually.

In primates, visual responses to stimuli can occur in subjects that think they are completely blind, a condition known as blindsight.[109,110,111] In addition, cats with V1 completely removed, and therefore likely unaware of visual stimuli, can detect obstacles, distinguish between patterns, and detect movement.[112] This condition would easily go undetected in dogs by both behaviour testing and ERG recording, because retinal function is largely unchanged and the problem involves brain activity.[113] In fact, some ganglion cells in normal animals bypass the visual cortex completely and innervate the superior colliculus directly, to permit unconscious head and eye movements.[55] If we are to accurately assess canine vision then behavioural and retinal testing are insufficient.

The visual evoked potential (VEP) addresses this concern to some degree because it does record brain activity via extracranial needle[107,114] or scalp electrodes.[115] The VEP signal consists of positive and negative peaks in a waveform, with each peak

representing a different stage of early postretinal visual processing. Peak 1, for example, might originate in the LGN and peak 2 in V1.[114] When the VEP is combined with ERG recording, the relative influences of the optic properties of the eye and early postretinal processing on visual acuity can be estimated.[105] Problems with VEPs, however, include the sparse literature on canine cortical anatomy combined with the precision required in electrode placement.[100] VEPs target mainly thalamocortical areas (LGN, V1, and V2).[107] The location of V1 has only recently been identified in dogs. As a result, researchers have often used cat cortex as a reference for electrode placement resulting in considerable signal variation and poor VEP standardization.[100]

This raises the second limitation of the VEP. Visual evoked potentials are recorded from outside the skull, so they are more sensitive to signals from outer layers of cortex.[108] For example, signals from posterior occipital sections of V1 and V2 might be over-represented while signals from anterior occipital cortex within the longitudinal fissure, or from temporal cortex, would be weaker. In addition, we have some idea of the areas responsible for producing different peaks in VEP recording of dogs (waveform generators)[107] but this understanding is imprecise.[115] Although the origin of a VEP signal can be localized to the occipital lobe, activity on a smaller scale, or activity anterior to V1 is difficult to pinpoint. Current thinking suggests that perception certainly depends on V1 in humans but that prefrontal cortex is also vital to conscious awareness.[116,117,118] Although more reliable than behaviour or ERG testing, the VEP is still severely limited as an objective assessment technique for visual perception because it cannot address activity in temporal or prefrontal cortices.

1.4 DEVELOPING fMRI TO ASSESS CANINE VISION

1.4.1 Canine fMRI: Cortical Limitations

Functional MRI has enormous potential to alleviate the concerns associated with existing tests for canine vision. By varying slice thickness and regions of interest, it is feasible to obtain entire maps of canine brains during visual presentations. Comparing functional maps of visually "normal" dogs with those suffering visual disease could reveal a great deal about the impacts of optical properties on brain activity. Developing functional map databases of dogs would be a valuable contribution to canine fMRI, as well, because the technique remains expensive. Correlating easily measured attributes of the visual system, like optical features, VEPs, or even behavioural responses with fMRI signals, could eventually help reduce costs.

If any of this potential is to be realized several concerns need to be addressed. Intrinsic characteristics of tissue in the neocortex, like plasticity, need to be accounted for when designing experiments. For example, young cats blinded during the first years of life revealed remarkable compensation in the anterior ectosylvian visual area (AEV). This region is normally exclusively visual but became completely responsive to auditory stimuli.[119] Similar cortical plasticity has also been well documented in adult animals,[120] and this phenomenon must be acknowledged when fMR images of visually deficient animals are analyzed. Their cortical functional anatomy could be very different from visually normal animals and could cause confusion during image interpretation.

A related issue to be addressed involves stimulus selection. Current visual testing suffers from its restriction to sub- and early cortical visual areas. To realize fMRI's potential, a range of stimulus types must eventually be used during experiments. Different areas of primate and cat brain are known to fire preferentially in response to shapes of different configuration and orientation, or movement in different directions.[66] By varying attributes of presented stimuli, researchers will be able to asses a wide range

of visual characteristics in different functional and anatomical cortical subunits. This would represent considerable progress for both veterinary clinicians and neuroscientists.

1.4.2 Canine fMRI: Anesthetic Limitations

By far the most pressing concern to be addressed regarding veterinary fMRI involves anesthesia. Electrodiagnostic and neuroimaging procedures demand that patients remain still so primates, cats, dogs and uncooperative humans (e.g. children), must be anesthetized. General anesthesia produces central nervous system (CNS) depression,[121] and cerebral cortex is generally the neural tissue most readily depressed in mammals.[122] This raises an obvious concern: How do we know that fMRI in anesthetized animals is representative of conscious brain activity? The answer is likely that we cannot know for sure, but that the advantages of neuroimaging data still outweigh the limitations, as long as anesthetic effects are understood and considered.[122]

Jezzard et al. reported the first account of BOLD fMR activity induced by visual stimuli in a non-human animal, and anesthesia played a key role in their results.[123] Visual stimuli evoked signal changes in V1 and V2 of anesthetized cats which is encouraging as it demonstrates BOLD signal changes in unconscious animals. The signal changes were between 0.7 - 2%, somewhat lower than those normally observed at 4T in humans, a finding attributed to anesthetic effects. This signal reduction is not particularly surprising, though, considering the known effects of anesthesia on other aspects of CNS activity (see below). Jezzard et al. also reported problems maintaining eye position in anesthetized animals and suggested that the use of a paralytic agent in conjunction with anesthesia might remedy this problem.[123]

That BOLD signals should exist in anesthetized animals is predictable as numerous reports exist of anesthetized humans displaying anesthetic awareness and post-operative recall,[124] a condition difficult to test in canine patients. Human patients occasionally retain memories of events during anesthesia which, although usually

unconscious (i.e. implicit), are remarkably accurate. This suggests that information processing and perception can occur during anesthesia if we acknowledge that memory is a form of residual perception.[125] Anesthesia which permits some level of implicit awareness is clearly not ideal for painful surgery, but could improve the quality of fMRI signals from anesthetized animals.

Propofol, isoflurane, and fentanyl / midazolam are three relatively safe and common anesthetic protocols in human practice,[126] and are considered below as candidates for use with canine fMRI. Of the three, isoflurane's CNS effects are probably best studied in dogs.[127,128] Understanding the effects of these regimes on other measures of cortical activity, like the EEG, and cerebral circulation, is important to predicting their potential effects on the MR signal.

Propofol: Potential Effects on fMRI

Propofol is a non-opioid, intravenous anesthetic agent widely used in a variety of human clinical applications including ambulatory, pediatric, and neuroanesthesia.[126] It is popular primarily due to its rapid metabolic clearance from the body[129,130] and the corresponding rapid recovery of patients, even after prolonged anesthetic maintenance.[126,129] Considerable patient variability in response to propofol exists, however, so close monitoring is required.[126] This variability may also limit the reliability of fMRI results between propofol anesthetized subjects.

Studies of propofol effects on CNS factors, like EEG activity, evoked responses, and cognitive recovery provide somewhat controversial results,[131] and are relatively rare in dogs. Most agree that cognitive function recovers quickly following anesthesia[126,131] and some evidence suggests that using propofol as both an induction and maintenance agent may improve this recovery,[132] especially if maintenance duration is relatively long.[133] Low doses of propofol cause an increase in human EEG activity, but at doses required to maintain unconsciousness, activity decreases with increasing dosage and

eventually burst suppression occurs.[134,135] Burst suppression certainly correlates with reduced brain activity. Propofol also has been linked to decreased cerebral blood flow (CBF) in humans[136] and dogs,[137] which will likely result in BOLD signal reduction via reduced oxyhemoglobin flow to the brain. On the other hand, propofol reduces the cerebral metabolic rate for O_2 ($CMRO_2$) in humans[136] and dogs,[137] and this could exert a contradictory effect by increasing the oxy- to deoxyhemoglobin ratio. The contradictory effect will likely be small, however, because propofol suppresses CBF by considerably more (approx. 50%) than $CMRO_2$ (approx. 30%) in both species.[136,137]

Several studies have addressed the issue of awareness during propofol anesthesia. Sung et al. observed no postoperative recall, but report more rapid recovery of memory ability upon emergence than occurred with thiopentone.[138] This suggests that the CNS may remain more active throughout propofol anesthesia. Dreaming could also play a role in fMRI during anesthesia by causing activity in visual areas and producing BOLD signal artifacts. Noble et al. found that 25% - 30% of patients dreamed during propofol anesthesia,[139] and Duval et al. report several case studies of patients anesthetized with propofol who recounted dreams that were influenced by events during surgery.[140] These patients later responded to hypnotic suggestions administered during surgery, though they displayed little explicit recall of events. We know that dose-dependant cerebral suppression occurs during propofol anesthesia,[134,135] but the results cited above suggest that some level of sensory processing can occur during the anesthetic period.

Propofol is a good candidate for use with canine fMRI because recovery occurs quickly, it is rapidly cleared from the body, and it can allow for some sensory processing during anesthesia. Variability in patient responses to propofol, however, is cause for concern if repeatable fMRI results are to be obtained. Also, reduced CBF will likely cause noticeable reductions in BOLD signal and reports of dreaming suggest that BOLD

signals unrelated to presented stimuli may occur. Dreaming and reduced CBF, however, may be limitations associated with most anesthetic agents.

Isoflurane: Potential Effects on fMRI

Inhalant anesthetics are often preferred because they can be easily administered and excreted via the lungs. Their use also permits anesthetic depth to be measured objectively and altered readily, despite the fact that inhalational anesthesia is generally characterized by longer induction and recovery times than propofol anesthesia.[141] Among the inhalants, isoflurane is a favorite in human practice because it allows for good muscle relaxation and stable cardiac rate and rhythm.[141]

Central nervous system effects of isoflurane, particularly relevant to BOLD fMRI, include a dose dependant EEG decrease which can lead to complete burst suppression in dogs.[127] This reduction in EEG activity may not accurately reflect anesthetic depth, however, as EEG responses of anesthetized humans are unrelated to pain-induced responses.[121] Interestingly, Hartikainen et al. report strong visual evoked responses in the EEG of humans during complete burst suppression, indicating that visual processing can occur in the mammalian brain under deep anesthesia.[142] Auditory evoked responses also have been observed during deep isoflurane anesthesia.[143] In contrast to propofol, isoflurane causes an increase in CBF in dogs[128] and humans[126], which could increase BOLD signal strength, although the CBF increase gradually decays over time in dogs when isoflurane is administered with nitrous oxide.[144] In addition, in humans the decrease in $CMRO_2$ is greater with isoflurane than that observed during propofol anesthesia[126] and this may contribute further to signal increase by altering the oxy- : deoxyhemoglobin ratio.

The issue of anesthetic recall and awareness also has been addressed for isoflurane. Roorda - Hrdlickova et al. observed implicit memory of events during balanced anesthesia that included isoflurane for both induction and maintenance[145] while

Ghoneim et al. report implicit recall during isoflurane anesthesia for both a behavioural suggestion and word learning.[146] On the other hand, Winograd et al. found no evidence for implicit learning of music played to anesthetized patients.[147] It seems clear, however, that some types of information processing can occur during isoflurane anesthesia. Dreaming under isoflurane also has been reported and this could affect BOLD signal strength. Noble et al. found that fewer patients tend to dream under isoflurane (approximately 12.5%) than under propofol (approximately 20%), although a greater percentage of the isoflurane patients experienced bad dreams (29% for isoflurane vs 5% for propofol).[139] The potential for dream activity, and increased CBF, suggest that isoflurane may cause some artifacts in fMR images.

Nonetheless, isoflurane is perhaps the best candidate for canine fMRI in large part because it is an inhalant for which anesthetic depth can be monitored easily.[141] Maintaining a light, stable plane of anesthesia, to allow for maximum cerebral activity and prevent changes in anesthetic depth, is especially important because many anesthetic effects on the CNS are known to be dose and depth dependant. It is likely a better candidate than other inhalants, as well, because the increase in CBF it causes is much smaller than that caused by halothane or enflurane in humans[126] and dogs.[148] Also encouraging is the fact that VEPs and AERs can be elicited during even very deep anesthesia in humans. Predicting which of propofol or isoflurane will allow for higher quality fMR images is difficult, however, because no direct comparisons exist and methods for EEG studies of anesthetic are not standardized.

Fentanyl / Midazolam: Potential Effects on fMR Images

Combinations of agents are often used to exploit a range of anesthetic characteristics and permit the use of smaller doses to reduce side effects[149]. For example, the hypnotic and reflex blocking effects of a non-opioid intravenous agent could complement the analgesic properties of an opioid narcotic.[129] This is referred to as

"balanced anesthesia", and the opioid, fentanyl, can be administered in combination with non-opioid, midazolam, to achieve this balance.

Opioids are the most commonly used drugs to treat acute and chronic pain in humans. They target the opiate receptors, widespread throughout the brain, and can cause both excitation and inhibition of neurons.[150] Generally, the opioids cause some respiratory depression and, to varying degrees, have an addictive potential which can be problematic with prolonged use.[149] Fentanyl is the most widely used opioid for human anesthesia, often preferred over morphine because it is more potent, has a shorter duration of action, and causes little of the histamine response characteristic of large morphine doses.[149]

In describing CNS and cortical effects of fentanyl anesthesia, recent human PET studies have been particularly revealing. Fentanyl effects seem to be highly localized and specific in the cerebral cortex, causing both inhibition and excitation depending on location. Firestone et al. report significant increases in regional CBF (rCBF) of cortical and subcortical areas in both hemispheres as a result of fentanyl.[150] This activity included the bilateral cingulates, prefrontal cortices and caudate nuclei. They also report significant deactivation in both prefrontal and temporal areas, as well as the cerebellum. Adler et al. observed both activation and deactivation in response to fentanyl in humans, as well.[151] These results illustrate, first of all, the important role functional imaging can play in describing anesthetic action. They also suggest that fentanyl could be a good candidate for fMRI studies restricted to visual cortex, in that it evokes little response there. Fentanyl dependant activation in temporal and prefrontal cortices, however, may interfere with the collection of imaging data associated with visual perception.

A few studies have addressed the issue of recall and awareness during fentanyl anesthesia. Positive verbal suggestions regarding the speed and comfort of postsurgical recovery, made in the presence of fentanyl anesthetized patients, appeared to improve

recovery following surgery.[152] Bennet reports two disturbing case studies of patients anesthetized under a balanced protocol, which included fentanyl, who were merely paralyzed during trauma surgery and experienced pain and explicit recall.[153] Utting suggests that, as the opioids are not true anesthetic drugs, any reduction in awareness they cause is likely an indirect effect, which explains why they are often used in conjunction with other agents, like midazolam.[154]

Midazolam is a non-opioid intravenous sedative with some similarity to propofol,[129] and EEG responses are similarly dose dependant for both agents.[155] Of particular importance to BOLD signals are midazolam's effects on cerebral circulation. Like propofol, midazolam results in reduced overall CBF and $CMRO_2$ in humans. The reduction, however, is considerably less under midazolam,[126] and this agent may allow for a more accurate representation of conscious BOLD signals than propofol.

Predicting the combined effects of fentanyl and midazolam is difficult because they may act on BOLD activity synergistically. Based on their individual actions, however, the combination of fentanyl and midazolam has great potential for fMRI investigations restricted to the visual cortex and the occipital lobe. Because fentanyl causes both localized activation and deactivation of temporal and prefrontal areas in humans, however, it may produce considerable artifact in areas anterior to the visual cortex during whole brain imaging of dogs. As our objective is to test visual perception, fentanyl / midazolam is unlikely to be the optimal fMRI anesthetic protocol.

Encouraging, for investigations of sensory processing is the fact that often anesthesia allows for implicit learning and even rare explicit recall of events, indicating that some level of sensory processing can occur. Most research on postoperative recall has focused on eliminating this phenomenon, as it is clearly undesirable during surgery. It could, however, be of potential benefit to canine fMRI. As fMRI is not a painful procedure, it would be humane to use light anesthesia and anesthetic protocols which

have been shown to allow implicit awareness and learning in humans. Light anesthesia could facilitate images that more accurately reflect conscious perception in dogs.

Predicting which of the three anesthetic protocols will allow for the best fMRI images is challenging because methods in anesthetic research are poorly standardized and considerable subjectivity is involved in the assessment of anesthetic depth.[126] Based on EEG, evoked potential, cerebral circulation, and functional imaging (PET) evidence, as well as the temporal and prefrontal effects of fentanyl and the difficulties inherent to monitoring and maintaining depth during intravenous anesthesia, isoflurane is likely the most reliable choice for use with whole brain imaging. Ensuring that recorded responses are elicited by presented stimuli, and not by fluctuations in anesthetic depth, will be vital to reducing artifacts. Isoflurane is particularly well suited to this role.

1.5 SUMMARY

Functional MRI is an advance in neuroimaging that relies on the magnetic resonance signal properties of oxygenated and deoxygenated hemoglobin to detect changes in regional cerebral blood flow, indicative of changes in neural activity. This technology has yielded considerable gains in the study of human cerebral cortex, particularly in the visual system, and could represent a valuable tool for veterinary ophthalmology.

The canine visual system shares some similarity with that of other mammals especially at early levels of anatomy and processing, but differences likely exist in visual cortex. It is known that V1 is similarly located near the occipital poles of both hemispheres, but our understanding of canine cortical anatomy essentially ends here. Intuitively, it seems likely that canine cortex is more similar to that of cats than primates, but this has not been investigated. Nonetheless, during visual stimulation of dogs one should expect to see BOLD signal changes in the occipital cortex and V1 as a minimum

indication of perception. Some activity in temporal and prefrontal cortices would be anticipated, as well.

Evaluating canine vision clearly suffers from the fact that dogs cannot communicate with the evaluator. In keeping with our anthropomorphic tendencies, humans tend to assume that quality of life for pets includes experiencing their surroundings visually. Whether or not this is true, conscious perception should, therefore, be the focus of a test for canine vision. Current techniques, like behavioural tests, ERG recording and the VEP ignore the fact that perception of visual stimuli, at least in primates, involves activity in visual, temporal, and prefrontal cortices and not simply in the retina or early postretinal regions. Theoretically, areas important to object recognition or motion processing could be completely non-functional in an animal with an apparently normal ERG or VEP. Functional MRI provides obvious advantages over other methods because it allows for whole brain functional imaging in real time, at a range of spatial scales,

Like other neuroimaging and electrodiagnostic techniques, fMRI requires that patients remain still. This clearly presents a challenge for the veterinarian. The use of anesthesia is an unfortunate but inevitable consequence of this requirement. However, it need not overly impair the quality of images obtained if the effects of anesthesia on the brain, and on fMRI, are understood. Anesthetic protocols in common clinical use, which represent good candidates for use with canine fMRI are propofol, isoflurane, and fentanyl / midazolam. On a comparative basis, at equal anesthetic depths, the combination of fentanyl / midazolam likely will allow for functional images which best reflect conscious activity in canine visual cortex. Fentanyl causes powerful localized activation and deactivation of temporal and prefrontal cortices in humans and, therefore, it may be a poor protocol for use when testing visual perception. It is extremely important that anesthetic depth remain constant throughout the imaging procedure, so it is likely

that isoflurane is better suited as an fMRI anesthetic. Anesthetic depth is much more easily estimated and maintained for an inhalant agent and, among the inhalant agents, isoflurane has a relatively minor impact on cerebral circulation.

1.6 REFERENCES

1. Myers LJ. Use of innate behaviors to evaluate sensory function in the dog. *Veterinary Clinics of North America: Small Animal Practice* 1991; **21**: 289-299.

2. Pyckett IL, Newhouse JH, Buonoanno FS, Brady TJ, Goldman MR, Kistler JP, Pohost GM *Principles of nuclear magnetic resonance imaging*. Radiology 1982; **143**: 157-168.

3. Kean DM, Smith MA. *Magnetic Resonance Imaging*. William Heinemann Medical Books, London, 1986.

4. Heiken JP, Glazer HS, Lee JKT, Murphy WA, Gado M. *Manual of Clinical Magnetic Resonance Imaging*. Raven Press, New York, 1986.

5. Le Bihan D, Karni A. Applications of magnetic resonance imaging to the study of human brain function. *Current Opinion in Neurobiology* 1995; **5**: 231-237.

6. Breger R, Kneeland JB. Basic physics of magnetic resonance imaging. In: *Cranial and Spinal Magnetic Resonance Imaging: An Atlas and Guide* (ed. Daniels DL, Haughton VM, Naidich, TP), Raven Press: New York, 1987; 1-4.

7. Sanders JA. Magnetic resonance imaging. In: *Functional Brain Imaging* (ed. Orrison WW, Lewine JD, Sander JA, Hartshorne MF) Mosby - Year Book Ltd: St Louis, 1995;145-186.

8. Edelman RR, Rubin JB, Buxton RB. (1990b) Flow. In: *Clinical Magnetic Resonance Imaging* (ed. Edelman RR, Heselink JR). WB Saunders Company: New York, 1990; 109-182.

9. Stehling MK, Turner R, Mansfield P. Echo-planar imaging: Magnetic resonance imaging in a fraction of a second. *Science* 1991; **254**: 43-50

10. Haase A. Snapshot FLASH MRI: Applications to T1, T2, and chemical shift imaging. *Magnetic Resonance in Medicine* 1990; **13**: 77-89.

11. Davis PC, Newman NJ. Advances in neuroimaging of the visual pathways. *American Journal of Ophthalmology* 1996; **121**: 690-705.

12. Edelman RR, Kleefield J, Wentz KU, Atkinson DJ. Basic principles of magnetic resonance imaging. In: *Clinical Magnetic Resonance Imaging* (ed. Edelman RR, Heselink JR), WB Saunders Company: New York, 1990b; 3-38.

13. Congar P, Khazipov R, Ben-ari Y. Direct demonstration of functional disconnection by anoxia of inhibitory interneurons from excitatory inputs in rat hippocampus. *Journal of Neurophysiology* 1995; **73**: 421-426.

14. Sanders JA, Orrison WW. Functional magnetic resonance imaging. In: *Functional Brain Imaging* (ed. Orrison WW, Lewine JD, Sanders JA, Hartshorne MF), Mosby - Year Book Ltd: St Louis, 1995; 239-326.

15. Phelps ME, Kuhl DE, Mazziota JC. Metabolic mapping of the brain's responses to visual stimulation: Studies in humans. *Science* 1981; **211**: 1445-1448.

16. Pritchard J, Rothman D, Novotny E, Petroff O, Kuwabura T, Avison M, Houseman A, Hanstock C, Shulman R. Lactate rise detected by 1H NMR in human visual cortex during physiologic stimulation. *Proceeding of the National Academy of Sciences USA* 1991; **88**: 5829-5831.

17. Fox PT, Raichle ME. Focal physiological uncoupling of cerebral blood flow and oxidative metabolism during somatosensory stimulation in human subjects. *Proceeding of the National Academy of Sciences USA* 1986; **83**: 1140-1144.

18. Belliveau JW, Kennedy DN, McKintry RC, Buchbinder BR, Weisskoff RM, Cohen MS, Vevea JM, Brady TJ, Rosen BR. Functional mapping of the human visual cortex by magnetic resonance imaging. *Science* 1991; **254**: 716-719.

19. Fox PT, Mintun MA, Raichle ME, Miezen FM, Allman JM, Van Essen DC. Mapping the human visual cortex with positron emission tomography. *Nature* 1986; **323**: 806-809.

20. Heistad DD, Kontos HA. Cerebral circulation. In: *Handbook of Physiology* Vol III, section 2 (ed. Shepard JT, Abboud FM) American Physiological Society: Bethesda, MD, 1983.

21. Iadecola C. Regulation of the cerebral microcirculation during neural activity. *Trends in Neuroscience* 1993; **16**: 206-214.

22. Lou HC, Edvinsson L, Mackenzie ET. The concept of coupling blood flow to brain function: revision required? *Annals of Neurololoqy* 1987; **22**: 289-297.

23. Pauling L, Coryell CD. The magnetic properties and structure of hemoglobin, oxyhemoglobin and carbon monoxyhemoglobin. *Proceedings of the National Academy of Sciences* USA 1936; **22**: 210-216.

24. Villringer A, Rosen BR, Belliveau JW, Ackerman JL, Lauffer RB, Buxton RB, Chao YS, Wedeen VJ, Brady TJ. Dynamic imaging with lanthanide chelates in normal brain: contrast due to susceptibility effects. *Magnetic Resonance in Medicine* 1988; **6**: 164-174.

25. Rosen BR, Belliveau JW, Aronen HJ, Kennedy D, Buchbinder BR, Fischman A, Gruber M, Glas J, Weisskoff RM, Cohen MS, Hochberg FH, Brady TJ. Susceptibility contrast imaging of cerebral blood volume: Human experience. *Magnetic Resonance in Medicine* 1991; **22**: 293-299.

26. Cohen MS. Rapid MRI and functional application. In: *Brain Mapping: The Methods* (ed. Toga AW, Mazziotta JC). Academic Press: San Diego, 1996; pp 223-255.

27. Detre JA, Leigh JS, Williams DS, Koretsky AP. Perfusion imaging. *Magnetic Resonance in Medicine* 1992; **23**: 37-45.

28. Williams DS, Detre JA, Leigh JS, Koretsky AP. Magnetic resonance imaging of perfusion using spin inversion of arterial water. *Proceedings of the National Academy of*

Sciences USA 1992; **89**: 212-216.

29. Kwong KK, Belliveau JW, Chesler DA, Goldberg IE, Weisskoff RM, Poncelet BP, Kennedy DN, Hoppel BE, Cohen MS, Turner R, Cheng H, Brady TJ, Rosen BR. Dynamic resonance imaging of human brain activity during primary sensory stimulation. *Proceedings of the National Academy of Sciences* USA 1992; **89**: 5675-5679.

30. Ellerman J, Garwood M, Hendrich K, Hinke R, Hu X, Kim S, Menon R, Merkle H, Ogawa S, Ugurbil K. Functional imaging of the brain by nuclear magnetic resonance. In: *NMR in Physiology and Biomedicine* (ed. Gillies RJ). Academic Press: San Diego, 1994; 137-150.

31. DeYoe EA, P, Neitz J, Miller D, Winans P. Functional magnetic resonance imaging (fMRI) of the human brain. *Journal of Neuroscience Methods* 1994; **54**: 171-187.

32. Thulborn KR, Waterton JC, Mathews PM, Radda GK. Oxygenation dependence of the transverse relaxation time of water protons in whole blood at high field. *Biochimica et Biophysica Acta* 1982; **714**: 265-270.

33. Ogawa S, Lee TM. Magnetic resonance imaging of blood vessels at high fields: In Vivo and in vitro measurements and image simulation. *Magnetic Resonance in Medicine* 1990; **16**: 9-18.

34. Turner R, Jezzard P, Wen H, Kwong KK, Le Bihan D, Zeffiro T, Balaban RS. Functional mapping of the human visual cortex at 4 and 15 T using deoxygenation contrast EPI. *Magnetic Resonance in Medicine* 1993; **29**: 277-279.

35. Ogawa S, Tank DW, Menon R, Ellerman JM, Kim S Merkle H Ugurbil K. Intrinsic signal changes accompanying sensory stimulation: Functional brain mapping with magnetic resonance imaging. *Proceedings of the National Academy of Sciences* USA 1992; **89**: 5951-5955.

36. Ogawa S, Lee TM, Nayak A, Glynn P Oxygenation-sensitive contrast in magnetic resonance imaging of rodent brain at high magnetic fields. *Magnetic Resonance in Medicine* 1990a; **14**: 68-78.

37. Ogawa S, Lee TM, Kay AR, Tank DW (1990b) Brain magnetic resonance imaging with contrast dependent on blood oxygenation. *Proceedings of the National Academy of Sciences* USA 1990b; 87: 9868-9872.

38. Bandettini PA, Wong EC, Hinks RS, Tifofsky RS, Hyde JS. Time course EPI of human brain function during task activation. *Magnetic Resonance in Medicine* 1992; **25**: 390-397.

39. Menon RS, Ogawa S, Strupp JP, Ugurbil K. Ocular dominance in human V1 demonstrated by functional magnetic resonance imaging. *Journal of Neurophysiology* 1997; **77**: 2780-2787.

40. Menon RS, Gati JS, Bradley G, Goodyear G, Luknowsky DC, Thomas CG. Spatial and temporal resolution of functional magnetic resonance imaging. *Biochemistry and Cell Biology* 1998; **76**: 560-571.

41. Engel SA, Rumelhart DE, Wandell BA, Lee AT, Glover GH, Chichilnisky E Shadlen MN. fMRI of human visual cortex. *Nature* 1994; **369**: 525.

42. Fox PT, Mintum MA, Reiman EM, Raichle ME. Enhanced detection of focal brain responses using intersubject, averaging and analyisis of subtracted PET images. *Journal of Cerebral Blood Flow and Metabolism* 1988; **8**:642-65.

43. Talairach J, Tournoux P. *Co-Planar Sterotactic Atlas of the Human Brain.* Georg Thiem Verlag, Stuttgart, 1988.

44. Sereno MI. Brain mapping in animals and humans. *Cognitive Neuroscience* 1998; **8**: 188-194.

45. Lai S, Hopkins AL, Haacke AM, Li D, Wasserman BA, Buckley P, Friedman L, Meltzer H, Hedera P, Friedland R. Identification of vascular structures as a major source of signal contrast in high resolution 2D and 3D functional activation imaging of the motor cortex at 15 T: Preliminary results. *Magnetic Resonance in Medicine* 1993; **30**: 387-392.

46. Kim SG, Ashe J, Georgopoulos AP, Merkle H, Ellerman JM, Menon RS, Ogawa S, Ugurbil K. Functional imaging of human motor cortex at high field. *Journal of Neurophysiology* 1993a; **69**: 297-302.

47. Grabowski TJ, Damasio AR. Improving functional imaging techniques. *Proceedings of the National Academy of Sciences* USA 1996; **93**: 14302-14303.

48. Buckner RL, Bandettini PA, O'Craven KM, Savoy RL, Petersen SE, Raichle ME, Rosen BR. Detection of cortical activation during averaged single trials of a cognitive task using functional magnetic resonance imaging. *Proceedings of the National Academy of Sciences* USA 1996; **93**: 14878-14883.

49. Boynton GM, Engel SA, Glover GH, Heeger DJ. Linear systems analysis of functional magnetic resonance imaging in human V1. *Journal of Neuroscience* 1996; **16**: 4207-4221.

50. Binder JR, Rao SM, Hammeke TA, Yetkin FZ, Jesmaniwicz A, Bandettini PA, Wong EC, Estrowski LD, Goldstein MD, Haughton VM, Hyde JS. Functional magnetic resonance imaging of human auditory cortex. *Annals of Neurology* 1994a; **35**: 662-672.

51. Binder JR, Rao SM, Hammeke TA, Frost JA, Bandettini PA, Hyde JS. Effects of stimulus rate on signal response during functional magnetic resonance imaging. Cognition and Brain Research 1994b; **2**: 31-38.

52. Dhankar MA, Wexler BE, Fulbright RK, Halwes T, Blamire AM, Schulman RG. Functional magnetic resonance imaging assessment of the human brain auditory cortex response to increasing word presentation rate. *Journal of Neurophysiology*; 1997; **77**: 476-483.

53. Kim SG, Ashe J, Hendrich K, Ellerman JM, Merkle H, Ugurbil K, Georgopoulos AP. Functional magnetic resonance imaging of motor cortex: Hemispheric asymetry and handedness *Science* 1993b; **261**: 615-617.

54. Rao SM, Binder JR, Bandettini PA, Hammeke TA, Yetkin FZ, Jesmanowicz A, Lisk LM, Morris GL, Mueller WM, Estowski LD. Functional magnetic resonance imaging of complex human movements. *Neurology* 1993; **43**: 2311-2318.

55. Reichert H. Sensory systems. In: *Introduction to Neurobiology*, Georg Thieme Verlag: Stuttgart, 1992; 85-119.

56. Eckert R. Neural processing and behaviour. In: *Animal Physiology: Mechanisms and Adaptations* (ed. Eckert R, Randall D, Augustine G). W H Freeman and Company: New York, 1988; 219-265.

57. De Lahunta A. *Veterinary Neuroanatomy and Clinical Neurology*. WB Saunders Company, Philadelphia, 1983.

58. Williams RW Hogan D, Preston E, Garraghty E.Target recognition and visual maps in the thalamus of achiasmatic dogs. *Nature* 1994; **367**: 637-639.

59. Van Essen DC. Visual areas of the mammalian cerebral cortex. *Annual Reviews in the Neurosciences* 1979; **2**: 227-263.

60. Hubel DH, Weisel TH. Receptive fields, binocular interaction and functional architecture in the cat's visual cortex. *Journal of Physiology* 1962; **160**: 106-154.

61. Gizzi MS, Katz E, Schumer RA, Movshon JA. Selectivity for orientation and direction of motion of single neurons in cat striate and extrastriate visual cortex. *Journal of Neurophysiology* 1990; **63**:1529-1543.

62. Tootell RBH, Anders MD, Sereno MI, Malach R. New images from human visual cortex. *Trends in Neuroscience* 1996; **19**: 481-489.

63. Hubel DH, Weisel TH. Receptive fields of single neurons in cat's striate cortex. *Journal of Physiology* 1959; **148**: 574-591.

64. Hubel DH, Weisel TH. Receptive fields and functional architecture of monkey striate cortex. *Journal of Physiology* 1968; **195**: 215-243.

65. Hubel DH, Weisel TH. Functional architecture of macaque monkey visual cortex. *Proceedings of the Royal Society of London [Biology]* 1977; 198: 1-59.

66. Hubel DH, Weisel TH. Anatomical demonstration of orientation columns in macaque monkey. *Journal of Comparative Neurology* 1978; **177**: 361-380.

67. Sereno MI, Dale AM, Reppas JB, Kwong KK, Belliveau JW, Brady TJ, Rosen BR, Tootell RBH. Borders of multiple visual areas in humans revealed by functional magnetic resonance imaging. *Science* 1995; **268**: 889-893.

68. DeYoe EA, Carman GJ, Bandettini P, Glickman S, Weiser J, Cox R, Miller D, Neitz J. Mapping striate and extrastriate visual areas in human cerebral cortex. *Proceedings of the National Academy of Sciences* USA 1996; **93**: 2382-2386.

69. Reppas JB, Niyogi S, Dale AM, Sereno MI, Tootell RBH. Representation of motion boundaries in retinotopic human visual cortical areas. *Nature* 1997; **388**: 175-179.

70. Tanaka K. Neuronal mechanisms of object recognition. *Science* 1993; **262**: 685-688.

71. Courtney SM, Ungerleider LG. What fMRI has taught us about human vision. *Current Opinion in Neurobiology* 1997; **7**: 554-561.

72. Tootell RBH, Mendola JD, Hadjikani NK, Ledden PJ, Liu AK, Reppas JB, Sereno MI, Dale AM. Functional analysis of V3A and related areas in human visual cortex. *Journal of Neuroscience* 1997; **17**: 7060-7078.

73. Tootell RBH, Reppas JB, Kwong KK, Malach R, Born RT, Brady TJ, Rosen BR, Belliveau JW. Functional analysis of human MT and related visual cortical areas using magnetic resonance imaging. *Journal of Neuroscience* 1995; **15**: 3215-3230.

74. Desimone R. Face-selective cells in the temporal cortex of monkeys. *Journal of Cognitive Neuroscience* 1991; **3**: 1-8.

75. Engel SA, Glover GH, Wandell BA. Retinotopic organization in human visual cortex and the spatial precision of functional MRI. *Cerebral Cortex* 1997a; **7**: 181-192.

76. Ungerleider LG, Mishkin M. Two cortical visual systems. In: *Analysis of Visual Behaviour* (ed. Ingle DJ, Goodale MA, Mansfield RJW). MIT Press: Cambridge, Mass, 1982; 549-586.

77. Livingstone M, Hubel DH. Segregation of form, color, movement and depth: Anatomy, physiology and perception. *Science* 1988; **240**: 740-749.

78. Goodale MA, Milner AD. Separate visual pathways for perception and action. *Trends in Neuroscience* 1992; **15**: 20-25.

79. Howard RJ, Brammer M, Wright I, Woodruff PW, Bullmore ET, Zeki S. A direct demonstration of functional specialization within motion-related visual and auditory cortex of the human brain. *Current Biology* 1996; **6**: 1015-1019.

80. Treue S, Maunsell JHR. Attentional modulation of visual motion processing in cortical areas MT and MST. *Nature* 1996; **382**: 539-541.

81. O'Craven KM, Rosen BR, Kwong KK, Treisman A, Savoy RL. Voluntary attention modulates fMRI activity in human MT-MST. *Neuron* 1997; **18**: 591-598.

82. Eden GF, VanMeter JW, Rumsey JM, Maisog JM, Woods RP, Zeffiro TA. Abnormal processing of visual motion in dyslexia revealed by functional magnetic resonance imaging. *Nature* 1996; **382**: 67-69.

83. Puce A, Allison T, Asgari M, Gore JC, McCarthy G. Differential sensitivity of human visual cortex to faces letterstrings and textures: a functional magnetic resonance imaging study. *Journal of Neuroscience* 1996; **16**: 5205-5215.

84. Courtney SM, Ungerleider LG, Keil K, Haxby JV. Transient and sustained activity in a distributed neural system for human working memory. *Nature* 1997; **386**: 608-611.

85. Malach R, Reppas JB, Benson RR, Kwong KK, Jiang H, Kennedy WA, Ledden PJ, Brady TJ, Rosen BR, Tootell RBH. Object- related activity by functional magnetic resonance imaging in human occipital cortex. *Proceedings of the National Academy of Sciences* USA 1995; **92**: 8135-8139.

86. Martin A, Wiggs C, Ungerleider LG, Haxby J V. Neural correlates of category - specific knowledge. *Nature* 1996; **379**: 649-652.

87. Lueck CJ, Zeki S, Friston KJ, Deiber MP, Cope P, Cunningham VG, Lammertsma AA, Kennard C, Frackowiak RSJ. The color center in the cerebral cortex of man. *Nature* 1989; **340**: 386-389.

88. Damasio A, Yamada T, Damasio H, Corbett J, McKee J. Central achromatopsia: Behavioural, anatomic and physiologic aspects. *Neurology* 1980; **30**: 1064-1071.

89. Sakai K, Watanabe E, Onodera Y, Uchilda I, Kato H, Yamamoto E, Koizumi H, Miyashita Y. Functional mapping of the human colour centre with echo-planar magnetic resonance imaging. *Proceedings of the Royal Society London [Biology]* 1995; **261**: 89-98.

90. Engel SA, Zhang X, Wandell BA. Colour tuning in human visual cortex measured with functional magnetic resonance imaging. *Nature* 1997b; **388**: 68-71.

91. Moran J, Desimone R. Selective attention gates visual processing in extrastriate cortex. *Science* 1985; **229**: 782-784.

92. Desimone R. Neural mechanisms for visual memory and their role in attention. *Proceedings of the National Academy of Sciencesi* USA 1996; **93**: 13494-13499.

93. McCarthy G, Blamire AM, Puse A, Nobre AC, Bloch G, Hyder F, Golgman Rakic P, Shulman RG. Functional magnetic resonance imaging of human prefrontal cortex activation during a spatial working memory task. *Proceedings of the National Academy of Sciences* USA 1994; **91**: 8690-8694.

94. Kosslyn SM, Thompson WL, Kim IJ, Alpert NM. Topographical representation of mental images in primary visual cortex. *Nature* 1995; **378**: 496-498.

95. Le Bihan D, Turner R, Zeffiro TA, Cuenod CA, Jezzard P, Bonnerot V. Activation of human primary visual cortex during visual recall: A functional magnetic resonance imaging study. *Proceedings of the National Academy of Sciences* USA 1993; **90**: 11802-11805.

96. Miller PE, Murphy CJ. Vision in dogs. *Journal of the American Veterinary Medical Association* 1996; **207**:1623-1634.

97. Kemp CM, Jacobson SG. Rhodopsin levels in the central retinas of normal miniature poodles and those with progressive rod-cone degeneration. *Experimental Eye Research* 1992; **54**: 947-956.

98. Peichl L. Topography of ganglion cells in the dog and wolf retina. *Journal of Comparative Neurology* 1992; **324**: 603-620.

99. Neitz J, Geist T, Jacobs GH. Color vision in the dog. *Visual Neuroscience* 1989; **3**: 119-125.

100. Ofri R, Dawson WW, Samuelson DA (1994) Mapping of the cortical area of central vision in dogs. *Progress in Comparative and Veterinary Ophthalmology* 1994; 4: 172-178.

101. Hubel DH, Weisel TH (1963) Shape and arrangement of columns in cat's striate cortex. *Journal of Physiology* 1963; **165**: 559-568.

102. Payne BR. Evidence for visual cortical area homologues in cat and macaque monkey. *Cerebral Cortex* 1992; **3**: 1-15.

103. Scannell JW, Sengpiel F, Tovee MJ, Becson PJ, Blakemore C, Young M. Visual motion processing in the anterior ectosylvian sulcus of the cat. *Journal of Neurophysiology* 1996; **76**: 895-907.

104. Ezeh PI, Myers LJ, Cummins KA, Whitley RD. Utilizing an optokinetic device in assessing the functional visual acuity of the dog. *Progress in Veterinary Neurology* 1990; **1**: 427-432.

105. Odom JV, Bromberg NM, Dawson WW. Canine visual acuity: retinal and cortical field potentials evoked by pattern stimulation. *American Journal of Physiology* 1983; **14**: R637-R641.

106. Ofri R, Dawson WW, Gelatt KN. Visual resolution in normal and glaucomatus dogs determined by pattern electroretinogram. *Progress in Veterinary and Comparative Ophthalmology* 1993; **3**:111-116.

107. Strain GM, Jackson RM, Tedford BL. Visual evoked potentials in the clinically normal dog. *Journal of Veterinary Internal Medicine* 1990; **4**: 222-225.

108. Sims MH, Ward DA. Response of pattern-electroretinograms (PERG) in dogs to alterations in the spatial frequency of the stimulus. *Progress in Veterinary and Comparative Ophthalmology* 1992; **2**: 106-112.

109. Humphrey NK, Weiskrantz L. Vision in monkeys after removal of the striate cortex. *Nature* 1967; **215**: 944-946.

110. Cowey A, Stoerig P. Blindsight in monkeys. *Nature* 1995; **373**: 247-249.

111. Weiskrantz L, Barbur JL, Sahraie A. Parameters affecting conscious versus unconscious visual discrimination with damage to V1. *Proceedings of the National Academy of Sciences* USA 1995; **92**: 6122-6126.

112. Winans SS. Visual form discrimination after removal of visual cortex in cats. *Science* 1967; **158**: 944-946.

113. Kaas JH. Vision without awareness. *Nature* 1995; **373**: 195.

114. Sims MH, Laratta LJ, Bubb WJ, Morgan RV. Waveform analysis and reproducibility of visual evoked potentials in dogs. *American Journal of Veterinary Research* 1989; **50**: 1823-1828.

115. Bischel P, Oliver JE, Coulter DB, Brown J. Recording of visual-evoked potentials in dogs with scalp electrodes. *Journal of Veterinary Internal Medicine* 1988; **2**: 145-149.

116. Nakamura RK, Mishkin M. Chronic 'blindness' following lesions of nonvisual cortex in monkeys. *Experimental Brain Research* 1986; **63**: 173-184.

117. Nakamura RK, Schein SJ, Desimone R. Visual responses from cells in striate cortex of monkeys rendered chronically blind by lesions of nonvisual cortex. *Experimental Brain Research* 1986; **63**: 185-90.

118. Sahraie A, Weiskrantz L, Barbur JL, Simmons SCR, Brammer MJ. Pattern of neuronal activity associated with conscious and unconscious processing of visual signals. *Proceedings of the National Academy of Sciences* USA 1997; **94**: 9406-9411.

119. Rauschecker JP, Korte M. Auditory compensation for early blindness in cat cerebral cortex. *Journal of Neuroscience* 1993; **13**: 4538-4548.

120. Mclean J, Palmer LA (1998) Plasticity of neuronal response properties in adult cat striate cortex. *Visual Neuroscience* 1998; **15**: 177-196.

121. Dwyer RC, Rampil IJ, Eger EI, Bennett HL. The electroencephalogram does not predict depth of isoflurane anesthesia. *Anesthesiology* 1994; **81**: 403-409.

122. Harvey RC, Sims MH, Greene SA. Neurologic disease. In *Lumb and Jones' Veterinary Anesthesia* (eds. Thurmon JC, Tranquill WJ, Benson GJ). Williams and Wilkins: Baltimore, 1996; 781-784.

123. Jezzard P, Rauschecker JP, Malonek D. An *in vivo* model for functional MRI in cat visual cortex. *Magnetic Resonance in Medicine* 1997; **38**: 699-705.

124. Trustman R, Dubovsky S, Titley R. Auditory perception during general anesthesia: Myth or fact. *International Journal of Clinical and Experimental Hypnosis* 1977; **25**: 88-105.

125. Kihlstrom JF, Schacter DL. Anesthesia, amnesia, and the cognitive unconscious. In *Memory and Awareness in Anesthesia* (ed. Bonke B, Fitch W, Millar K). Swets and Zeitlinger: Amsterdam, 1990; 21-44.

126. Smith DS, Fisher SM. Neuroanesthesia and neurologic diseases. In: *Dripps, Eckenhoff, Vandam Introduction to Anesthesia* (ed. Longnecker DE, Murphy FL). WB Saunders Philadelphia, 1992; 382-395.

127. Newberg RE, Milde JH, Michenfelder JD. The cerebral metabolic effects of isoflurane at and above concentrations that suppress cortical electrical activity. *Anesthesiology* 1983; **59**: 23-28.

128. Newberg RE, Michenfelder JD (1983) Cerebral protection by isoflurane during hypoxemia or ischemia. *Anesthesiology* 1983; **59**: 29-35.

129. Kennedy SK (1992) Nonopiod intravenous anesthetics. In *Dripps, Eckenhoff, Vandam: Introduction to Anesthesia* (ed. Longnecker DE, Murphy FL). WB Saunders: Philadelphia, 1992; 91-101.

130. Shafer SL. Advances in propofol pharmacokinetics and pharacodynamics. *Journal of Clinical Anesthesia* 1993; **5**: 14S-21S

131. Sneyd JR, Kamra SK, Davidson B, Kishimoto T, Kadoya C, Domino EF. Electrophysiologic effects of propofol sedation. *Anesthesia and Analgesia* 1994; **79**: 1151-1158.

132. DeGrood PMRM, Harbers JBM, Van Egmond J, Crul JF. Anesthesia for laparoscopy. A comparison of five techniques including propofol, etomidate, thiopentone, and isoflourane. *Anesthesia* 1987; **42**:815-823.

133. Valanne J. Recovery and discharge of patients after long propofol infusion vs isoflurane anesthesia for ambulatory surgery. *Acta Anaesthesiology Scandanavia* 1992; 36: 530-533.

134. Jones JG. Use of evoked potentials in the EEG to measure depth of anesthesia. In: *Consciousness, Awareness and Pain in General anesthesia* (ed.Rosen M, Lunn JM). Butterworths: London, 1987; 132-149.

135. Van Hemelrijk J, Tempelhoff JM, White PF, Jellish WS. EEG assisted titration of propofol infusion during neuroanesthesia: Effect of nitrous oxide. *Journal of Neurosurgery and Anesthesia* 1992; **4**: 11-20.

136. Pinaud M, Lelausque JN, Chetanneau A, Fauchoux N, Menegalli D, Souron R. Effects of propofol on cerebral hemodynamics and metabolism in patients with brain trauma. *Anesthesiology* 1990; **73**: 404-409.

137. Artu AA, Shapiro Y, Bowdle, TA. Electroencephalogram, cerebral metabolic and vascular responses to propofol anesthesia in dogs. *Journal of Neurosurgery and Anesthesia* 1992; **4**: 99-109.

138. Sung YF, Tillette, T, Freniere S, Powell RW. Retrograde amnesia, anterograde amnesia and impaired recall by using either thiopentone or propofol as induction and maintenance anesthetic agents. In: *Memory and Awareness in Anesthesia* (ed. Bonke B, Fitch W, Millar K). Swets and Zeitlinger: Amsterdam, 1990; 176-180.

139. Noble DW, Power I, Spence AA, Weatheril D. Sleep and dream in relation to hospitalization, anesthesia and surgery. A preliminary analysis of the first 100 patients. In *Memory and Awareness in Anesthesia* (ed. Bonke B, Fitch W, Millar K). Swets and Zeitlinger: Amsterdam, 1990; 219-225.

140. Duval M, Cogliolo P, Santangelo E, Villanin R, Cuocolo R. Memory for intraoperative events and its psychological consequences. In *Memory and Awareness in Anesthesia* (ed. Bonke B, Fitch W, Millar K). Swets and Zeitlinger: Amsterdam, 1990; 244-249.

141. Miller FL, Marshall BE.The inhaled anesthetics. In: *Dripps, Eckenhoff, Vandam: Introduction to Anesthesia* (ed. Longnecker DE, Murphy FL). WB Saunders: Philadelphia, 1992; 77-90.

142. Hartikainen K, Rorarius, M, Makela K, Perakyla J, Varila E, Jantti V. Visually evoked bursts during isoflurane anesthesia. *British Journal of Anesthesia* 1995; **74**: 681-685.

143. Michenfelder JD.The interdependency of cerebral functional and metabolic effects following massive doses of thiopental in the dog. *Anesthesiology* 1974; **41**: 231-236.

144. Turner DM, Kassell NF, Sasaki T, Comair YG, Boarini DJ, Beck DO. Time dependent change in cerebral and cardiovascular parameters in isoflurane-nitrous oxide anesthetized dogs. *Neurosurgery* 1984; **14**: 144-151.

145. Roorda - Hrdlickova V, Wolters G, Bonke B, Phaf RH. Unconscious perception during general anesthesia, demonstrated by an implicit memory task. In: *Memory and Awareness in Anesthesia* (ed. Bonke B, Fitch W, Millar K). Swets and Zeitlinger: Amsterdam, 1990; 150-154.

146. Ghoneim MM, Block RI, Sum Ping ST Ali MA, Hoffman JG. Learning without recall during anesthesia. In: *Memory and Awareness in Anesthesia* (ed. Bonke B, Fitch W, Millar K). Swets and Zeitlinger: Amsterdam, 1990; 161-169.

147. Winograd E, Sebel PS, Golgman WP, Clifton CL. Indirect assessment of memory for music under anesthesia. In: *Memory and Awareness in Anesthesia* (ed. Bonke B, Fitch W, Millar K). Swets and Zeitlinger: Amsterdam, 1990; 181-184.

148. Short CE, Otto KA. Nervous system: Effects of anesthetics on central nervous system function. In*: Lumb and Jones' Veterinary Anesthesia* (ed. Thurman JC, Tranquill WJ, Benson GJ). Williams and Wilkins: Baltimore, 1996; 171-181.

149. O'Hara DA. Opioids in anesthesia practice. In: *Dripps, Eckenhoff, Vandam: Introduction to Anesthesia* (ed. Longnecker DE, Murphy FL). WB Saunders:Philadelphia, 1992; 102-109.

150. Firestone LL, Gyulai F, Mintun M, Adler LJ, Urso K, Winter PM. Human brain activity response to fentanyl imaged by positron emission tomography. *Anesthesia and Analgesia* 1996; **82**: 1247-1251.

151. Adler LJ, Gyulai FE, Diehl DJ, Mintun MA, Winter PM, Firestone LL. Regional brain activity changes associated with fentanyl analgesia elucidated by positron emission tomography. *Anesthesia and Analgesia* 1997; **84**: 120-126.

152. Evans C, Richardson PH. A double-blind randomized placebo-controlled study of therapeutic suggestions during general anesthesia. In: *Memory and Awareness in Anesthesia* (ed. Bonke B, Fitch W, Millar K). Swets and Zeitlinger: Amsterdam, 1990; 120-130.

153. Bennett HL. Memory for trauma surgery: Trauma victims talk back. In: *Memory and Awareness in Anesthesia* (ed. Bonke B, Fitch W, Millar K). Swets and Zeitlinger: Amsterdam, 1990; 237-243.

154. Utting JE. Clinical aspects of awareness during anesthesia. In: *Memory and Awareness in Anesthesia* (ed. Bonke B, Fitch W, Millar K). Swets and Zeitlinger: Amsterdam, 1990; 259-271.

155. Veselis RA, Reinsel R, Marino P, Sommer S, Carlon GC. The effects of midazolam on the EEG during sedation of critically ill patients. *Anesthesia* 1993; **48**: 463-470.

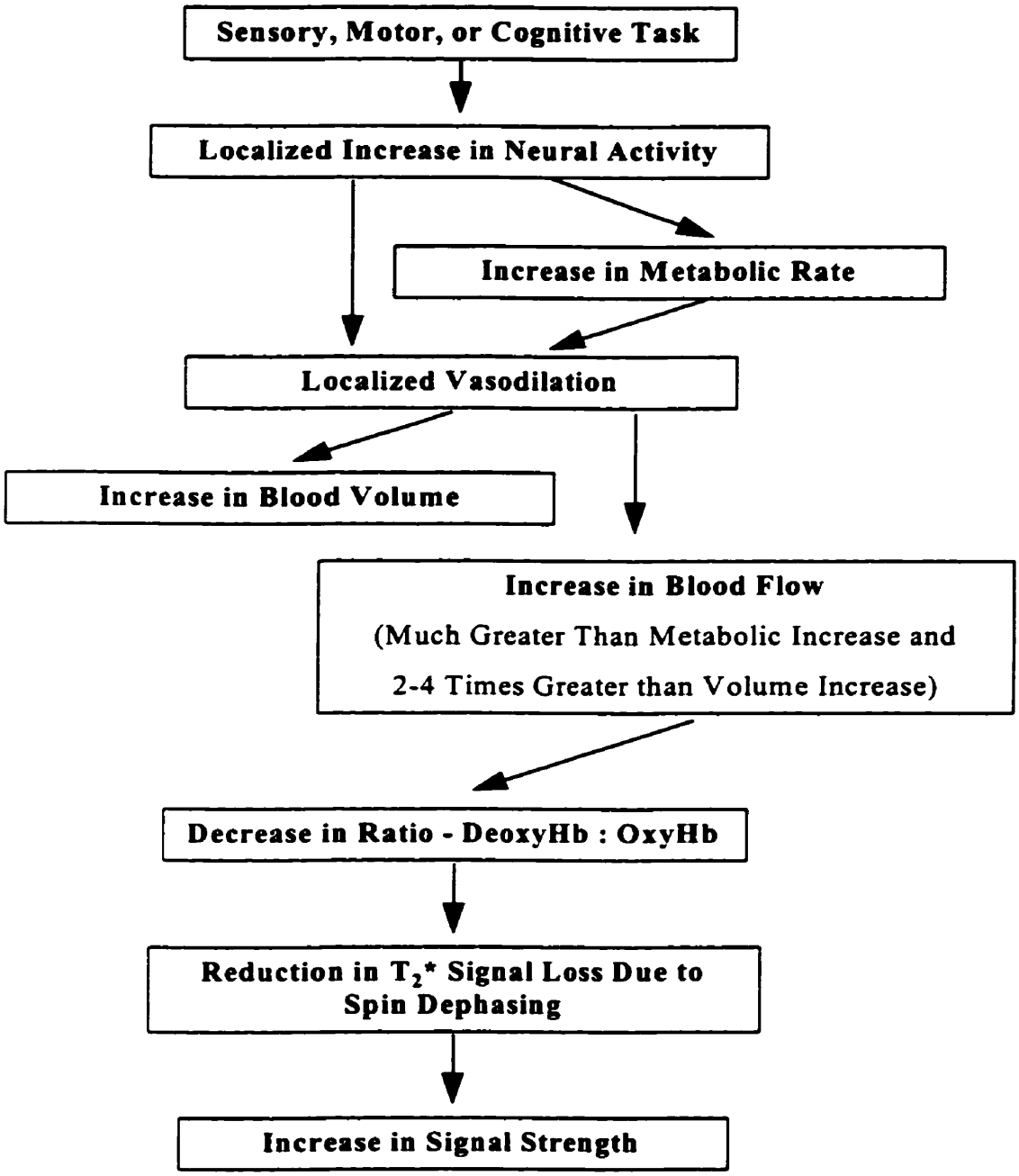

Figure 1.1 Mechanism of the BOLD (blood oxygenation level dependant) principle, currently used widely for fMRI. Hb represents hemoglobin. (modified from DeYoe et al.[31])

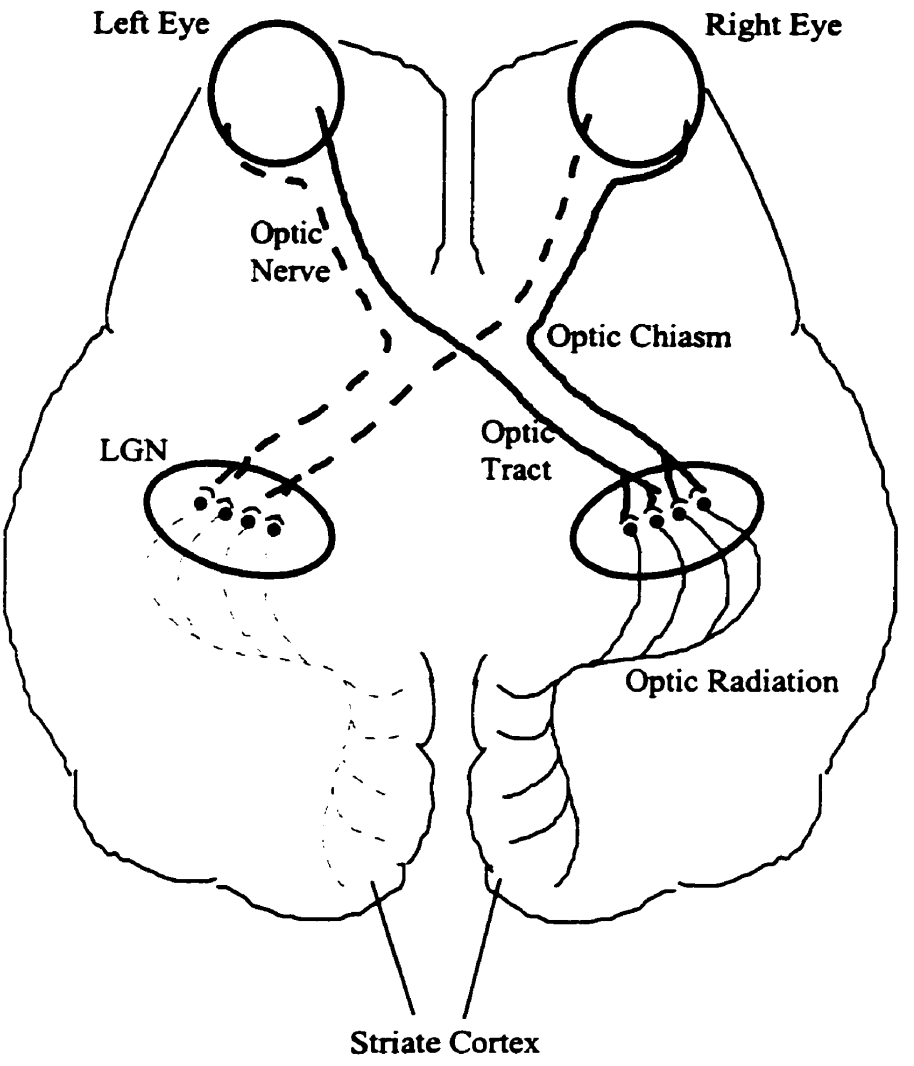

Figure 1.2 Schematic diagram of early postretinal neural pathways in the mammalian brain. Images that appears to our left are initially processed in the right LGN (lateral geniculate nucleus) and striate cortex (solid lines) and those to our right in the left LGN and striate cortex (dashed lines). Not to scale. (modified from Reichert[55])

Figure 1.3 Some of the retinotopic, ventral stream, and dorsal stream areas in the human brain, identified by fMRI. The outlined areas of the dorsal view of cerebral cortex (A) and mid-sagittal view of the right cerebral hemisphere (B) approximately correspond with the area shown in C where the occipital and occipitotemporal cortices have been flattened and functional subunits labelled. The • represents a reference point near the calcarine sulcus common to all three figures. Retinotopic areas include V1, V2, V3, V3a, VP, and V4v; MT is the dorsal stream region shown; and LO is the ventral stream region shown. (modified from Tootell et al.[61])

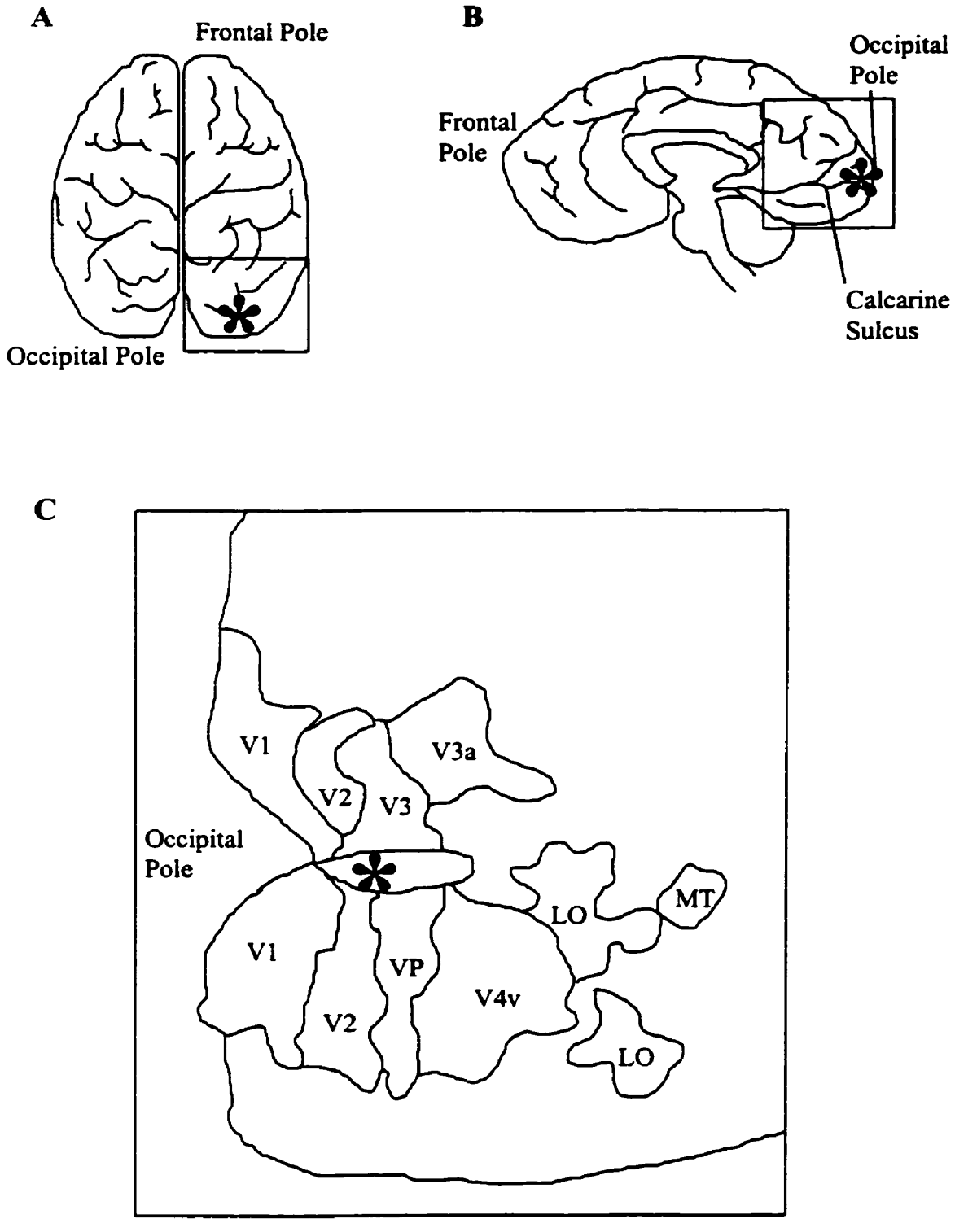
A
Frontal Pole
Occipital Pole
B
Occipital Pole
Frontal Pole
Calcarine Sulcus
C
V1
V3a
V2
V3
Occipital Pole
LO
MT
V1
VP
V4v
V2
LO

CHAPTER TWO.

2.1 GENERAL INTRODUCTION AND OBJECTIVES

Current tests for canine vision are subjective and poorly standardized[1,2] and, because of our inability to communicate verbally with animals, few alternatives exist. Functional magnetic resonance imaging (fMRI) has proven enormously productive in human vision research,[3] and has been used to investigate brain activity of non-human primates[4] and cats.[5] This relatively new technique in neuroimaging may represent a potential tool to assess canine vision.

Blood Oxygenation Level Dependant (BOLD) fMRI provides an indirect but nonetheless accurate spatial and temporal representation of neural activity in the brain based on MR signals associated with the oxygenation of flowing blood in cortical microvasculature.[6] The high spatial resolution of fMRI and the fact that it is non-invasive make it particularly attractive over other neurobiological methods in that these features permit the investigator to focus on very small functional subunits of brain tissue in living subjects.[3,7]

The long term goal of this research is to exploit the attractive characteristics of fMRI in the development of an objective test of canine vision. Clinical applications of such a test would include the evaluation of treatments in use for diseases like glaucoma. Currently, to treat such visual problems in dogs, the veterinary ophthalmologist relies on techniques similar to those used in humans with little conclusive evidence that they improve or spare vision. The potential research applications of canine fMRI are numerous and diverse and include experiments addressing retinotopy, visual processing of form, colour and motion, and learning in a new mammalian animal model.

2.2 ANATOMIC REGIONS ASSOCIATED WITH VISION IN ANESTHETIZED DOGS

Although the functional organization of the feline brain has been well studied, canine cerebrum has received little attention in the literature. In fact, many assumptions about the organization of the dog brain are based on our understanding of cats and other mammals. Investigating activity in areas assumed to play a role in vision for dogs using fMRI could help confirm or refute these assumptions. Identifying brain regions which produce reliable signals in response to vision will also be important to the development of a clinical test for canine vision.

One assertion of veterinary neuroanatomists is that an estimated 75% of optic nerve fibres decussate at the optic chiasm in dogs,[6] although little direct evidence has been collected to support this claim. Resolving the issue, conclusively, has implications for experimental design, particularly when developing appropriate stimuli for future studies of the canine brain, as well as for the development of a clinical test for canine vision using fMRI.

The goals of this study with respect to functional neuroanatomy were:

1. To examine both the amount of signal change and the size of activated areas within both the lateral geniculate nucleus of the thalamus and the occipital lobe of the cerebral cortex in anesthetized dogs.
2. To compare both of these quantitative measures of image quality, within both regions of interest, in anesthetized dogs presented with binocular stimuli and in the same dogs presented with monocular stimuli.
3. To compare the two quantitative measures of image quality in the right and left halves of each region of interest during monocular stimulus presentations.

2.3 THE OPTIMAL ANESTHETIC

Like all neuroimaging techniques, fMRI is very sensitive to subject movement[9] so clearly anesthesia will be required if canine subjects are to be scanned. Anesthesia is known to affect, mostly in an inhibitory fashion, neural activity in the brain as well as cerebral blood flow and cerebral blood oxygenation.[10] It follows that images obtained from anesthetized dogs will likely involve weaker signals than those obtained from awake subjects. Understanding anesthetic effects on fMRI will permit us to better interpret data obtained during canine imaging. To date anesthesia has rarely been used with fMRI because cooperative human patients can remain still throughout the procedure. Accordingly, the present study could also be relevant to imaging work with non-cooperative human patients, like small children or adults suffering mental illness.

The goals of this study with respect to anesthesia were twofold:

1. To obtain fMR images from dogs anesthetized with 3 clinically common and safe anesthetic agents representing three different categories of anesthesia: a) the inhalent agent, isoflurane; b) the non-opioid intravenous agent, propofol; and c) the opioid agent fentanyl given in intravenous combination with the non-opioid midazolam.
2. To compare quantitative measures of image quality (i.e. amount of signal change and size of activated regions) within anatomic brain regions of interest known to play a role in vision in other animals (and assumed to in dogs), specifically the lateral geniculate nucleus in the thalamus and the occipital lobe of the cerebral cortex.

2.4 REFERENCES

1. Myers LJ. Use of innate behaviors to evaluate sensory function in the dog. *Veterinary Clinics of North America: Small Animal Practice* 1991; **21**: 289-299.

2. Odom JV, Bromberg NM, Dawson WW. Canine visual acuity: retinal and cortical field potentials evoked by pattern stimulation. *American Journal of Physiology* 1983; **14**: R637-R641.

3. Tootell RBH, Mendola JD, Hadjikani NK, Ledden PJ, Liu AK, Reppas JB, Sereno MI, Dale AM. Functional analysis of V3A and related areas in human visual cortex. *Journal of Neuroscience* 1997; **17**: 7060-7078.

4. Steffanacci L, Reber P, Costanza J, Wong E, Buxton R, Zola S, Squire L, and Albright T. fMRI of monkey visual cortex. *Neuron* 1998; 20:1051-1057.

5. Jezzard P, Rauschecker JP, Malonek D. An *in vivo* model for functional MRI in cat visual cortex. *Magnetic Resonance in Medicine* 1997; **38**: 699-705.

6. Ogawa S, Tank DW, Menon R, Ellerman JM, Kim S Merkle H Ugurbil K. Intrinsic signal changes accompanying sensory stimulation: Functional brain mapping with magnetic resonance imaging. *Proceedings of the National Academy of Sciences* USA 1992; **89**: 5951-5955.

7. Menon RS, Gati JS, Bradley G, Goodyear G, Luknowsky DC, Thomas CG. Spatial and temporal resolution of functional magnetic resonance imaging. *Biochemistry and Cell Biology* 1998; **76**: 560-571.

8. DeLahunta AD. *Veterinary Neuroanatomy and Clinical Neurology 2nd edn.* WB Saunders Company: Philadelphia, 1983.

9. Ellerman J, Garwood M, Hendrich K, Hinke R, Hu X, Kim S, Menon R, Merkle H, Ogawa S, Ugurbil K. Functional imaging of the brain by nuclear magnetic resonance. In: *NMR in Physiology and Biomedicine* (ed. Gillies RJ). Academic Press: San Diego, 1994; 137-150.

10 . Smith DS, Fisher SM. Neuroanesthesia and neurologic diseases. In: *Dripps, Eckenhoff, Vandam Introduction to Anesthesia* (ed. Longnecker DE, Murphy FL). WB Saunders Philadelphia, 1992; 382-395.

CHAPTER THREE

FUNCTIONAL MRI ACTIVITY IN THE THALAMUS AND OCCIPITAL CORTEX OF ANESTHETIZED DOGS INDUCED BY MONOCULAR AND BINOCULAR STIMULATION.

3.1 ABSTRACT

The neuroanatomy of the mammalian visual system has received considerable attention through electrophysiological study of cats and non-human primates, and through neuroimaging of humans. Canine functional neuroanatomy, however, has received much less attention, limiting our understanding of canine vision and the visual pathways. As an early step in the application of blood oxygenation level dependant (BOLD) functional magnetic resonance imaging (fMRI) for veterinary use, a comparison of visual activity in the thalamus and occipital cortex of anesthetized dogs presented with binocular and monocular visual stimuli was carried out. Activity in the left and right thalamus and occipital cortex during monocular stimulation was also compared. Six beagles were presented with a vertical grating visual stimulus and scanned at 4 Tesla. Each dog was scanned twice under each of 3 anesthetic protocols (isoflurane, propofol, and fentanyl / midazolam). We found: 1. significant BOLD activation in the lateral geniculate nucleus (LGN) of the thalamus and the occipital cortex; 2. a significantly larger area of activation in the LGN during monocular stimulation than during binocular stimulation; and 3. that activity in the hemisphere contralateral to the stimulus was not significantly greater than that ipsilateral to it.

3.2 INTRODUCTION

The functional neuroanatomy of the mammalian visual system has received considerable attention since the ground breaking electrophysiological studies of Hubel and Weisel.[1,2] Their work recording intracellular and extracellular neural activity in cats and monkeys is the basis for our understanding of the functional architecture of visual brain areas, especially with respect to the retinotopic organization of receptive fields and the processing of form and movement. More recently, interest in directly addressing human visual processing, combined with waning acceptance of relatively invasive research techniques, has motivated the development of neuroimaging methods. The most recent and powerful of these is blood oxygenation level dependant (BOLD) functional magnetic resonance imaging (fMRI). Blood oxygenation level dependant fMRI depicts neural activity in the brain in real time with extremely high spatial resolution.[3] The technique has permitted researchers to address questions regarding human visual processing and has confirmed that many of the patterns reported by researchers like Hubel and Weisel for other mammals are preserved in humans.[3,4] Recent work confirming that reliable and reproducible images can be obtained from animals under general anesthesia[5,6,7] suggests there is considerable potential for research and clinical use of fMRI in veterinary neurology and ophthalmology.

Blood oxygenation level dependant fMRI depends on the principle that increased activity in cerebral cortex leads to an increase in metabolic activity[8] and blood flow[9,10] localized to the site of activity. The increase in flow exceeds the metabolic increase and the rate of oxygen extraction from the cerebral microvasculature, which produces an increase in the ratio of oxygenated : deoxygenated hemoglobin.[11,12] Deoxyhemoglobin causes attenuation of magnetic resonance signal.[13] An increased oxy : deoxyhemoglobin ratio therefore results in a signal increase corresponding to areas of neural activity, called the BOLD effect, in appropriately weighted MR images.[14,15] To

detect the BOLD effect, acquired images of the brain are divided into equal sized discrete volume elements, or voxels. Data acquired during a control phase and a stimulus presentation phase are compared within each voxel. Those in which a significant change in BOLD signal occurs are superimposed on a corresponding anatomic MR image.[4]

The functional neuroanatomy of cat and non-human primate vision has received more attention in the literature than that of the dog but some notable studies have addressed canine visual processing. Visual evoked potentials (VEPs) have been used to investigate early postretinal visual activity, presumably in the thalamus and early visual cortices.[16] One limitation of VEP, however, is the scarcity of reference information on canine cortical functional anatomy to use when positioning VEP electrodes. Ofri et al. began resolving this issue using electrode recording to map the area of central vision (area centralis) in dogs.[17] This area overlaps with the boundary of primary and secondary visual cortex in mammals and is a primary target of VEP recording.[18] They localized area centralis near the medial border of the posterior occipital lobe at the junction of the marginal and endomarginal gyri. These results are consistent with findings in other mammals and may provide a starting point for comparison with fMRI results.

The long term goal of our research is the development of BOLD fMRI as a means to assess canine vision. In the present study, anesthetized dogs were presented with binocular and monocular visual stimulation and scanned to address the questions: 1) Can reliable, anatomical patterns of BOLD activity be obtained from the brains of anesthetized dogs; 2) Do patterns of neural activity in relevant brain regions differ between monocular and binocular stimulation; and 3) Does neural activity differ in the left and right halves of relevant brain regions during monocular stimulation?

3.3 METHODS

3.3.1 Animals

Six purpose bred beagles (1 male, 5 female; mean mass 9.75 ± 0.88 (± 1 SD) kg) were obtained from the University of Guelph Central Animal Facility, Guelph, Ontario, Canada and were transported to the Animal Care and Veterinary Services facilities at the University of Western Ontario, London, Ontario where they were housed during the experimental period. Each dog underwent a rigorous ophthalmic examination, including slit lamp biomicroscopy, indirect ophthalmoscopy, applanation tonometry and streak retinoscopy, prior to being included in the study. Dogs were fasted for 12 hours prior to each experiment but permitted free access to water. All procedures met with the approval of both the University of Western Ontario Council on Animal Care and the University of Guelph Animal Care Committee.

3.3.2 Imaging

A Siemens Varians 4 Tesla Whole Body Magnetic Resonance Scanner housed at the Robart's Research Institute at the University of Western Ontario was used for all experiments. The visual stimulus was a 20 cm by 20 cm vertical grating pattern with 10 black and 10 white bars that alternated position at 5 Hz, and was back-projected from a digital projector (NEC Corporation model MT800, Tokyo, Japan) onto a screen 60 cm from the subject's eyes. Dogs' eyelids were held open using non-magnetic, insulated copper speculae. Surgical tape was used during monocular experiments to hold the left eyelid closed. Due to limited time available for individual imaging sessions only right eye monocular stimulation was performed. To prevent corneal dehydration, an elastoviscous, clear corneal shield (Hylashields Nite®, i-med Pharma Inc., Pointe-Claire, Quebec) was applied to each eye immediately prior to speculum insertion.

Functional MRI experiments consisted of 10 alternating 9 s periods of stimulus activation followed by corresponding 30 s periods of inactivation. This sequential task

activation paradigm permits data obtained during the rest state and activation state to be averaged. This provides a mean baseline signal strength and a mean activation signal strength for comparison, increases the statistical power of voxel by voxel comparison, and improves signal to noise ratio.[13] Experiments were first performed with both eyes open and then performed again with the left eye taped closed.

For each experiment, 4 shot (i.e. spatial encoding of single slice data was achieved using 4 identical pulse sequences), echo-planar, T2*-weighted whole brain magnetic resonance images depicting BOLD contrast were obtained with a radio-frequency (RF) knee coil for RF transmission and reception. The functional images were obtained in contiguous dorsal sections with echo time (TE) = 15 ms, repetition time (TR) = 750 ms, flip angle = 60°, 64 x 64 matrix, field of view (FOV) =12.8 cm (2 mm in-plane resolution), and slice thickness = 2 mm. Immediately following binocular experiments, and immediately prior to monocular experiments, 3D magnetization-prepared Turbo FLASH (Fast Low Angle Shot) T1-weighted anatomical images of each dog brain were acquired with TE = 6.5 ms, TR = 12.4 ms, flip angle = 11°, and inversion time = 500ms. Anatomical volumes were acquired in the same FOV as, and in register with, the functional images so that functional data could be superimposed on anatomic images. Head movement was restricted using foam padding within the RF knee coil.

The analysis software Stimulate was used for image processing.[18] Cross correlation analysis was used for voxel by voxel comparison which permitted the reference function, to which the time course of BOLD signal was compared, to shift. This accommodated hemodynamic delays between neural activity and factors underlying the BOLD effect. Statistical significance for the cross-correlation was set initially at $p < 0.10$ and improved to $p < 0.05$ by restricting significance to clusters with a minimum size of 3 significant voxels.[19] These voxel clusters were then superimposed onto the T1-weighted anatomic images.

Once image processing was complete, regions which included the lateral geniculate nucleus (LGN) of the thalamus and the occipital cortex were identified on each image and these areas were used as specific regions of interest (ROI) for further analysis. In all dogs, the LGN region consisted of 2 bilateral rectangular volumes, as symetrical as possible, transecting 5 dorsal slices at the level of the thalamus in the diencephalon (see Figure 3.1). Within each slice, boundaries of the 2 sections of this ROI were placed as equidistant as possible laterally from the third ventricle and medially from the lateral ventricles. The occipital ROI was a larger rectangular volume beginning in the first dorsal slice where the cerebellum could no longer be observed and proceeding dorsally through 7 slices. Within each slice, the caudal boundary for this ROI was placed at the occipital pole and the rostral boundary was placed just caudal to the pseudosylvian fissure. For comparisons of activity in the left and right hemispheres of the brain, each ROI was divided along the longitudinal fissure into left and right halves. For each ROI and half-ROI, the number of significant voxels was determined as a percentage of the total number of voxels within the ROI. The mean percentage signal change (between the control and activation states) was also calculated. These measures were used for further analysis.

3.3.3 Anesthesia

Binocular and monocular fMRI experiments were performed on all 6 dogs anesthetized under each of 3 different anesthetic protocols: 1) the inhalant, isoflurane (AErrane®, Janssen, North York, Ontario); 2) the non-opioid intravenous agent, propofol (Rapinovet®, Schering Plough Animal Health, Point-Claire, Quebec); and 3) a combination of the opioid intravenous agent, fentanyl (Abbott Laboratories Ltd., Toronto, Ontario), and non-opioid, midazolam (Versed®, Hoffman La Roche Ltd. Mississauga, Ontario). The results of comparisons between binocular results under the 3 anesthetics are reported elsewhere.[7] To avoid data loss resulting from movement artifacts, and to

facilitate comparison of results within dogs, each dog was scanned twice under each agent for a total of 36 experimental sessions. The order of anesthetic agent used for each dog was chosen randomly. At least 72 hours passed between experimental sessions on any dog to minimize carry-over effects. Prior to each experimental session mydriasis was achieved using 0.5% tropicamide drops (Diotrope®, Dioptic Laboratories, Markham, Ontario), dogs were premedicated with 0.01 mg/kg glycopyrolate (Sabex Inc., Boucherville, Quebec), intramuscularly, and a 20 gauge cephalic catheter was placed for fluid administration.

Target doses of each agent known to maintain a relatively light, comparable and stable depth of general anesthesia were selected.[20] Bolus induction was used for the I.V. regimes (propofol, 4-6 mg/kg; fentanyl / midazolam, 10-20 ug/kg and 0.5 mg/kg, respectively) and mask induction for isoflurane. Once anesthetized, dogs were intubated, transported a short distance to the MR scanning room, and placed on 100% oxygen, or oxygen and isoflurane. A neuromuscular block was produced using atracurium besylate (Sabex Inc., Boucherville, Quebec) at 0.3 mg/kg I.V. This minimized muscle movement and facilitated central fixation of a relaxed eye. Intermittent positive pressure ventilation was employed using a volume limited ventilator (Airshields® Ventimeter®, Air-Shields Inc., Hatboro, Pennsylvania) with a respiratory frequency of 10 breaths per minute and a tidal volume of 15 ml/kg.

A constant drip infusion was used for anesthetic maintenance with the I.V. agents (propofol, 0.4 mg/kg/min; fentanyl / midazolam 0.80 ug/kg/min and 8.0 ug/kg/min, respectively), administered via a microdrip (Baxter Corporation, Toronto, Ontario) from a pre-loaded volume limiting system (Buretrol®, Baxter Corporation, Toronto, Ontario). Actual infusion doses were calculated by dividing the volume of infusion used during an imaging session by the total time of the session. Intravenous anesthetics were diluted

with saline (anesthetic:saline, 1:3) to facilitate more accurate infusion and to simultaneously achieve fluid replacement through the same venous access. Inhalant anesthesia (1.6% end-tidal, expired isoflurane) was maintained using a precision vaporizer (Forane®, Cyprane Ltd., Keighley Yorkshire, England) and a modified Bain breathing system at a fresh gas flow sufficient to prevent rebreathing(150 ml/kg). The Bain system was modified by extending both the inlet and exhaust tubing to 10 m. Dogs were maintained on a 0.9% NaCl infusion (Baxter Corporation, Toronto, Ontario) at 5 ml/kg/hr during isoflurane anesthesia. Experiments in which actual induction or infusion doses exceeded the mean of all doses ± 2 standard deviations were excluded from further analyses.

A gas monitor (Criticare Poet® IQ, Criticare Systems Inc., Waukesha, Wisconsin) was used to monitor inspired and end-tidal, expired CO_2 and O_2 levels during all experiments, as well as inspired and end-tidal, expired isoflurane during isoflurane experiments. These factors were recorded for the 10 min immediately prior to a scanning session as well as immediately following a session. Unfortunately, they could not be monitored throughout scanning sessions because the powerful magnetic field surrounding the scanner prohibited any metal containing equipment from being placed within a 10 m radius. This distance exceeded the sampling capabilities of the anesthetic monitor. Heart rate and oxygen saturation were monitored throughout each session using a pulse oximeter (Nonin Medical Inc. model 8600FO, Minneapolis, Minnesota) and fibre-optic cable. Each animal was covered with a blanket while anesthetized to maintain body temperature and prevent hypothermia.

3.3.4 Statistical Analysis

Comparisons of percentage signal change and number of significant voxels as a percentage of ROI size between binocular and monocular experiments, and between the left and right halves of each ROI during monocular experiments, were based on a split

plot design[21] within the Randomized Complete Blocks Design (RCBD).[21] The SAS systems general linear models procedure (Proc GLM)[22] was used to detect trial by anesthetic treatment effects on the differences between monocular and binocular activity and between left and right brain activity. If a significant trial by treatment interaction was not detected the difference between binocular minus monocular data and zero, and between left brain minus right brain data and zero from both ROIs was tested for significance using Proc GLM. This model averaged results from trials 1 and 2 for each dog. If a significant trial by anesthetic treatment effect was detected, then SAS Proc Mixed[23] was used to test whether differences varied from zero between trials and anesthetic agents separately. Significance for all tests was assessed at $p < 0.05$.

3.4 RESULTS

Comparisons of the effects of the 3 anesthetic agents on BOLD imaging with binocular stimulation, and the infusion doses of the 3 anesthetic agents are reported elsewhere.[7] The results below were obtained from the same dogs during the same sessions. Six of 36 experimental sessions were excluded from analysis; 5 due to motion artifacts and 1 because anesthetic infusion dose exceeded the pre-determined exclusion criterion of the mean $\pm$ 2 SD.

Representative images obtained during binocular and monocular stimulation and corresponding time courses of BOLD activity from the LGN are presented in Figure 3.1. The LGN and a large area of occipital cortex were the focus of further analysis since significant voxels were reliably recorded in both of these regions, and because both areas have a known visual function in other mammals. The few significant voxels observed outside of the 2 ROIs were excluded from further analysis because we could not confirm whether their significance was visual in origin or reflective of oscillatory activity unrelated to vision.

The interactive effects of trial and anesthetic agent on the difference between both quantitative measures of BOLD activity in both ROIs between the right eye and binocular stimulation are shown in Table 3.1. Anesthetic agent and trial had a significant interactive effect on the difference between mean percentage signal change in the LGN region obtained during binocular and right eye stimulus presentations, so SAS Proc Mixed[23] was used to compare differences in this category between binocular and monocular stimulation. In the other three categories no significant anesthetic / trial interactions occurred so Proc GLM[22] was used to compare data obtained during binocular and right eye stimulation.

Comparisons of the differences between results of binocular and monocular stimulation for both measures of BOLD activity in both ROIs are presented in Figure 3.2. A significant difference in the percentage of significant voxels in the LGN region was detected between binocular and right eye stimulus presentations ($F = 6.14$, $p = 0.01$, $df = 7$). No other significant differences were detected.

Images obtained during stimulus presentations to the right eye alone were analyzed also using the procedure described above. After ROIs were divided along the longitudinal fissure, data collected from the left and right halves of the brain were compared. Results of Proc GLM testing for effects of anesthetic agent / trial interactions on differences between activity in left and right halves of each ROI are summarized in Table 3.2. No significant anesthetic / trial interactions were detected so Proc GLM was used to compare both the mean percentage signal change, and number of significant voxels as a percentage of ROI size between left and right halves of both ROIs (Figure 3.3). There were no significant differences in either variable between the left and right halves of either ROI. Individual animal BOLD signal data are presented in Appendices I-III.

3.4 DISCUSSION

This study is the first to investigate functional neuroanatomy in the canine visual system using fMRI. Brain activity was recorded in anesthetized dogs presented with a visual stimulus when both eyes were open and when the left eye was covered. In both cases, neural activity was reliably elicited in the LGN of the thalamus and the occipital cortex. This supports the widely accepted assumption that these areas play a role in visual processing in dogs, as they do in humans,[24] cats,[25,26] and non-human primates.[27] Our results also support the work of Ofri et al. who localized the area of central vision in dogs to a region near the medial border of the posterior occipital lobe.[17] The two regions of interest (LGN and occipital cortex) were selected for further analysis because of their known visual function in other animals combined with the reliability of responses in these regions in the present study.

There were no obvious qualitative differences between images or time courses of activity obtained during monocular and binocular stimulation. A significant trial by anesthetic treatment effect was detected for only 1 of 4 monocular versus binocular comparisons. In that instance, data were separated in terms of trial and anesthetic group by using SAS Proc Mixed for analysis. Although not obvious from boxplots of their respective distributions, under the 3 anesthetic agents used, the size of activated area relative to ROI size was significantly greater during monocular stimulation than during binocular in the LGN region. In addition, percentage signal change was not different between monocular and binocular stimulation in the LGN and neither measure differed in the occipital ROI. These results are surprising because ROIs included both right and left halves for comparison of monocular and binocular experiments. During monocular stimulation fewer nerve fibres propagate activity to the LGN because 1 of 2 optic nerves does not receive stimulus dependant activity from the covered retina. It might therefore be expected that less total, bilateral activity would occur during monocular presentations.

Instead, in the present study, either a slightly larger bilateral area was significantly active or there was no difference in activity. An explanation for this unexpected result could involve problems with precise control of anesthesia during fMRI, as reported elsewhere.[7] Due to our relatively small sample size results may have been vulnerable to variation associated with inconsistencies in anesthetic dose.

Properties of the visual stimulus and the visual system could also account for the absence of greater BOLD activity during binocular as opposed to monocular stimulation. If the stimulus was intense enough to saturate visual processing at the level of the LGN during monocular presentations, then adding the activity of nerve fibres from the second optic nerve during binocular stimulation would not increase activity in the LGN. Experiments addressing the dependance of visual activity on stimulus properties in anesthetized dogs as measured by BOLD imaging should be one priority of future research.

Another unexpected finding of this study involved comparisons between activity in the left and right halves of each ROI, in light of widely accepted assumptions regarding axon decussation at the optic chiasm. It has been estimated that 75% of optic tract fibres decussate at the chiasm on route to the LGN in dogs, compared with 65% in cats and 50% in humans.[25] If this estimate is accurate then during monocular stimulus presentations we would expect both a stronger signal and a larger area of neural activity in the contralateral half of the LGN region than in the ipsilateral half. If only 1 eye and 1 optic nerve is stimulated, and if 75% of the fibres in this optic nerve decussate, then activity should be more pronounced contralateral to the stimulated eye. In the present study, however, there was no significant difference between either mean percentage signal change, or the percentage of significant voxels per ROI in the left and right LGN when only the right eye was open. Conceivably, this result may reflect a statistical error arising from violation of equal variance assumptions and inconsistencies in anesthetic

dose. We did test for anesthetic effects on differences between left and right halves of both ROIs, and found no significant effects; nevertheless, given the relatively small sample size, the analysis may have been vulnerable to variance effects.

An alternative explanation could involve the ROI selection method employed in this study, specifically with respect to subtle variation in the sizes of right and left halves of the LGN ROI. In most human fMRI studies, image data are compared to a standardized reference brain based on the Talairach coordinate system, permitting precise ROI localization.[28] A canine brain coordinate system is not available. Regions of interest were drawn as individual rectangles on a computer screen, creating subtle variation in size between ROIs in the left and right halves of the brain. To incorporate ROI size differences into the analysis and minimize the impact of this variation, the number of significant voxels per ROI as a percentage of ROI size was calculated. If the relative size of the left ROI varied considerably more than the number of significant voxels within it, as compared to the right LGN ROI, however, the ability to detect statistical differences between activity ipsilateral and contralateral to the stimulated eye could have been reduced.

A plausible neuroanatomic explanation for this unexpected finding also exists, however, in that the degree of decussation at the optic chiasm in dogs may be overestimated in the literature. In other words, a greater proportion of optic tract fibres might innervate ipsilateral LGN in dogs than has previously been supposed. Animals like fish and some birds, for whom predator detection and avoidance has been an important evolutionary consideration, tend to have a lateral eye position and almost complete or at least substantial decussation at the optic chiasm.[25] Predatory animals, like cats and especially primates, on the other hand, tend to have more frontally fixated eyes and less cross-over at the chiasm: between 65 and 50%.[25,29] In the absence of direct data on dogs, then, it is possible that the estimate of 75% is excessive, given that dogs have

clearly evolved as predators and that eye position in most breeds is fixated more frontally than laterally. Further study addressing brain activity during monocular stimulus presentations with larger sample sizes would help resolve this question.

The issue of inter-specific neuroanatomic variation raises another interesting issue. Human involvement in canine evolutionary development has produced enormous intra-specific variation in dogs for any number of genetic traits. Few species on earth exhibit a size range as large as that between Great Dane to Shi-Tsu, for example. Based on the wide range of functions for which dogs have been bred, it is logical to assume that neuroanatomic differences also exist. Ofri et al. compared the location of area centralis in the occipital cortices of sight hounds (greyhounds) and scent hounds (beagles) and did detect a significant difference in its location along the anterior-posterior axis.[17] Other differences in the visual systems of dog breeds have also been noted. The visual streak of the retina (analogous to the fovea in humans), for example, varies considerably between wolf-like breeds, with an elongate streak adapted for scanning the horizon and beagles, with a more diffuse, ovoid visual streak.[30] This variation suggests that fMRI results may differ between dog breeds. Comparative studies of different breeds would be an especially interesting area for future fMRI research in dogs.

Functional MR images can be recorded from anesthetized dogs presented with both binocular and monocular visual stimuli. Surprisingly, quantitative measures of BOLD activity were not significantly greater during binocular than monocular stimulus presentations. In fact, a significantly larger region within the LGN ROI was activated during monocular stimulation. Significant differences between the left and right halves of LGN and occipital cortex during monocular stimulation were also not observed. Both of these results are unexpected, based on widely held assumptions about the canine visual

system, and further support the potential of fMRI to address research questions in veterinary neurology and ophthalmology.

3.6 REFERENCES

1. Hubel DH, Weisel TN. Receptive fields, binocular interaction and functional architecture in the cat's visual cortex. *Journal of Physiology* 1962; **160**:106-154.

2. Hubel DH, Weisel TN. Receptive fields and functional architecture of monkey striate cortex. *Journal of Physiology* 1968; **195**: 215-243.

3. Tootell RBH, Mendola JD, Hadjikani NK, Ledden PJ, Liu AK, Reppas JB, Sereno MI, Dale AM. Functional analysis of V3A and related areas in human visual cortex. *Journal of Neuroscience* 1997; **17**: 7060-7078.

4. Menon RS, Ogawa S, Strupp JP, Ugurbil K. Ocular dominance in human V1 demonstrated by functional magnetic resonance imaging. *Journal of Neurophysiology* 1997; **77**: 2780-2787.

5. Jezzard P, Rauschecker JP, Malonek D. An *in vivo* model of functional MRI in cat visual cortex. *Magnetic Resonance in Medicine* 1997; **38**: 699-705.

6. Lahti KM, Ferris CF, Li F, Sotak CH, King JA. Comparison of evoked cortical activity in concious and propofol anesthetized rats using functional MRI. *Magnetic Resonance in Medicine* 1998; **41**: 412-416.

7. Willis C, Quinn R, McDonell W, Gati J, et al, Functional MRI as a tool to assess vision in dogs: The optimal anesthetic. Veterinary Ophthalmology, submitted (Chapter 4, this thesis).

8. Pritchard J, Rothman D, Novotny E, Petroff O, Kuwabura T, Avison M, Houseman A, Hanstock C, Shulman R. Lactate rise detected by 1H NMR in human visual cortex during physiologic stimulation. *Proceeding of the National Academy of Sciences USA* 1991. **88**: 5829-5831.

9. Fox PT, Raichle ME. Focal physiological uncoupling of cerebral blood flow and oxidative metabolism during somatosensory stimulation in human subjects. *Proceeding of the National Academy of Sciences USA* 1986, **83**: 1140-1144.

10. Belliveau JW, Kennedy DN, McKintry RC, Buchbinder BR, Weisskoff RM, Cohen MS, Vevea JM, Brady TJ, Rosen BR. Functional mapping of the human visual cortex by magnetic resonance imaging. *Science* 1991; **254**: 716-719.

11. Bandettini PA, Wong EC, Hinks RS, Tifofsky RS, Hyde JS. Time course EPI of human brain function during task activation. *Magnetic Resonance in Medicine* 1992 **25**: 390-397.

12. Kwong KK, Belliveau JW, Chesler DA, Goldberg IE, Weisskoff RM, Poncelet BP, Kennedy DN, Hoppel BE, Cohen MS, Turner R, Cheng H, Brady TJ, Rosen BR. Dynamic resonance imaging of human brain activity during primary sensory stimulation. *Proceedings of the National Academy of Sciences* USA 1992; **89**: 5675-5679.

13. Villringer A, Rosen BR, Belliveau JW, Ackerman JL, Lauffer RB, Buxton RB, Chao YS, Wedeen VJ, Brady TJ. Dynamic imaging with lanthanide chelates in normal brain: contrast due to susceptibility effects. *Magnetic Resonance in Medicine* 1988; **6**: 164-174.

14. Ogawa S, Lee TM. Magnetic resonance imaging of blood vessels at high fields: In Vivo and in vitro measurements and image simulation. *Magnetic Resonance in Medicine* 1990; **16**: 9-18.

15. Ogawa S, Tank DW, Menon R, Ellerman JM, Kim S Merkle H Ugurbil K. Intrinsic signal changes accompanying sensory stimulation: Functional brain mapping with magnetic resonance imaging. *Proceedings of the National Academy of Sciences* USA 1992; **89**: 5951-5955.

16. Strain GM, Jackson RM, Tedford BL. Visual evoked potentials in the clinically normal dog. *Journal of Veterinary Internal Medicine* 1990; **4**: 222-225.

17. Ofri R, Dawson WW, Samuelson DA. Mapping of the cortical area of central vision in dogs. *Progress in Comparative and Veterinary Ophthalmology* 1994; 4: 172-178.

18. Strupp JP. A GUI based fMRI analysis software package. *Neuroimage* 1996; **3**: 5607.

19. Forman SD, Cohen JD, Fitzgerald M, Eddy WF, Mintum MA, Noll DC. Improved assessment of significant activation in functional magnetic resonance imaging (fMRI): Use of a cluster-size threshold. *Magnetic Resonance in Medicine* 1995; **33**: 636-647.

20. Thurmon JC, Tranquill WJ, Benson GJ. *Lumb and Jones' Veterinary Anesthesia*. Williams and Wilkins, Baltimore, 1996.

21 Snedecor GW, Cochran WC. *Statistical Methods*. 8th edn, Iowa State University Press: Iowa, 1989.

22. SAS Institute Inc. *SAS/STAT User's Guide Version 6*. 4th edn, SAS Institute Inc.: Cary NC, 1989.

23. SAS Institute Inc. *SAS/STAT Software: Changes and enhancements through release 6.12*. SAS Institute Inc.: Cary NC, 1997.

24. Reichert H. *Introduction to Neurobiology*. Georg Thieme Verlag; Stuttgart, 1992.

25. De Lahunta A. *Veterinary Neuroanatomy and Clinical Neurology* 2nd edn. WB Saunders: Philadelphia; 1983.

26. Hubel DH, Weisel TH. Receptive field's of single neurons in cat's striate cortex. *Journal of Physiology* 1959; **148**: 574-591.

27. Hubel DH, Weisel TH. Anatomical demonstration of orientation columns in macaque monkey. *Journal of Comparative Neurology 1978*; **177**: 361-380.

28. Talairach J, Tournoux P. *Co-Planar Stereotactic Atlas of the Human Brain*. Georg Thieme Verlag, Stuttgart, 1988.

29. Herron MA, Martin JE, Joyce JR. Quantitative study of the decussating optic axons in the pony, cow, sheep and pig. *American Journal of Veterinary Research* 1978; **39**: 1137-1145.

30. Piechl L. Topography of ganglion cells in the dog and wolf retina. *Journal of Comparative Neurology* 1992 **324**: 603-620.

Table 3.1 Evaluation of interactive effects of trial by anesthetic treatment on the differences in BOLD fMR signal obtained during monocular and binocular stimulus presentations. Two measures of the signal (mean percentage signal change, PSC; and percentage of significant voxels per ROI, SVX) were assessed in 2 regions of interest (lateral geniculate nucleus, LGN; and occipital cortex, OCC).[≠]

Variable	F	p
LGN PSC	4.53	0.05*
LGN SVX	1.05	0.39
OCC PSC	2.24	0.17
OCC SVX	0.02	0.98

[≠] Randomized complete blocks design, SAS general linear model procedure (Proc GLM)[22] to detect significant trial by anesthetic treatment effects with 2 degrees of freedom; n = 30. Significance shown by (*).

Table 3.2 Evaluation of interactive effects of trial by anesthetic treatment on the differences in BOLD fMR signal observed in the left and right brain hemispheres during monocular stimulus presentations. Two measures of the signal (mean percentage signal change, PSC; and percentage of significant voxels per ROI, SVX) were assessed in 2 regions of interest (lateral geniculate nucleus, LGN; and occipital cortex, OCC).[≠]

Variable	F	p
LGN PSC	1.58	0.29
LGN SVX	0.37	0.69
OCC PSC	0.46	0.65
OCC SVX	0.80	0.48

[≠] Randomized complete blocks design, SAS general linear model procedure (Proc GLM)[22] to detect significant trial by anesthetic treatment effects with 2 degrees of freedom; n = 30.

Figure 3.1 Blood Oxygenation Level Dependant (BOLD) Functional MR images in multiple dorsal sections (A, B) and corresponding BOLD signal time courses (C, D) from a dog anesthetized with fentanyl / midazolam and presented with a vertical grating visual stimulus with the left eye covered (A,C) and with both eyes open (B,D). All functional data were obtained using 4 shot echo-planar imaging weighted for T2*. Images were divided into discrete volume elements (voxels) in a 64 X 64 matrix with in plane resolution = 2 mm and slice thickness (i.e. between adjacent dorsal sections) = 2 mm. Within each voxel cross correlation was used to detect increases in BOLD signal linked to repeated periods of stimulus presentation. Voxels in which a significant increase in BOLD signal was detected were then superimposed on 3D magnetization prepared Turbo FLASH (Fast Low Angle Shot) anatomic images as coloured pixels. Bright yellow pixels represent those with the largest percentage signal change. A region of interest, which included the lateral geniculate nucleus of the thalamus, is outlined on 5 sections. The number of significant voxels as a percentage of total ROI size was used as one quantitative measure of image quality for further analysis and the mean percentage BOLD signal change was another quantitative measure. ROIs were always selected in the same slices and were as close in size as possible between experiments. Percentage signal changes were calculated by comparing baseline and activation BOLD signals based on the time courses of stimulus presentation (bottom traces in C and D).

A.

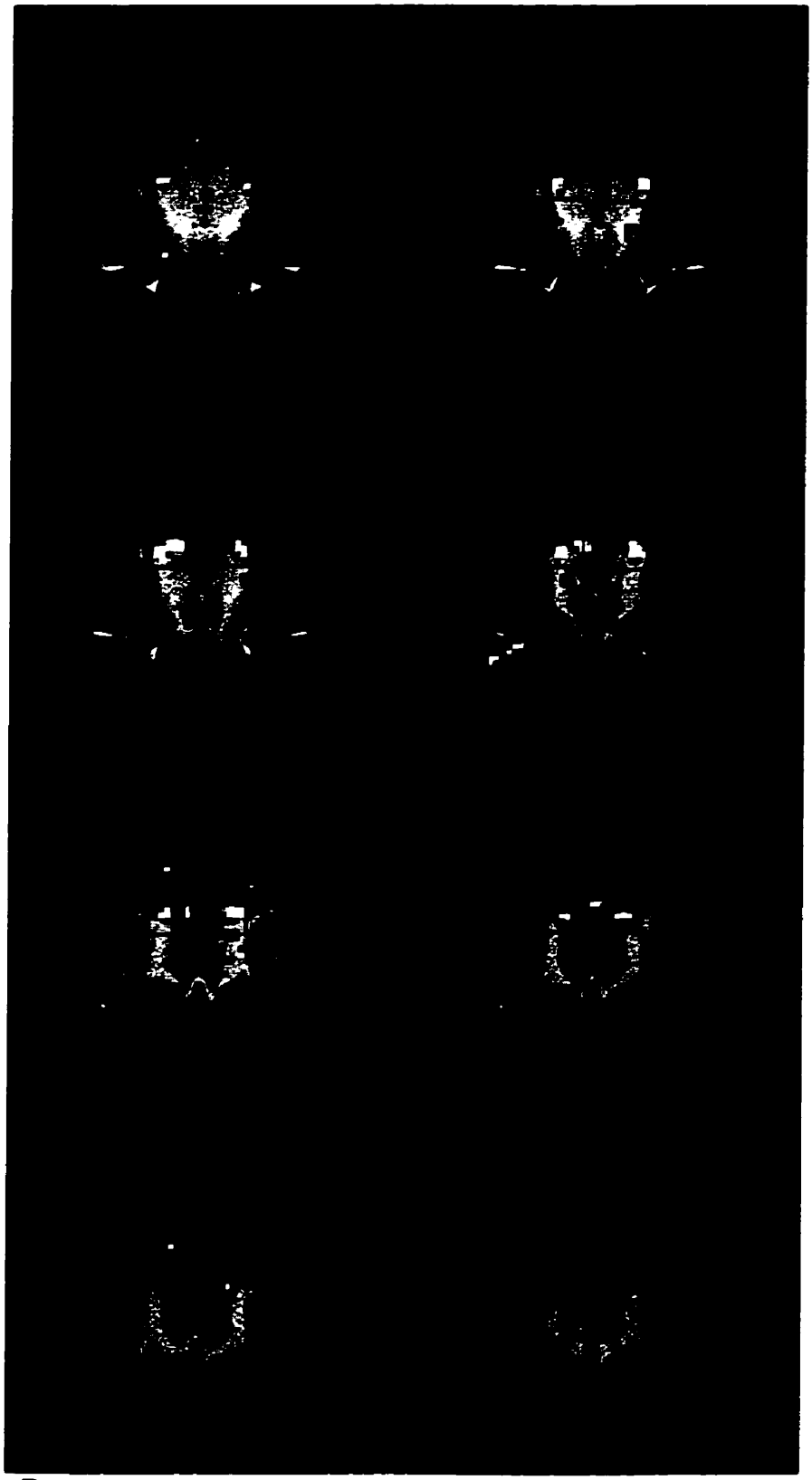

B.

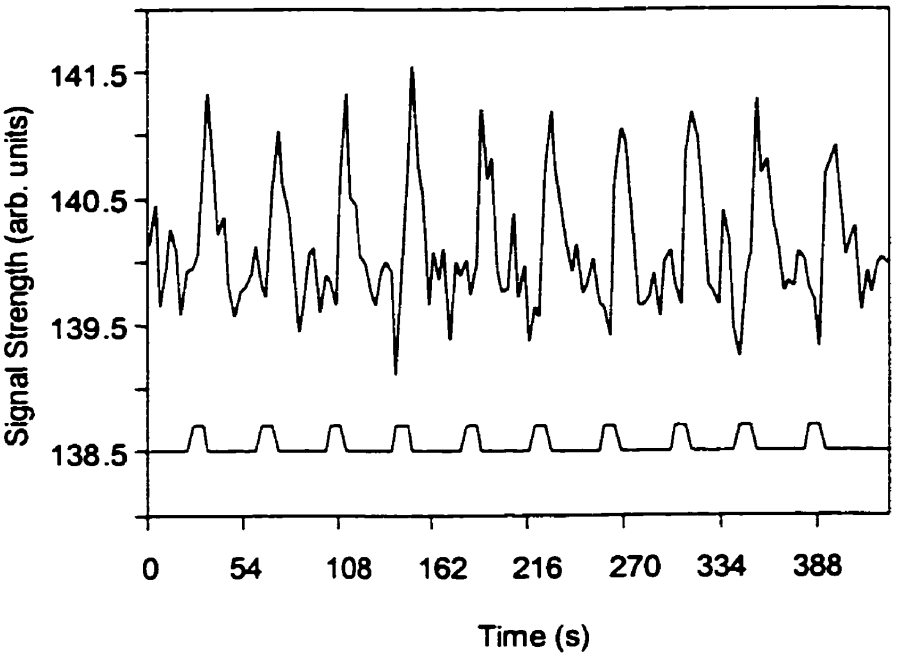

C (monocular)

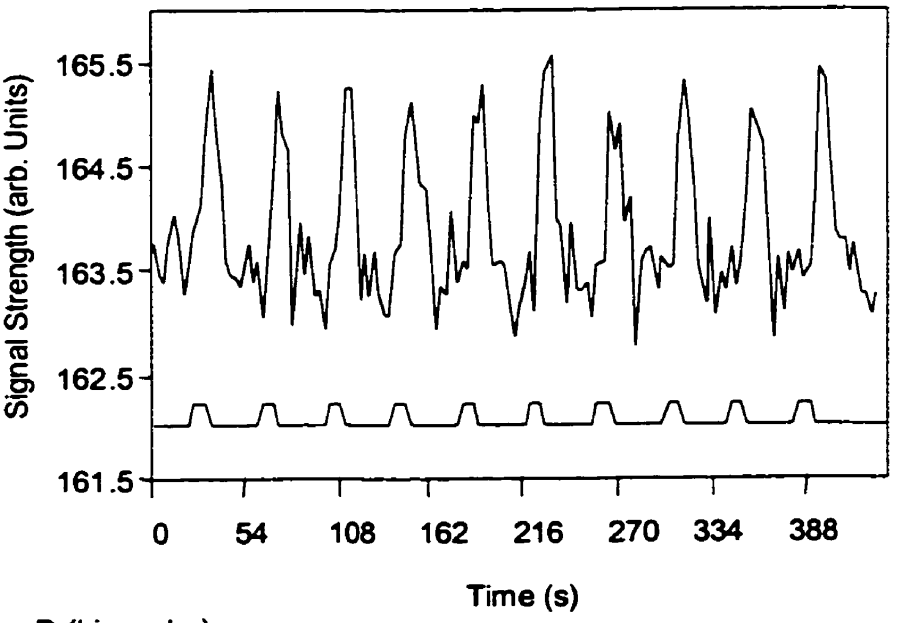

D (binocular)

Figure 3.2 Boxplots of data obtained during BOLD fMRI from 6 dogs anesthetized under each of 3 different anesthetic agents during binocular and monocular stimulus presentations. A) Mean percentage BOLD signal change in the lateral geniculate nucleus (LGN) region of interest. B) Number of significant voxels / ROI as a percentage of ROI size in the LGN region. C) Mean percentage signal change in the occipital lobe (OCC) region. D) Number of significant voxels as a percentage of ROI size in the OCC region. Analysis was performed using SAS Proc GLM[23] if no trial by anesthetic interaction was found on preliminary analysis (B, C, D), or using SAS Proc Mixed[24] if there was a significant interaction. A significant difference ($p < 0.05$) was found between activity during binocular and monocular stimulus presentations only for the number of significant voxels / ROI as a percentage of voxel size in the LGN region ($B\ F = 6.14$, $p = 0.01$, $df = 7$). For clarity, box plots for each anesthetic agent are presented, despite the fact that the anesthetic used had no effect on differences between activity induced by monocular and binocular stimulus presentations. Horizontal lines from top to bottom on each boxplot represent the 90th, 75th, median, 25th and 10th percentiles respectively. Dots represent data points outside this range.

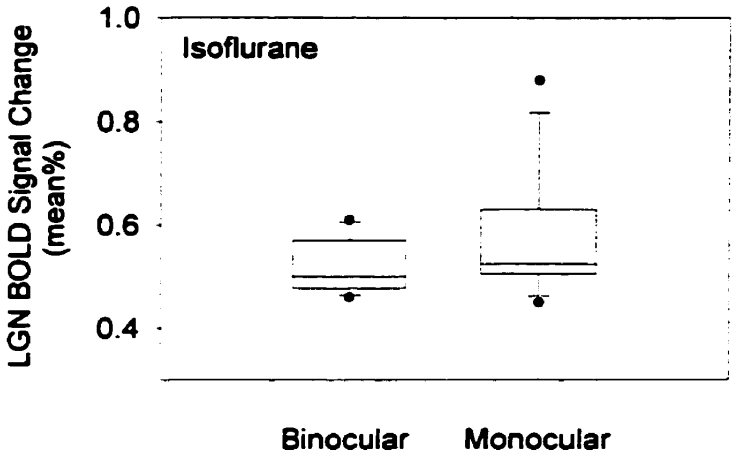
Isoflurane
LGN BOLD Signal Change (mean%)
1.0
0.8
0.6
0.4
Binocular
Monocular

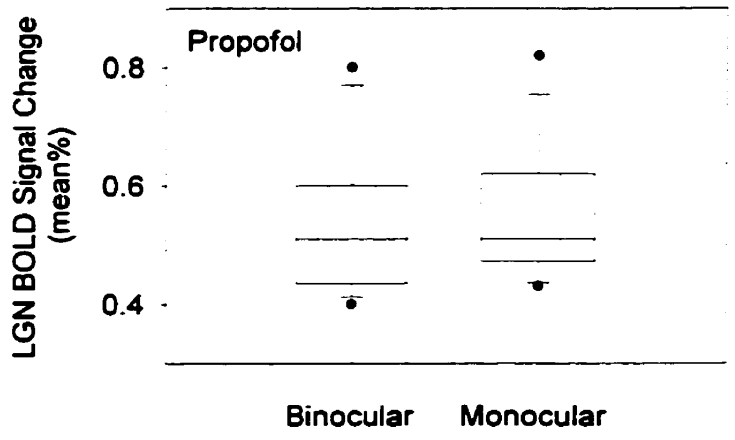
Propofol
LGN BOLD Signal Change (mean%)
0.8
0.6
0.4
Binocular
Monocular

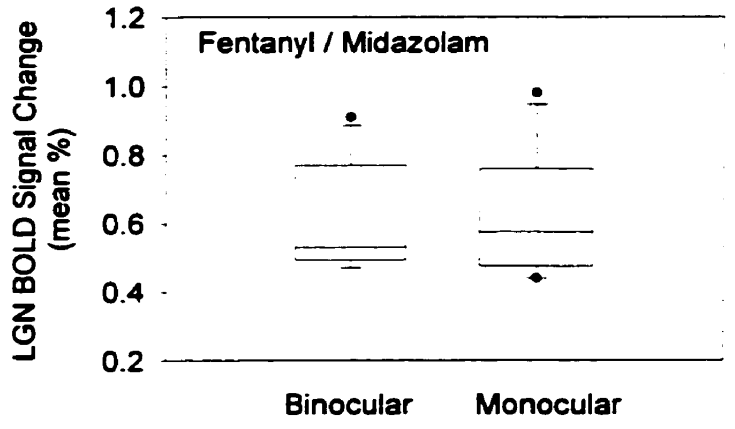
Fentanyl / Midazolam
LGN BOLD Signal Change (mean %)
1.2
1.0
0.8
0.6
0.4
0.2
Binocular
Monocular

A

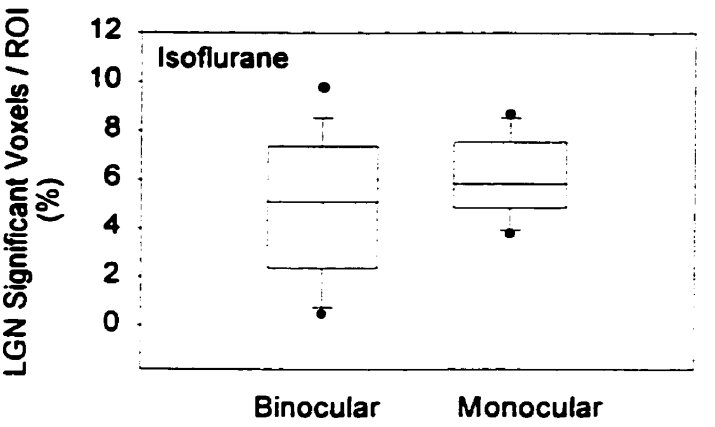
Isoflurane
LGN Significant Voxels / ROI (%)
12
10
8
6
4
2
0
Binocular
Monocular

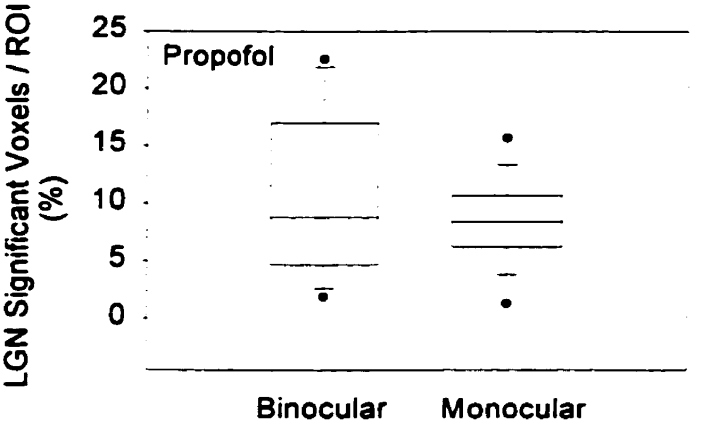
Propofol
LGN Significant Voxels / ROI (%)
25
20
15
10
5
0
Binocular
Monocular

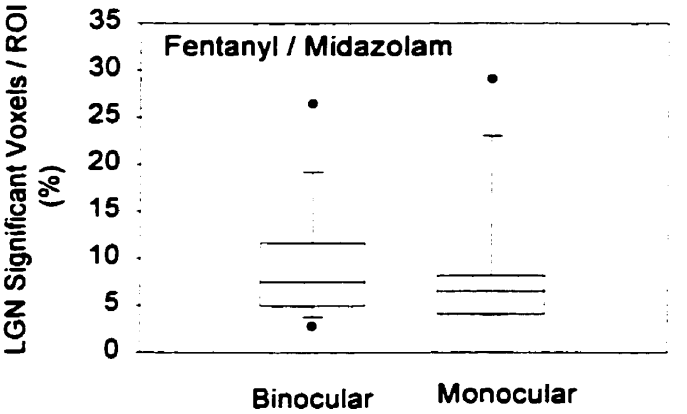
Fentanyl / Midazolam
LGN Significant Voxels / ROI (%)
35
30
25
20
15
10
5
0
Binocular
Monocular

B

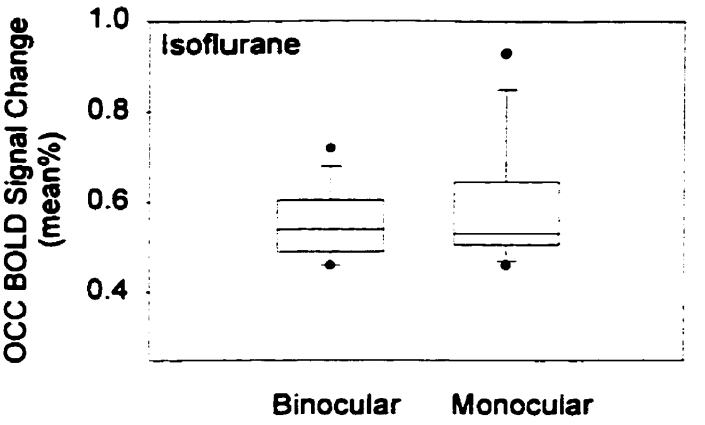
Isoflurane
OCC BOLD Signal Change (mean%)
1.0
0.8
0.6
0.4
Binocular
Monocular

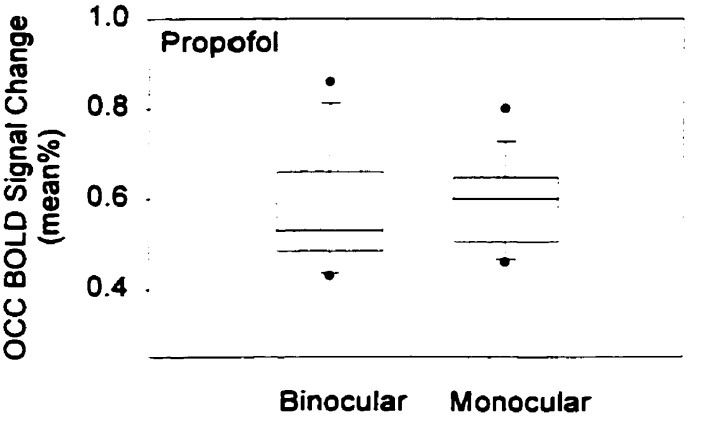
Propofol
OCC BOLD Signal Change (mean%)
1.0
0.8
0.6
0.4
Binocular
Monocular

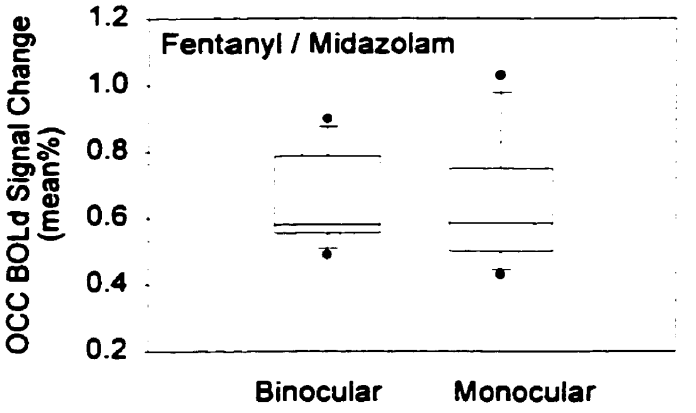
Fentanyl / Midazolam
OCC BOLd Signal Change (mean%)
1.2
1.0
0.8
0.6
0.4
0.2
Binocular
Monocular

C

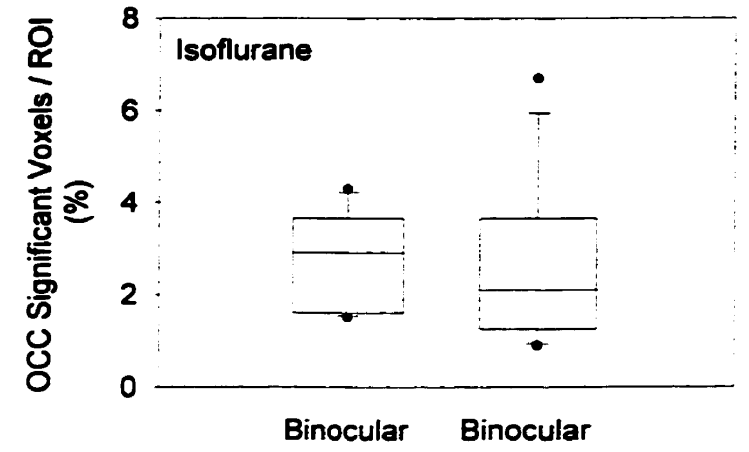
Isoflurane
OCC Significant Voxels / ROI (%)
8
6
4
2
0
Binocular
Binocular

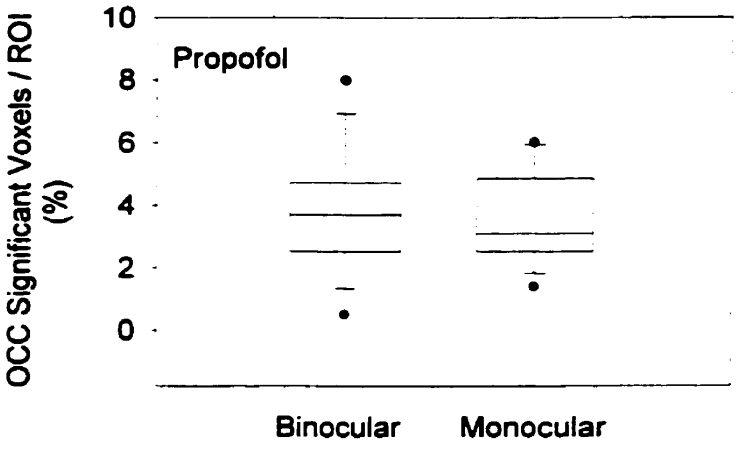
Propofol
OCC Significant Voxels / ROI (%)
10
8
6
4
2
0
Binocular
Monocular

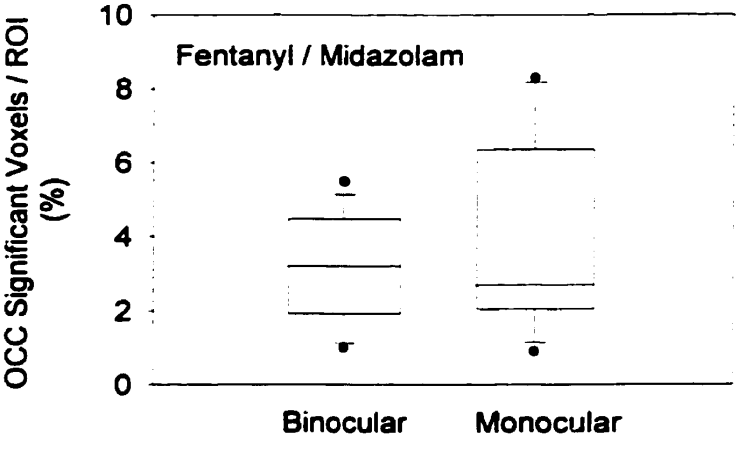
Fentanyl / Midazolam
OCC Significant Voxels / ROI (%)
10
8
6
4
2
0
Binocular
Monocular

D

Figure 3.3 Boxplots of data obtained during BOLD fMRI from the left and right hemispheres of 6 dogs anesthetized under each of 3 different anesthetic agents during monocular stimulus presentations. A) Mean percentage BOLD signal change in the lateral geniculate nucleus (LGN) region of interest. B) Number of significant voxels / ROI as a percentage of ROI size in the LGN region. C) Mean percentage signal change in the occipital lobe (OCC) region. D) Number of significant voxels as a percentage of ROI size in the OCC region. Analysis was performed using SAS Proc GLM,[23] as no trial by anesthetic interactions were found on preliminary analysis. There were no significant differences between activity in the left and right halves of each ROI. For clarity, box plots for each anesthetic agent are presented, despite the fact that the anesthetic used had no effect on differences between activity induced by monocular and binocular stimulus presentations. Horizontal lines from top to bottom on each boxplot represent the 90th, 75th, median, 25th and 10th percentiles respectively. Dots represent data points outside this range.

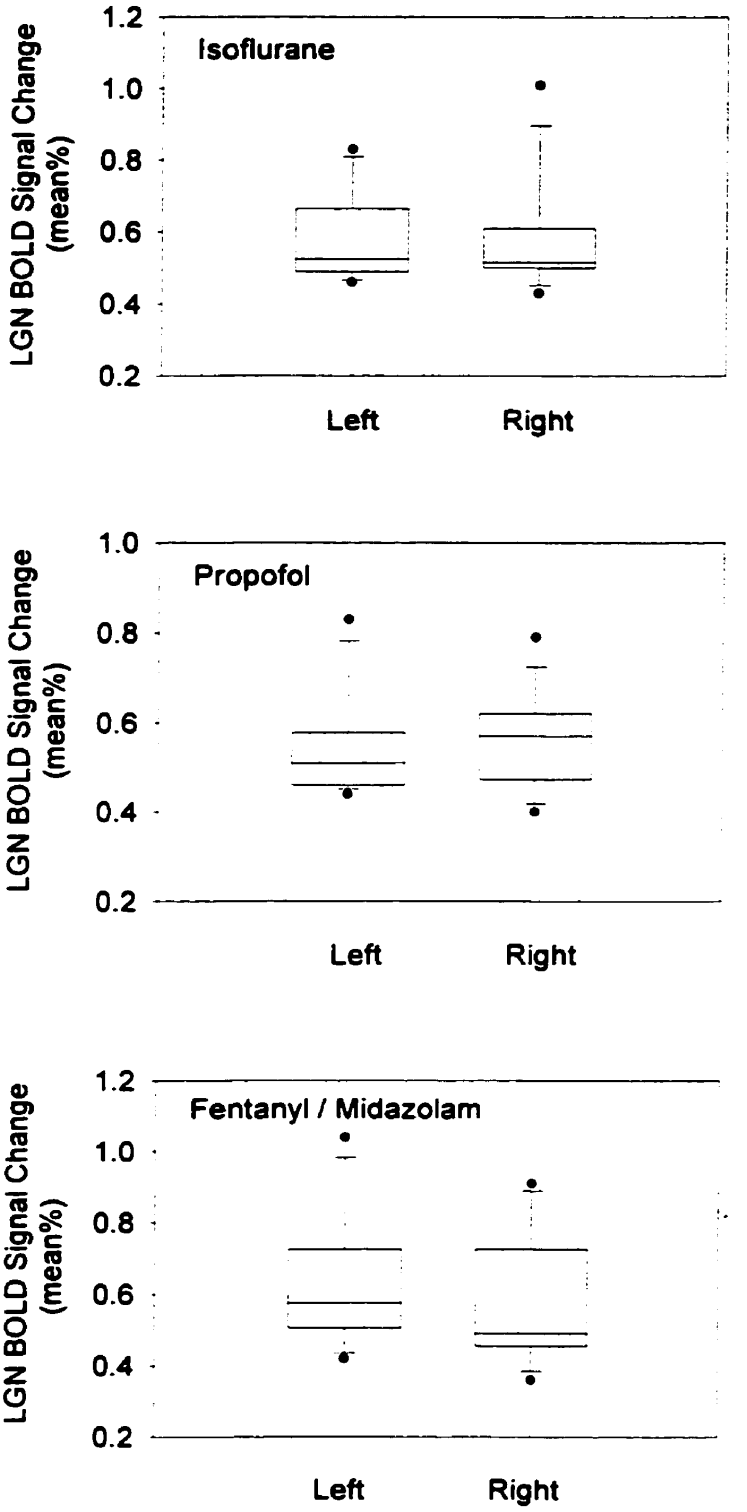
Isoflurane
LGN BOLD Signal Change (mean%)
1.2
1.0
0.8
0.6
0.4
0.2
Left
Right
Propofol
LGN BOLD Signal Change (mean%)
1.0
0.8
0.6
0.4
0.2
Left
Right
Fentanyl / Midazolam
LGN BOLD Signal Change (mean%)
1.2
1.0
0.8
0.6
0.4
0.2
Left
Right

A

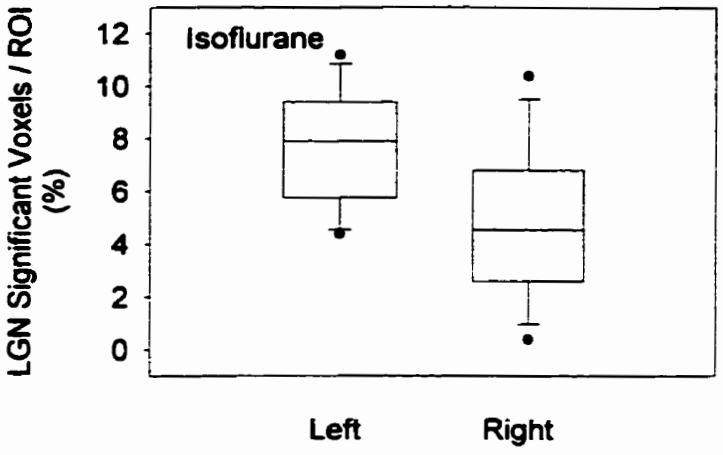
Isoflurane
LGN Significant Voxels / ROI (%)
12
10
8
6
4
2
0
Left
Right

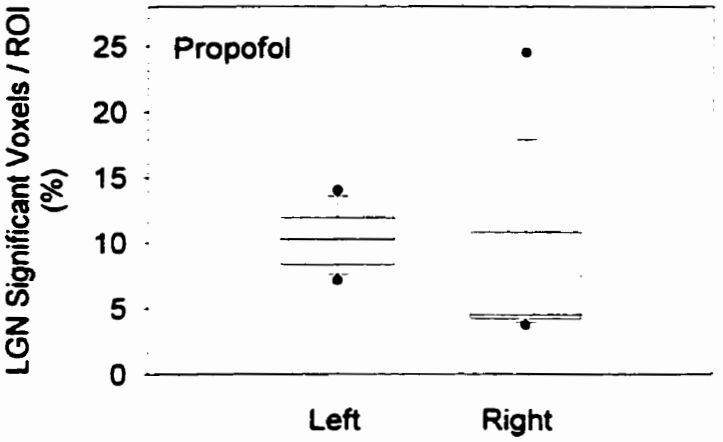
Propofol
LGN Significant Voxels / ROI (%)
25
20
15
10
5
0
Left
Right

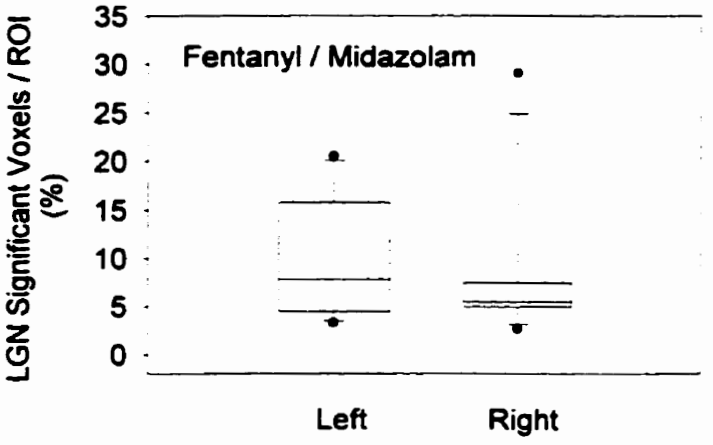
Fentanyl / Midazolam
LGN Significant Voxels / ROI (%)
35
30
25
20
15
10
5
0
Left
Right

B

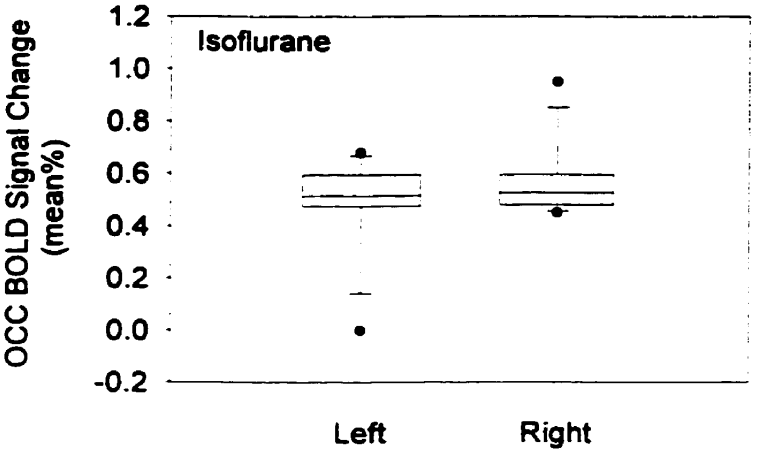
Isoflurane
OCC BOLD Signal Change (mean%)
1.2
1.0
0.8
0.6
0.4
0.2
0.0
-0.2
Left
Right

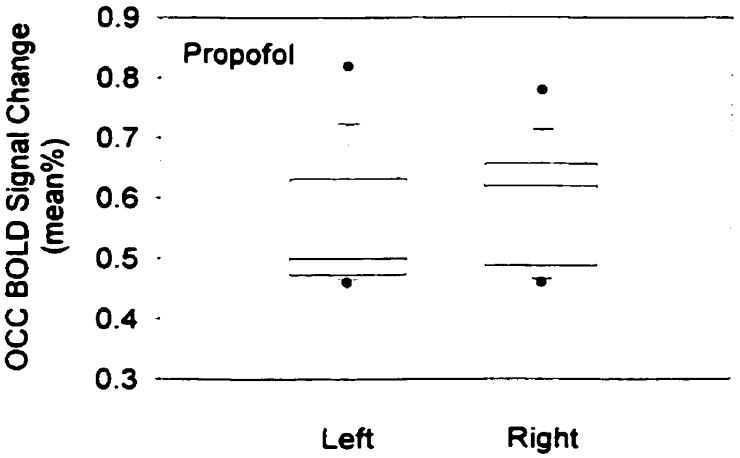
Propofol
OCC BOLD Signal Change (mean%)
0.9
0.8
0.7
0.6
0.5
0.4
0.3
Left
Right

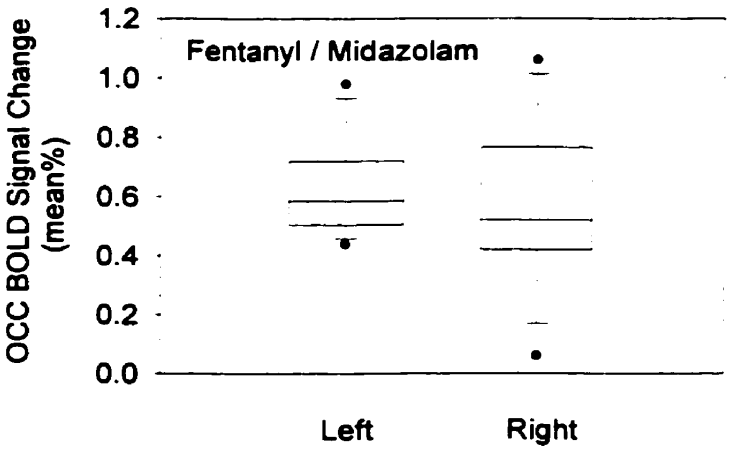
Fentanyl / Midazolam
OCC BOLD Signal Change (mean%)
1.2
1.0
0.8
0.6
0.4
0.2
0.0
Left
Right

C

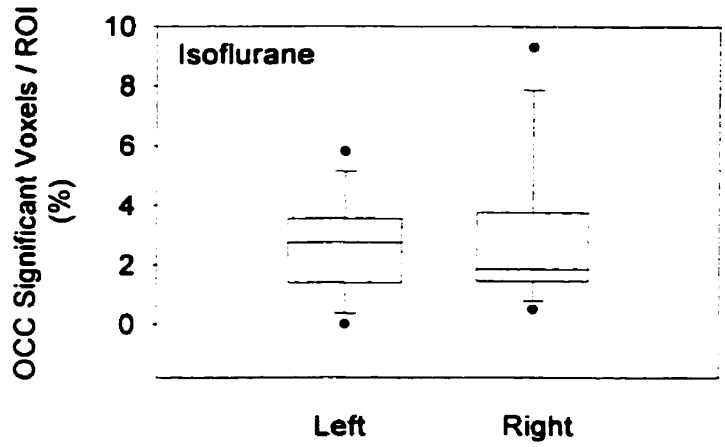
Isoflurane
OCC Significant Voxels / ROI (%)
10
8
6
4
2
0
Left
Right

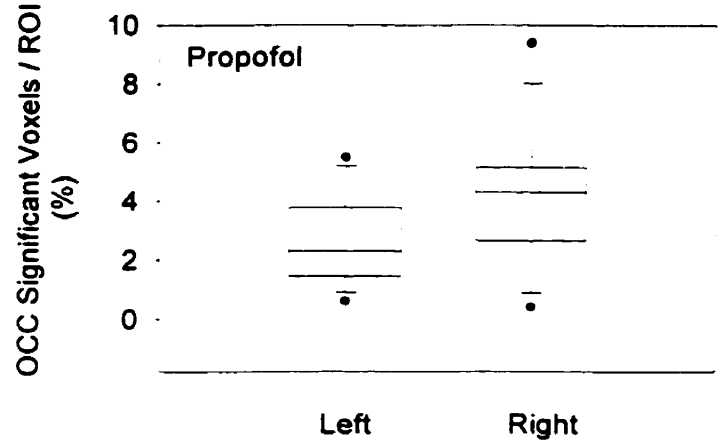
Propofol
OCC Significant Voxels / ROI (%)
10
8
6
4
2
0
Left
Right

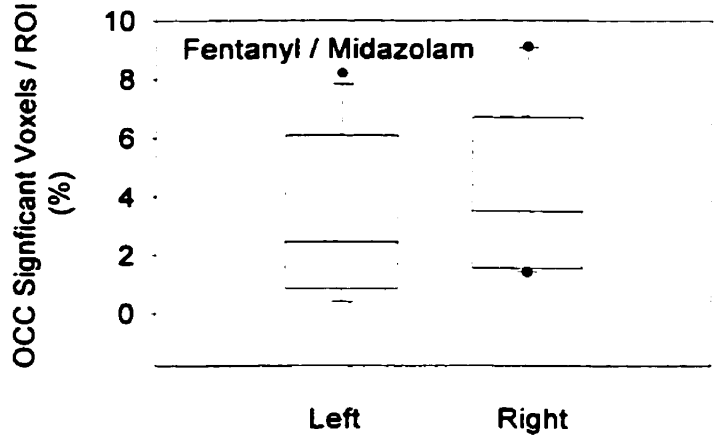
Fentanyl / Midazolam
OCC Signficant Voxels / ROI (%)
10
8
6
4
2
0
Left
Right

D

CHAPTER FOUR

FUNCTIONAL MRI AS A TOOL TO ASSESS VISION IN DOGS: THE OPTIMAL ANESTHETIC

4.1 ABSTRACT

Functional magnetic resonance imaging (fMRI) is a recent advance in neuroimaging which provides a picture of brain activity with excellent spatial resolution. Current methods used to evaluate canine vision are poorly standardized and vulnerable to bias. Functional MRI may represent a valuable method of testing vision in dogs if the impacts of anesthesia on fMRI are understood. Six dogs were scanned during visual stimulation, each under 3 different anesthetic protocols (isoflurane, propofol, fentanyl / midazolam) to address the questions: 1) Can visually evoked fMR signals be reliably recorded in anesthetized dogs? and 2) Which anesthetic agent permits the least suppression of visually induced fMR signal in dogs? This study confirms that visual stimuli reliably elicit neural activity and fMR signal change in anesthetized dogs. No significant differences in images acquired under the 3 anesthetics were found, and there was no significant relationship between anesthetic dose and brain activity. Images obtained during isoflurane anesthesia were more consistent between dogs than those obtained with the other 2 agents. This reduced variation may reflect the fact that inhalant anesthesia is more easily controlled than intravenous anesthesia under conditions associated with high field fMRI.

4.2 INTRODUCTION

Evaluating visual function presents the veterinary clinician with a range of challenges. The most obvious of these involves the inability of animals to communicate their perceptions verbally. The Snellen chart, effective for human visual testing, cannot be used. Instead, potentially biased and poorly standardized visual tests are employed. Several methods are currently in use to evaluate canine visual function and all have inherent limitations. Behavioural techniques, like the menace response, evaluate an animal's reactions to stimuli but are open to influence from distraction in the testing environment.[1] Electroretinography (ERG) records retinal activity during visual stimulation,[2,3] and therefore evaluates receptor function, but fails to record visual activity in the brain where perception actually occurs. The visual evoked potential (VEP) of the electroencephalogram (EEG) has the advantage that it does record brain activity, presumably from the thalamus and from primary visual cortex (V1).[4,5] As there are few descriptions of canine cerebral functional anatomy in the literature, the feline cortex is used as a reference for electrode placement when recording VEPs in dogs, leading to poor standardization of the technique and unreliable results.[6] Due to the limitations associated with all of these methods not only is assessment of visually normal animals difficult, but objective evaluations of surgical and pharmacological treatments for visual disease are unavailable.

Blood oxygenation level dependant (BOLD) functional magnetic resonance imaging (fMRI) is a relatively new technique in medical imaging which reveals neural activity in the brain with high spatial resolution. BOLD fMRI depends on the principle that increased activity in cerebral cortex (e.g. visual cortex in response to a visual stimulus) leads to an increase in metabolic activity,[7] and a more pronounced increase in blood flow, localized to the site of neural activity.[8,9] Since the increase in blood flow exceeds the metabolic increase and the rate of oxygen extraction from the cerebral

microvasculature, an increase in the ratio of oxygenated : deoxygenated hemoglobin results.[10,11] Deoxyhemoglobin is paramagnetic[12] and causes attenuation of magnetic resonance signal.[13] The increased oxy : deoxyhemoglobin ratio therefore causes a signal increase, localized to areas of increased neural activity, in properly weighted MR images.[14,15] To detect this BOLD effect statistically, acquired images of the brain are divided into equal sized discrete volume elements, or voxels. Images obtained during repeated stimulus presentation periods are then compared on a voxel by voxel basis to those obtained during repeated control periods. Voxels in which a significant change in BOLD signal occurs are superimposed on a corresponding anatomic MR image.[16]

This new technique has been a highly productive tool for human neuroscientists, particularly with respect to the visual system. One study of particular interest addressed dyslexia in humans.[17] Using fMRI, the authors demonstrated that the medial temporal area (MT) of the brain in dyslexic patients was not activated by movement in the visual field, although there is activation of this region in normal patients presented with moving stimuli. Subtle defecits in cognitive processing of visual motion by dyslexics were also observed during behavioural tests, suggesting a link between motion and language processing and confirming the fMRI results. Functional MRI has also revealed a great deal about the processing of shape and form in the human visual system,[18] as well as the functional neuroanatomy of visual perception and memory.[19] If several logistic concerns can be addressed BOLD fMRI could be similarly beneficial to veterinary research.

Blood oxygenation level dependant fMRI is highly sensitive to subject movement[20] so anesthesia will be a necessary limitation imposed on veterinary applications of the technique. Results of a pilot study by our group revealed that functional MR images could be obtained from anesthetized dogs and suggested that anesthesia was the most influential variable affecting image quality.[21] In the present

study, the effects of 3 clinically common anesthetic protocols (isoflurane, propofol and a combination of fentanyl / midazolam) on fMRI were compared during visual stimulation in dogs. Two specific questions were addressed: 1) Can BOLD signal changes be reliably and repeatably elicited by visual stimuli in anesthetized dogs? 2) Do differences in the quality of fMR images exist when different anesthetic agents are used? To our knowledge this study is the first detailed account of fMRI in dogs.

4.3 METHODS

4.3.1 Animals

Six purpose bred beagles (1 male, 5 female; mean mass 9.75 ± 0.88 kg (± 1 SD)), obtained from the University of Guelph Central Animal Facility, Guelph, Ontario, Canada, were transported to the Animal Care and Veterinary Services facilities at the University of Western Ontario, London, Ontario where they were housed during the experimental period. To establish normality, each dog underwent a thorough ophthalmic examination including slit lamp biomicroscopy, indirect ophthalmoscopy, applanation tonometry, and streak retinotopy. Dogs were fasted for 12 hours prior to each experiment but permitted free access to water. All procedures met with the approval of both the University of Western Ontario Council on Animal Care and the University of Guelph Animal Care Committee.

4.3.2 Imaging

All experiments were performed on a Siemens Varians 4 Tesla Whole Body Magnetic Resonance Scanner housed at the Robarts Research Institute at the University of Western Ontario. The visual stimulus, a 20 cm by 20 cm vertical grating pattern with 10 black and 10 white bars that alternated position at 5 Hz, was back-projected from a digital projector (NEC Corporation model MT800, Tokyo, Japan) located behind the observation window, onto a screen 60 cm from the subject's eyes.

The animals' eyelids were held open using non-magnetic, insulated copper speculae. To prevent corneal dehydration, an elastoviscous, clear corneal shield (Hylashields Nite®, i-med Pharma Inc., Pointe-Claire, Quebec) was applied to each eye immediately prior to speculum insertion.

Each fMRI experiment lasted approximately 7 min and consisted of 10 alternating 9 s periods of stimulus activation followed by corresponding 30 s periods of inactivation. This sequential task activation paradigm permits averaging of image data obtained during the rest state and activation state to increase statistical power during voxel by voxel comparison and improve signal to noise ratio.[13] For each experiment 4 shot (i.e. spatial encoding of single slice data was achieved using 4 identical pulse sequences), echo-planar T2*-weighted whole brain magnetic resonance images depicting BOLD contrast were obtained with a radio-frequency (RF) knee coil (designed for MR imaging of the human knee but ideally sized for a beagle head) for RF transmission and reception. The functional images were obtained in contiguous dorsal sections with echo time (TE) = 15 ms, repetition time (TR) = 750 ms, flip angle = 60°, 64 x 64 matrix, field of view (FOV) =12.8 cm (2 mm in-plane resolution), and slice thickness = 2 mm. Immediately following each experiment corresponding whole brain, 3D magnetization-prepared Turbo FLASH (Fast Low Angle Shot) T1-weighted anatomical images of each dog were acquired with TE = 6.5 ms, TR = 12.4 ms, flip angle = 11°, and inversion time = 500 ms. These anatomical volumes were acquired in the same FOV as the functional images so that functional data could be superimposed on anatomic images. Head movement was restricted using foam padding within the RF knee coil.

Image processing was performed using the analysis software Stimulate.[22] Voxel by voxel comparison of rest and task state functional images was performed using cross-correlation analysis. This permitted the reference function, to which the time

course of BOLD signal was compared, to shift with the acquired signal and accommodate hemodynamic delay between neural activity and the factors underlying the BOLD effect. Statistical significance for the cross- correlation was set initially at $p < 0.10$ and was improved to $p < 0.05$ by restricting significance to clusters with a minimum size of 3 significant voxels.[23] These voxel clusters were then superimposed onto the T1-weighted anatomic images.

Once image processing was complete, regions which included the lateral geniculate nucleus (LGN) of the thalamus and the occipital cortex were identified on each image. These areas were used as specific regions of interest (ROI) for further analysis. In all dogs, the LGN region consisted of 2 bilateral and as symmetrical as possible rectangular volumes transecting 5 dorsal slices at the level of the thalamus in the diencephalon (see Figure 4.1A). Within each slice, boundaries of the 2 sections of this ROI were placed as equidistant as possible laterally from the third ventricle and medially from the lateral ventricles. The occipital ROI was a larger rectangular volume beginning in the first dorsal slice where the cerebellum could no longer be observed and proceeding dorsally through 7 slices (see Figure 4.1B). Within each slice, the caudal boundary for this ROI was placed at the occipital pole and the rostral boundary was placed just caudal to the pseudosylvian fissure.

For each anesthetic agent and ROI the number of significant voxels was determined as a percentage of the total number of voxels within the ROI, and the mean percentage signal change (between the rest and activation states) was calculated. These quantitative measures of BOLD activity were used for further analysis. Qualitative assessment of both the images themselves and the time courses of activation with respect to stimulus presentations was also performed.

4.3.3 Anesthesia

Functional MRI experiments were performed on all 6 dogs anesthetized under each of 3 different anesthetic protocols: 1) the inhalant, isoflurane (AErrane®, Janssen, North York, Ontario); 2) the non-opioid intravenous agent, propofol (Rapinovet®, Schering Plough Animal Health, Point-Claire, Quebec); and 3) a combination of the opioid intravenous agent, fentanyl (Abbott Laboratories Ltd., Toronto, Ontario), and non-opioid, midazolam (Versed®, Hoffman La Roche Ltd., Mississauga, Ontario). To avoid data loss resulting from movement artifacts, and to facilitate comparison of results within dogs, each dog was scanned twice under each agent for a total of 36 experimental sessions (6 dogs X 3 anesthetics X 2 trials). The order of anesthetic agent used for each dog was chosen randomly and the minimum time between consecutive studies on any dog was 72 hours.

Prior to each experimental session, mydriasis was achieved using 0.5% tropicamide drops (Diotrope®, Dioptic Laboratories, Markham, Ontario), 0.01 mg/kg glycopyrolate (Sabex Inc. Boucherville, Quebec) was given intramuscularly and a cephalic catheter was placed.

Target doses of each agent known to maintain a relatively light, comparable and stable depth of general anesthesia were selected (Table 4.1).[24] Bolus doses (propofol, 4-6 mg/kg; fentanyl / midazolam, 10-20 ug/kg and 0.5 mg/kg, respectively) were used for induction with the I.V. regimes and, mask induction was used for isoflurane. Once anesthetized, the dogs were intubated, transported a short distance to the MR scanning room, and placed on 100% oxygen, or oxygen and isoflurane. A neuromuscular block was produced using atracurium besylate (Sabex Inc., Boucherville, Quebec) at 0.3 mg/kg I.V. This minimized muscle movement and facilitated central fixation of a relaxed eye. Intermittent positive pressure ventilation was employed using a volume limited

ventilator (Airshields® Ventimeter®, Air-Shields Inc., Hatboro, Pennsylvania) with a respiratory frequency of 10 breaths per minute and a tidal volume of 15 ml/kg.

Maintenance of I.V. anesthesia was achieved using an infusion of propofol (0.4 mg/kg/min), or fentanyl / midazolam (0.80 ug/kg/min and 8.0 ug/kg/min, respectively), administered via a microdrip (Baxter Corporation, Toronto, Ontario) from a pre-loaded volume limiting system (Buretrol®, Baxter Corporation, Toronto, Ontario). Actual infusion doses were calculated by dividing the volume of infusion used during an imaging session by the total time of the session. The intravenous anesthetics were diluted with saline (anesthetic:saline, 1:3) to facilitate more accurate infusion and to simultaneously achieve fluid replacement through the same venous access.

Inhalant anesthesia (1.6% end-tidal, expired isoflurane) was maintained using a precision vaporizer (Forane®, Cyprane Ltd., Keighley Yorkshire, England) and a modified Bain breathing system at a fresh gas flow sufficient to prevent rebreathing(150 ml/kg). The Bain system was modified by extending both the inlet and exhaust tubing to 10 m. Dogs were maintained on a 0.9% NaCl infusion (Baxter Corporation, Toronto, Ontario) at 5 ml/kg/hr during isoflurane anesthesia. Experiments in which actual induction or infusion doses exceeded the mean of all doses ± 2 standard deviations were excluded from further analyses.

A gas monitor (Criticare Poet® IQ, Criticare Systems Inc., Waukesha, Wisconsin) was used to monitor inspired and end-tidal expired CO_2 and O_2 levels during all experiments, as well as inspired and end-tidal expired isoflurane during isoflurane experiments. These factors were recorded for the 10 min immediately prior to a scanning session, as well as immediately following a session, but they could not be monitored throughout scanning sessions. The powerful magnetic field surrounding the scanner prohibited any metal containing equipment from being placed within a 10 m radius, a

distance which exceeded the sampling capabilities of the gas monitor. Heart rate and oxygen saturation were monitored throughout each session using a pulse oximeter (Nonin Medical Inc. model 8600FO, Minneapolis, Minnesota) and fibre-optic cable. Each animal was covered with a blanket while anesthetized to maintain body temperature and prevent hypothermia.

4.3.4 Statistical Analysis

Comparisons of percentage BOLD signal change, and the number of significant voxels per ROI as a percentage of ROI size were performed based on the Randomized Complete Blocks Design (RCBD). The SAS systems general linear models procedure (Proc GLM)[25] was used to detect trial by anesthetic treatment interactions for both measures of image quality within each ROI. If no significant trial by treatment effects were detected, Proc GLM[25] was used to test for drug treatment effects by averaging results from trial 1 and trial 2 for each dog and comparing between anesthetics using a method analogous to repeated measures ANOVA. If a significant trial by treatment effect did occur, SAS Proc Mixed[26] was used to detect simple treatment effects within trial 1 and trial 2 separately. Linear regression analysis for anesthetic dose by both fMRI variables was performed using Statistix (Version 1.0, Analytical Software) by averaging data from trial 1 and trial 2 for each dog, when no significant trial by treatment effects were detected. When a trial by treatment interaction was detected, linear regression was performed by plotting data from the first trial for each dog against anesthetic dose. Significance for all analyses was assessed at $p < 0.05$.

4.3 RESULTS

Data from 36 experimental sessions were processed. Five sessions were excluded due to motion artifacts and 1 fentanyl / midazolam session was excluded because anesthetic infusion dose exceeded the mean ± 2 S.D. Despite these

exclusions, at least 1 of 2 trials for each dog under each anesthetic was included in all analyses.

Target and actual infusion doses of each anesthetic agent are provided in Table 4.1. Infusion doses and end-tidal CO_2 levels for all dogs are also presented in Appendix IV. Pulse oximetry data for all dogs are presented in Appendices V-VI. In all dogs, and under all 3 anesthetic agents, significant BOLD signal change of between 0.3 and 1.1% was elicited by visual stimulation. Representative images and the corresponding time courses of activity from 1 dog under fentanyl / midazolam anesthesia are shown in Figure 4.1. Voxels in which BOLD signal change correlated with the time course of stimulus presentation appear as coloured pixels on the anatomic image, the bright yellow pixels representing the greatest signal change between the control state and activation state.

No obvious qualitative trends with respect to fMR image quality were observed between the 3 anesthetic protocols. With all 3 anesthetics, significant activity in response to visual stimulation was observed consistently, though not exclusively, in a region which included the LGN of the thalamus, and throughout the occipital lobe of cerebral cortex. These regions were included in ROIs for all further analyses.

Results of the randomized complete blocks design (RCBD) general linear models procedure (Proc GLM)[25] to detect trial by treatment effects for both fMR variables in both regions of interest are presented in Table 4.2. Only the log transformed percentage of significant voxels within the LGN region was significantly affected by trial treatment interactions (log transform was applied based on the residual plot of these data). This trial by treatment effect occurred because there was a significant difference between observations from the first fentanyl / midazolam trial and first isoflurane trial ($F = 2.73$, $p = 0.02$, $df = 10$), but not between observations from the second trials for these protocols ($F = -0.76$, $p = 0.47$, $df = 10$). Based on this discrepancy, data from the 2 trials were

considered separately during further analysis and SAS Proc Mixed[28] was employed. All data met the normality assumptions of the general linear model, but equal variance assumptions may have been violated.

End-tidal CO_2 levels for each experiment were also analysed. The mean of end-tidal CO_2 levels recorded at the start and the end of an experiment was used because the magnetic field prohibited continuous use of the gas monitor throughout scanning sessions. No significant trial by treatment interaction effects ($F = 0.06$, $p = 0.94$, $df = 2$) were observed for recorded end tidal CO_2 values using Proc GLM. A treatment effect for CO_2 was significant ($F = 1.45$, $p = 0.03$, $df = 2$), however, because CO_2 values recorded under fentanyl / midazolam (47.1 ± 4.9 mm Hg) were significantly greater than under propofol (43.4 ± 2.5 mm Hg); end tidal CO_2 values under isoflurane (45.6 ± 3.0 mm Hg) did not differ significantly from values obtained under either of the other protocols.

Comparisons of mean percentage BOLD signal change and significant voxels / ROI between the 3 different anesthetics are presented in Figure 4.2. No significant differences were observed for any category. Based on their distributions, however, data obtained under isoflurane, especially for significant voxels / ROI in both the LGN and occipital regions seems qualitatively less variable (Figure 4.2, Table 4.3). Unfortunately, a definitive statistical test of equal variance is not available using the RCBD model.

Some variation in anesthetic dose between experiments was unavoidable, especially for the intravenous agents. To determine if this variation had an effect on BOLD activity, linear regression analyses were performed for anesthetic dose against both percentage signal change and significant voxels per ROI (Figures 4.3 – 4.5). No significant relationship between anesthetic dose and either measure of BOLD signal was observed in either ROI.

4.4 DISCUSSION

A pilot study by our group demonstrated, for the first time, that neural activity can be recorded from the brains of anesthetized dogs using BOLD fMRI.[21] The current study confirms the results of the pilot study and is the first to compare effects of different anesthetic protocols on fMRI activity in any animal. Our results are consistent with fMRI data recorded from visual cortex in cats anesthetized with isoflurane.[27] Mean percentage signal changes (0.3 – 1.1% for the present study) are considerably less than those observed with a repeated visual stimulus presentation paradigm in awake humans. This is not surprising given the fact that general anesthesia depresses central nervous system activity by definition and also reduces basal cerebral blood flow.[28] Lahti et al. compared somatosensory fMR responses of rats, awake and restrained, as well as during propofol anesthesia, and noted the anesthetic inhibition of BOLD activity.[29] The use of 100% oxygen for ventilation in the present study may have further compounded signal attenuation. Changes in the ratio of deoxy : oxyhemoblobin between the control state and the stimulus presentation state, the basis of the BOLD effect, may have been reduced because of high levels of dissolved oxygen in the blood. The use of N_2O and O_2, in combination, may be more appropriate for future canine fMRI studies to limit this potential source of signal loss. Despite reduced signal strength, BOLD activity has been reproducible in all fMRI studies of anesthetized animals to date, including the present study.

A methodological problem reported by Jezzard et al. involved maintaining eye position in anesthetized animals during presentations of visual stimuli.[28] They relied on the use of corrective lenses to fixate an animal's gaze on the stimulus and reported some complications with this method. In the present study, the neuromuscular block provided by atracurium was an effective alternative. It resulted in a centrally fixated,

relaxed eye position and helped reduce other muscle movements, to which fMRI is extremely sensitive.[27,30]

There were no obvious qualitative differences in images obtained under isoflurane, propofol or fentanyl / midazolam anesthesia. Activity was detected in brain areas known to play a role in visual processing in other mammals, with all three anesthetic regimes. In cats roughly 80% of optic tract fibres terminate and synapse in the lateral geniculate nucleus (LGN) of the thalamus. Lateral geniculate fibres in turn innervate visual cortex in the occipital lobes.[31] This organization is preserved in non-human primates and humans,[32] and almost certainly in dogs, although direct data are not available. Based on this known functional mammalian anatomy, and on the significant BOLD activity observed in these areas in the present study, a LGN region of interest (ROI) and an occipital ROI were selected for further analysis. This excluded the few significant voxels outside of ROIs that could have been associated with visual activity, or could simply have reflected non visual, oscillatory brain activity which by chance matched the time course of stimulus presentation.

Within both ROIs the mean percentage signal change between rest and stimulus presentation, as well as the number of significant voxels as a percentage of ROI size under the 3 different anesthetic agents, were compared. Although no significant differences were detected, there appeared to be less variation in responses under isoflurane anesthesia than under either of the I.V. protocols. This may reflect logistic complications of intravenous anesthetic infusion when working with a powerful MR scanner. A 4 T magnetic field is many times more powerful than the earth's magnetic field and, as such, interferes with electronic and mechanical equipment. All apparatus for anesthetic monitoring and delivery, therefore, had to be kept a minimum of 10 m from the MR scanner. This meant that drip infusion rate for I.V. anesthetic maintenance had to be set manually, prior to the onset of scanning, and could not be adjusted until the

completion of the hour long session. Over an hour, slight variations in drip rate could have caused considerable differences in the total volume of anesthesia administered. In addition, a change in leg position within the RF coil might have increased resistance to the infusion, adding to variation in the I.V. anesthetic dose. In contrast, the isoflurane dose was set as a percentage of inspired gas using a dial on an anesthesia machine and was confirmed using the gas monitor. Both pieces of equipment were located the required 10 m from the magnet. The use of an intravenous infusion pump would have facilitated more precise control of I.V. anesthetic dose. Despite the observed variation in dose, significant dose dependant effects of anesthesia on fMRI were not detected. This observation suggests that the influence of anesthesia on fMRI may not be dose dependant.

It remains plausible, however, that the increased variation in percentage signal change and percentage of significant voxels / ROI with I.V. administered protocols reflects reduced precision of anesthetic administration during imaging. One would expect that with increasing anesthetic dose, and therefore increased anesthetic depth, neural activity and BOLD signal would be reduced. Dose dependant inhibitory relationships between both isoflurane and propofol and measures of cerebral activity, like the EEG, have been reported.[33,34] We may have failed to detect a significant relationship between anesthetic dose and BOLD signal because the range of doses to which these dogs were exposed was too small to elucidate the correlation. One methodological objective of the study, in fact, was to maintain anesthetic dose as closely as possible between experiments. Variation likely occurred because of difficulties associated with maintaining a constant anesthetic infusion from a considerable distance. Further study using a wider range of anesthetic doses would help resolve this issue.

Blood carbon dioxide levels may have influenced the results of this study, as well, because of the considerable influence on cerebral blood flow exerted by CO_2.[24] A

statistically significant difference in end-tidal CO2 between the three anesthetic protocols was detected, though the small range of values (43.4 ± 2.5 - 47.1 ± 4.9 mm Hg) may not have been biologically significant. We did attempt to maintain CO_2 levels as closely as possible by ensuring dogs were stabilized with an end-tidal CO_2 level of between 38-42 mm Hg before being placed in the scanner. With continuous monitoring, changing CO_2 levels could have been detected quickly and addressed by modifying ventilation rate or tidal volume. Variation was also compounded by the fact that dogs were very briefly disconnected from ventilation during removal from the scanning room at the end of each session. This may have caused CO_2 accumulation so that values recorded at the end of the session overestimated end-tidal levels as they actually occurred during imaging.

Despite these potential sources of variation, reproducible BOLD signals in brain regions with known visual functions in other mammals were recorded. The reliability of fMRI results during anesthesia has important clinical and research implications. Restraining animals during fMRI is problematic because neural activity associated with factors such as stress or motor output against the restraints could confound data associated with the stimulus of interest. In addition, eye movements cannot be restrained, so fMRI investigations of visual activity are virtually impossible in awake animals, except perhaps in highly trained non-human primates. Also, if fMRI is eventually to have clinical application in veterinary medicine, the stress associated with restraint is unlikely to be accepted by pet owners. Human implications also exist in that, currently, human patients incapable of remaining still for extended periods (i.e. small children, the mentally ill) are not canididates for fMRI. Establishing, then, that fMR signals can be reproducibly recorded under general anesthesia is an important finding.

Our results demonstrate that BOLD signal change, and useful fMR images can be reliably elicited using visual stimulation in anesthetized dogs under 3 different anesthetic protocols. This is particularly encouraging for both clinical and research

application of fMRI in veterinary medicine, especially with respect to vision. We did not find differences in fMR activity between anesthetic agents, or dose dependant relationships between anesthesia and fMRI. It does seem, however, that isoflurane permitted more consistent BOLD activity than the intravenous anesthetic protocols. This may reflect the fact that inhalant anesthesia is more easily controlled under conditions associated with fMRI.

4.5 REFERENCES

1. Myers LJ. Use of innate behaviors to evaluate sensory function in the dog. *Veterinary Clinics of North America: Small Animal Practice* 1991; **21**: 289-299.

2. Odom JV, Bromberg NM, Dawson WW. Canine visual acuity: retinal and cortical field potentials evoked by pattern stimulation. *American Journal of Physiology* 1983; **14**: R637-R641.

3. Sims MH, Ward DA. Response of pattern-electroretinograms (PERG) in dogs to alterations in the spatial frequency of the stimulus. *Progress in Veterinary and Comparative Ophthalmology* 1992; **2**: 106-112.

4. Sims MH, Laratta LJ, Bubb WJ, Morgan RV. Waveform analysis and reproducibility of visual evoked potentials in dogs. *American Journal of Veterinary Research* 1989; **50**: 1823-1828.

5. Strain GM, Jackson RM, Tedford BL. Visual evoked potentials in the clinically normal dog. *Journal of Veterinary Internal Medicine* 1990; **4**: 222-225.

6. Ofri R, Dawson WW, Samuelson DA (1994) Mapping of the cortical area of central vision in dogs. *Progress in Comparative and Veterinary Ophthalmology* 1994; 4: 172-178.

7. Pritchard J, Rothman D, Novotny E, Petroff O, Kuwabura T, Avison M, Houseman A, Hanstock C, Shulman R. Lactate rise detected by 1H NMR in human visual cortex during physiologic stimulation. *Proceeding of the National Academy of Sciences USA* 1991. **88**: 5829-5831.

8. Fox PT, Raichle ME. Focal physiological uncoupling of cerebral blood flow and oxidative metabolism during somatosensory stimulation in human subjects. *Proceeding of the National Academy of Sciences USA* 1986, **83**: 1140-1144.

9. Belliveau JW, Kennedy DN, McKintry RC, Buchbinder BR, Weisskoff RM, Cohen MS, Vevea JM, Brady TJ, Rosen BR. Functional mapping of the human visual cortex by magnetic resonance imaging. *Science* 1991; **254**: 716-719.

10. Bandettini PA, Wong EC, Hinks RS, Tifofsky RS, Hyde JS. Time course EPI of human brain function during task activation. *Magnetic Resonance in Medicine* 1992 **25**: 390-397.

11. Kwong KK, Belliveau JW, Chesler DA, Goldberg IE, Weisskoff RM, Poncelet BP, Kennedy DN, Hoppel BE, Cohen MS, Turner R, Cheng H, Brady TJ, Rosen BR. Dynamic resonance imaging of human brain activity during primary sensory stimulation. *Proceedings of the National Academy of Sciences* USA 1992; **89**: 5675-5679.

12. Pauling L, Coryell CD. The magnetic properties and structure of hemoglobin, oxyhemoglobin and carbon monoxyhemoglobin. *Proceedings of the National Academy of Sciences* USA 1936 **22**: 210-216.

13. Villringer A, Rosen BR, Belliveau JW, Ackerman JL, Lauffer RB, Buxton RB, Chao YS, Wedeen VJ, Brady TJ. Dynamic imaging with lanthanide chelates in normal brain: contrast due to susceptibility effects. *Magnetic Resonance in Medicine* 1988; **6**: 164-174.

14. Ogawa S, Lee TM. Magnetic resonance imaging of blood vessels at high fields: In Vivo and in vitro measurements and image simulation. *Magnetic Resonance in Medicine* 1990; **16**: 9-18.

15. Ogawa S, Tank DW, Menon R, Ellerman JM, Kim S Merkle H Ugurbil K. Intrinsic signal changes accompanying sensory stimulation: Functional brain mapping with magnetic resonance imaging. *Proceedings of the National Academy of Sciences* USA 1992; **89**: 5951-5955.

16. Menon RS, Ogawa S, Strupp JP, Ugurbil K. Ocular dominance in human V1 demonstrated by functional magnetic resonance imaging. *Journal of Neurophysiology* 1997; **77**: 2780-2787.

17. Eden GF, VanMeter JW, Rumsey JM, Maisog JM, Woods RP, Zeffiro TA. Abnormal processing of visual motion in dyslexia revealed by functional magnetic resonance imaging. *Nature* 1996; **382**: 67-69.

18. Ungerleider LG, Mishkin M. Two cortical visual systems. In: *Analysis of Visual Behaviour* (ed. Ingle DJ, Goodale MA, Mansfield RJW) MIT Press: Cambridge, Mass., 1982; 549-586.

19. Courtney SM, Ungerleider LG, Kell K, Haxby JV. Transient and sustained activity in a distributed neural system for human working memory. *Nature* 1997; **386**: 608-611.

20. Sanders JA, Orrison WW. Functional magnetic resonance imaging. In: *Functional Brain Imaging* (ed. Orrison WW, Lewine JD, Sanders JA, Hartshorne MF), Mosby - Year Book Ltd: St Louis, 1995; 239-326.

21. Quinn R, Gati J, Parent J, Menon R, Nicolle D, Tingey D. Visualizing cortical activity in the dog utilizing functional magnetic resonance imaging (abstract). *28th Annual Meeting of the American College of Veterinary Ophthalmologists*. 1997.

22. Strupp JP. A GUI based fMRI analysis software package. *Neuroimage* 1996; **3**: 5607.

23. Forman SD, Cohen JD, Fitzgerald M, Eddy WF, Mintum MA, Noll DC. Improved assessment of significant activation in functional magnetic resonance imaging (fMRI): Use of a cluster-size threshold. *Magnetic Resonance in Medicine* 1995; **33**: 636-647.

24. Thurmon JC, Tranquill WJ, Benson GJ. *Lumb and Jones' Veterinary Anesthesia*. Williams and Wilkins, Baltimore, 1996.

25. SAS Institute Inc. *SAS/STAT User's Guide Version 6*. 4th edn, SAS Institute Inc.: Cary NC, 1989.

26. SAS Institute Inc. *SAS/STAT Software: Changes and enhancements through release 6.12*. SAS Institute Inc.: Cary NC, 1997.

27. Jezzard P, Rauschecker JP, Malonek D. An *in vivo* model of functional MRI in cat visual cortex. *Magnetic Resonance in Medicine* 1997; **38**: 699-705.

28. Ueki M, Mies G, Hossman K-A. Effects of alpha-chloralose, halothane, pentobarbitol and nitrous oxide anesthesia on metabolic coupling in somatosensory cortex of rats. *Acta Anesthesiology Scandinavia* 1992; **36**: 318-322.

29. Lahti KM, Ferris CF, Li F, Sotak CH, King JA. Comparison of evoked cortical activity in concious and propofol anesthetized rats using functional MRI. *Magnetic Resonance in Medicine* 1998; **41**: 412-416.

31. Hajnal JV, Myers R, Oatridge A, Schwieso JE, Young IR, Bydder GM. Artifacts due to stimulus correlated motion in functional imaging of the brain. *Magnetic Resonance in Medicine* 1994; **31**: 283-291.

32. De Lahunta A. *Veterinary Neuroanatomy and Clinical Neurology* 2nd edn. WB Saunders: Philadelphia; 1983.

33. Reichert H. *Introduction to Neurobiology*. Georg Thieme Verlag: Stuttgart; 1992.

34. Jones JG Use of evoked potentials in the EEG to measure depth of anesthesia. In Consciousness, Awareness and Pain in General Anesthesia (ed. Rosen M, Lunn JM), Butterworths: London, 1987;

35. Newberg RE, Milde JH, Michenfelder JD. The cerebral metabolic effects of isoflurane at and above concentrations that suppress cortical electrical activity. *Anesthesiology* 1983; **59**: 23-28.

Table 4.1. Anesthetic target doses and actual doses for isoflurane, propofol and fentanyl / midazolam used to anesthetize dogs for BOLD fMRI. Intravenous agents were administered using a drip infusion and isoflurane using a vaporizer and Bain circuit. One experiment was excluded (*) from subsequent analysis because the dose exceeded the mean ± 2 standard deviations. N/A = not available.

		Isoflurane (end-tidal%)	Propofol (mg/kg/min)	Fentanyl (ug/kg/min)	Midazolam (ug/kg/min)
Dog	Target	1.6	0.40	0.80	8.0
Bibi1.		N/A	0.20	0.50	5.0
Bibi2		1.4	0.26	0.83	8.3
Pakum1		N/A	0.36	1.30	13.0
Pakum2		1.4	N/A	0.40	4.0
Starr1		1.3	0.27	1.30	13.0
Starr2		1.5	0.36	0.90	9.0
Shadow1		1.3	0.44	0.89	8.9
Shadow2		1.4	0.33	0.88	8.8
Diosa1		1.6	0.33	1.70*	17*
Diosa2		1.3	0.36	0.92	9.2
Broadway1		1.6	0.33	0.90	9.0
Broadway2		1.8	0.36	0.75	7.5
Mean		1.5	0.33	0.94	9.4
S.D.		0.2	0.07	0.35	3.5

Table 4.2. Evaluation of trial by anesthetic effects on differences between 3 anesthetic treatments for 2 measures of BOLD signal (mean percentage signal change, PSC; and percentage of significant voxels per ROI, SVX) in 2 regions of interest (lateral geniculate nucleus, LGN; and occipital cortex, OCC).[≠]

Variable	F	p
LGN PSC	0.50	0.62
LGN SVX (log transformed)	4.41	0.04*
OCC PSC	0.67	0.54
OCC SVX	0.19	0.83

[≠] Randomized complete blocks design, SAS general linear model (Proc GLM)[25] to detect significant drug by trial effects with 2 degrees of freedom; n = 30.
* Significant difference.

Table 4.3. Standard deviations of BOLD fMRI data obtained from 6 dogs for 2 quantitative measures of image quality (mean percentage signal change, PSC; and number of significant voxels / ROI as a percentage of ROI size, SVX) in 2 regions of interest (lateral geniculate nucleus, LGN; and occipital lobe, OCC). A statistical test for equal variance is unavailable using the statistical model employed. Qualitatively, standard deviations for isoflurane data are smaller that those for propofol and fentanyl / midazolam data, especially for SVX in both ROIs.

Variable	Fentanyl / Midazolam	Propofol	Isoflurane
LGN PSC	0.17	0.13	0.11
LGN SVX	6.70	7.25	2.37
OCC PSC	0.15	0.15	0.14
OCC SVX	1.60	2.06	1.09

Figure 4.1 Blood Oxygenation Level Dependant (BOLD) Functional MR, whole brain images in dorsal sections (A, B) with corresponding BOLD activity time courses (C, D) from a dog anesthetized under fentanyl / midazolam and presented with a vertical grating visual stimulus. All functional data were obtained using 4 shot echo-planar imaging weighted for T2*. Images were divided into discrete volume elements (voxels) in a 64 X 64 matrix with in plane resolution = 2 mm and slice thickness = 2 mm. Within each voxel, cross correlation was used to detect increases in BOLD signal linked to repeated period of stimulus presentation. Voxels in which a significant increase in BOLD signal was detected were then superimposed on 3D magnetization prepared Turbo FLASH (Fast Low Angle Shot) anatomic images as coloured pixels. Bright yellow voxels are those with the greatest signal change between control and activation. Two regions of interest (ROIs) were selected based on regions where activation was reliably observed and where visual activity has been reported in other animals. Their boundaries appear as thin lines on A and B. The first ROI (A) included the lateral geniculate nucleus (LGN) of the thalamus and the second (B) included much of the occipital lobes of both cerebral hemispheres. The number of significant voxels as a percentage of total ROI size was used as one quantitative measure of image quality for further analysis and the mean percentage signal change was used as another. ROIs were always selected in the same slices, based on the same anatomical landmarks between dogs and anesthetics. Percentage signal changes were calculated by comparing baseline and activation BOLD signals, based on the time courses of stimulus presentation (bottom traces in C and D) and BOLD signal in the LGN region (C) and occipital region (D) over the course of each experiment. Arb. units = arbitrary units.

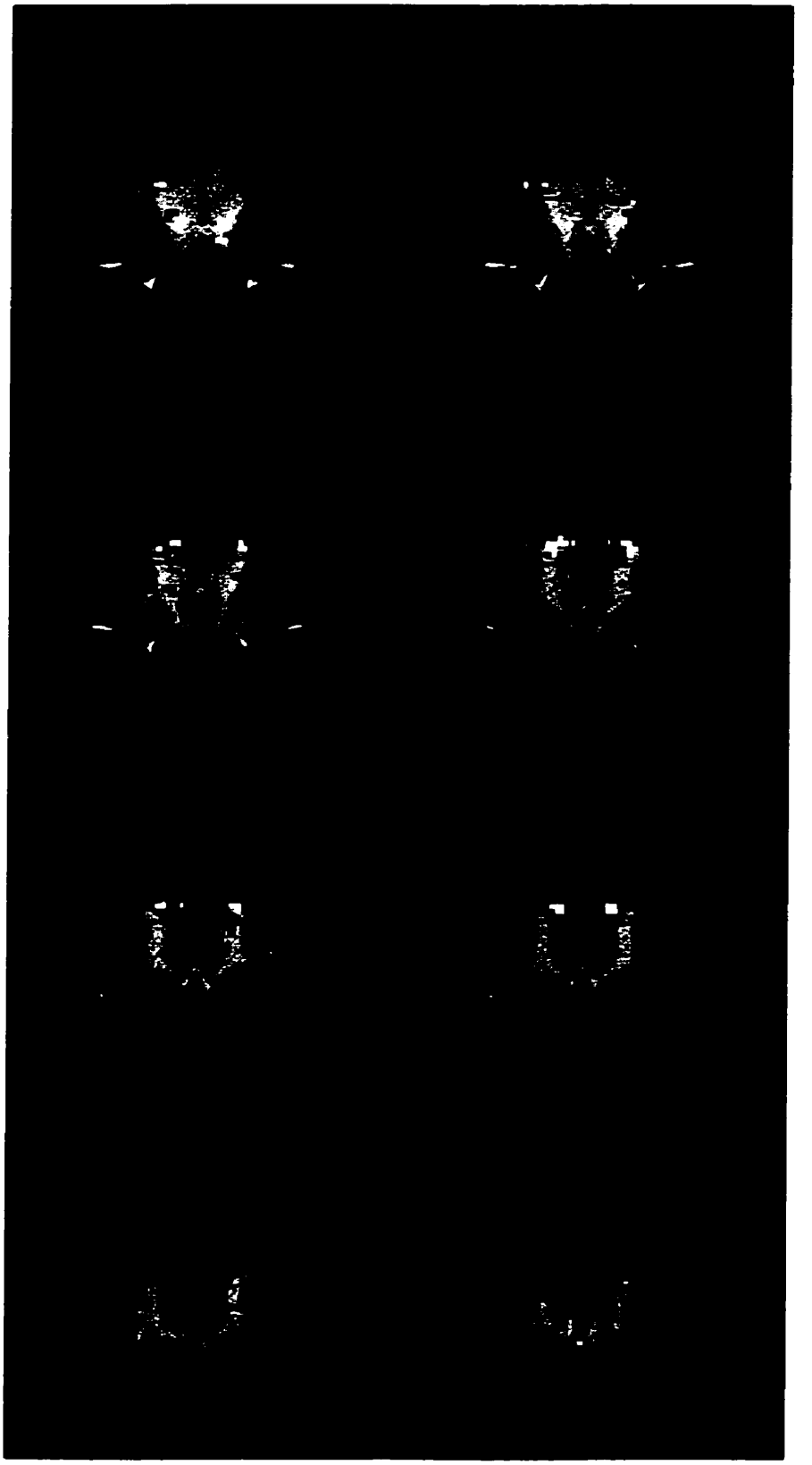

A.

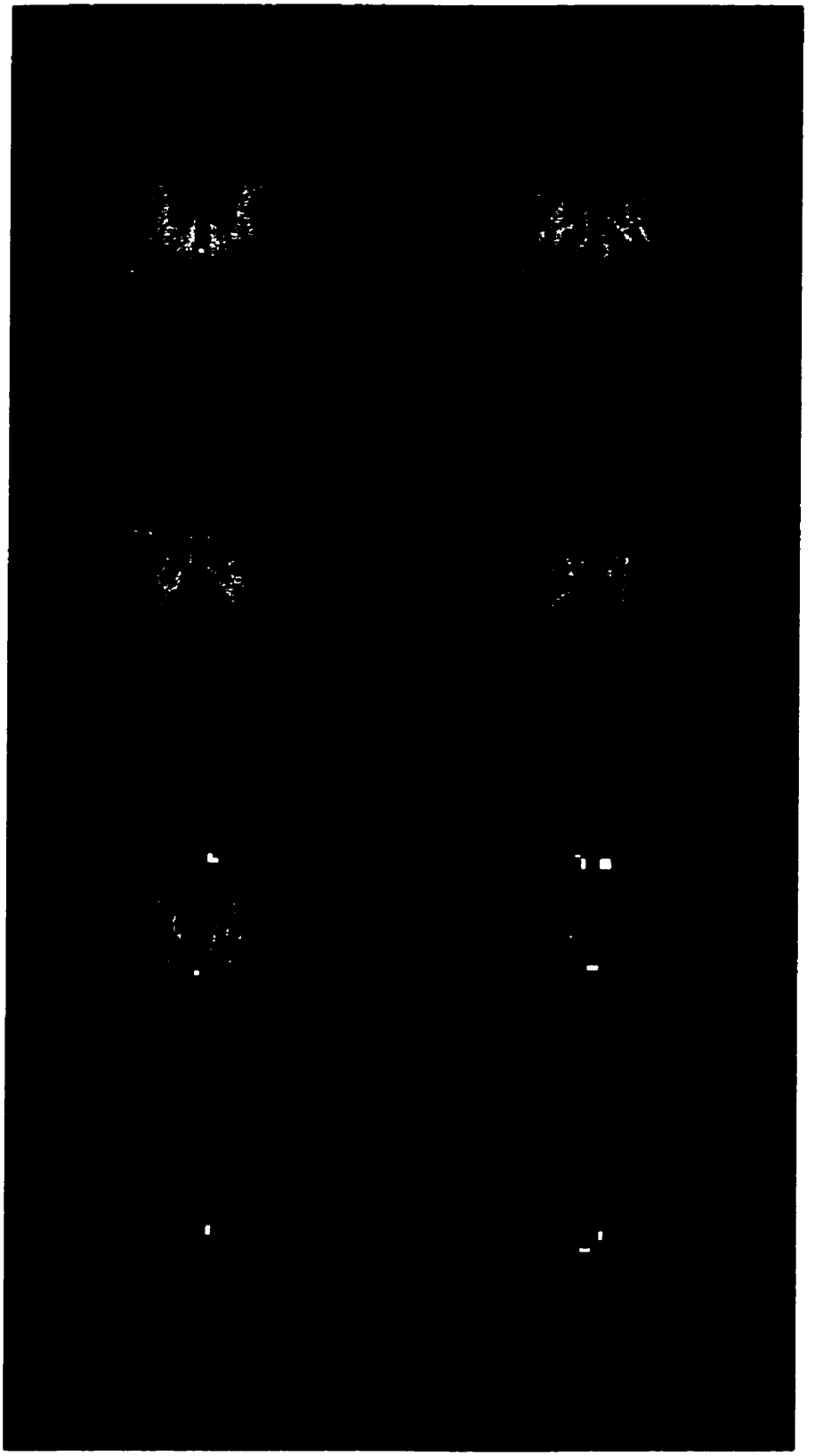

B.

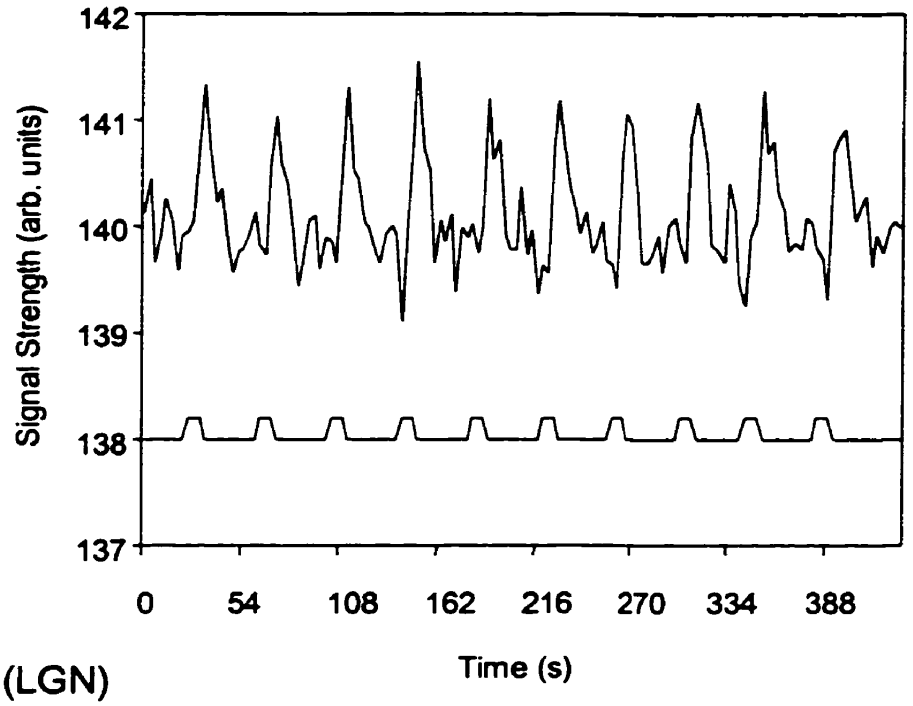

C (LGN)

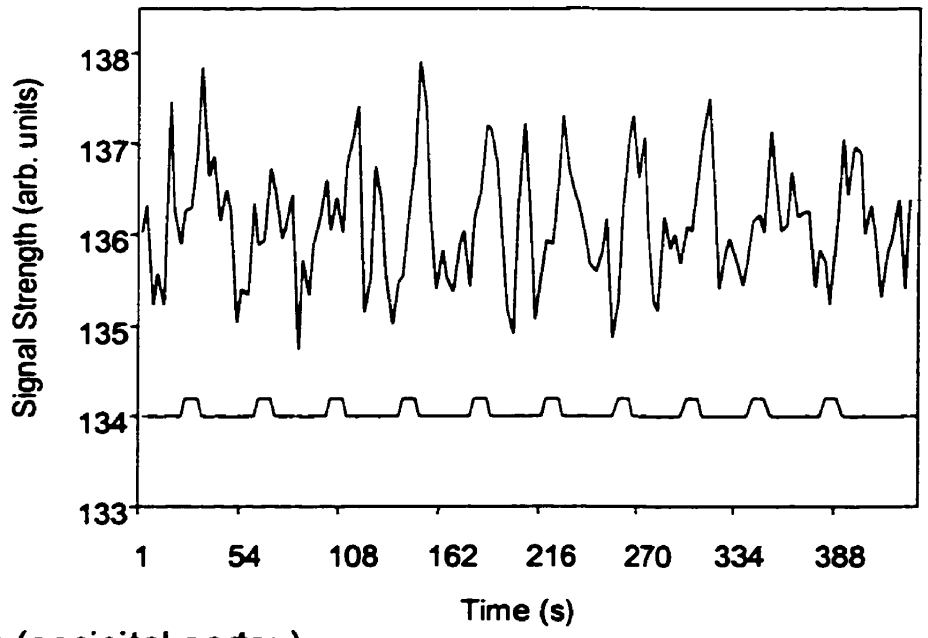

D (occipital cortex)

Figure 4.2. Boxplots of 2 quantitative measures of blood oxygenation level dependant (BOLD) fMR images in 2 regions of interest (ROIs) obtained from 6 anesthetized dogs. The bottom and top lines of each box represent the 25th and 75th percentiles, respectively, and the middle line represents the median. Horizontal lines below and above boxes represent the 10th and 90th percentiles, respectively, and black dots represent data points outside this range. Each dog was anesthetized under 3 anesthetic agents: fentanyl / midazolam (Fent), propofol (Prop), and isoflurane (Iso). There were no significant differences in the lateral geniculate nucleus (LGN) ROI for mean percentage BOLD signal changes (A, $F = 1.97$, $p = 0.19$, $df = 2$), or for percentage of significant voxels per ROI (B, $F = 1.57$, $p = 0.26$, $df = 2$) under the 3 different anesthetic agents, nor were differences significant in the occipital ROI between mean percentage signal changes (C, $F = 3.0$, $p = 0.10$, $df = 2$) or percentage of significant voxels per ROI (D, $F = 1.4$, $p = 0.56$, $df = 2$) under the 3 different anesthetic agents. The randomized complete blocks design general linear model procedure[25], analogous to repeated measures ANOVA, was used to test 3 of the 4 categories because it permitted averaging of data from repeated trials. This procedure was not valid for comparison of number of significant voxels / ROI as a percentage of voxel size in the LGN region because a significant trial by treatment effect had previously been detected (Table 4.2). These data were compared using SAS Proc Mixed,[26] which considers trials individually. Although not testable statistically using the model employed, the variance of all 4 categories under isoflurane anesthesia is less than under the other anesthetic agents (Table 4.3), particularly in B and D.

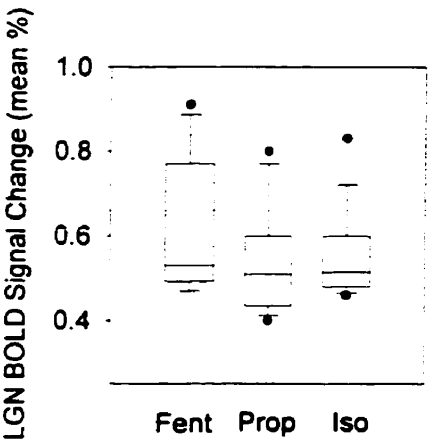
LGN BOLD Signal Change (mean %)
1.0
0.8
0.6
0.4
Fent
Prop
Iso

A.

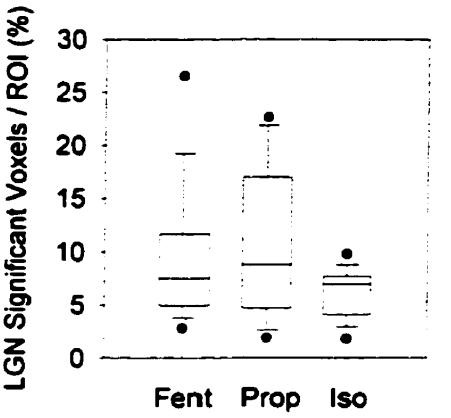
LGN Significant Voxels / ROI (%)
30
25
20
15
10
5
0
Fent
Prop
Iso

B.

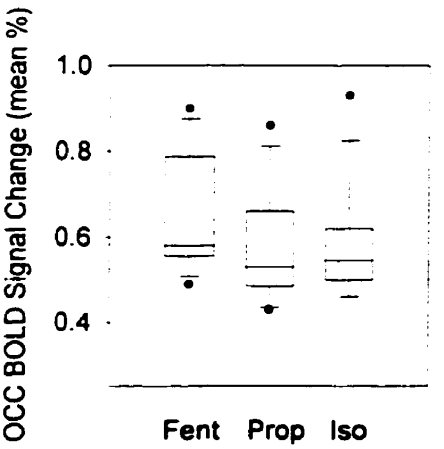
OCC BOLD Signal Change (mean %)
1.0
0.8
0.6
0.4
Fent
Prop
Iso

C.

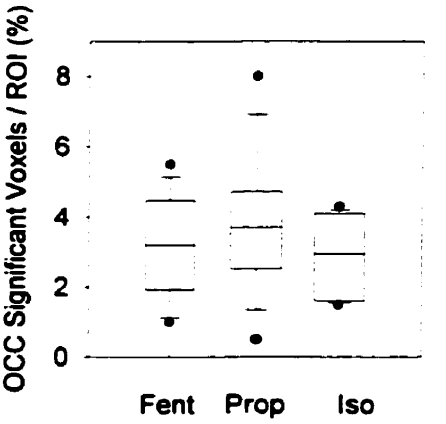
OCC Significant Voxels / ROI (%)
8
6
4
2
0
Fent
Prop
Iso

D.

Figure 4.3. Scatter plots of 2 quantitative measures of BOLD fMR image quality in 2 brain regions of interest (ROIs) against isoflurane dose, obtained during visual stimulation in isoflurane anesthetized dogs. Linear regression analyses were performed. There was no significant relationship between mean percentage BOLD signal change in the lateral geniculate nucleus (LGN) ROI (A, $r^2 = 0.14$, $F = 0.49$, $p = 0.53$, $df = 4$) and no significant relationship between the number of significant voxels / ROI as a percentage of voxel size and dose in the LGN region (B, $r^2 = 0.05$, $F = 0.21$, $p = 0.67$, $df = 5$). There was no significant relationship between mean percentage BOLD signal change and dose in the occipital (OCC) ROI (C, $r^2 = 0.48$, $F = 2.8$, $p = 0.19$, $df = 4.$) or between dose and number of significant voxels / ROI as a percentage of ROI size in the OCC region (D, $r^2 = 0.001$, $F = 0.94$, $p = 0.94$, $df = 5$). Each data point represents the mean of 2 experimental sessions for a single dog if data from both sessions were available.

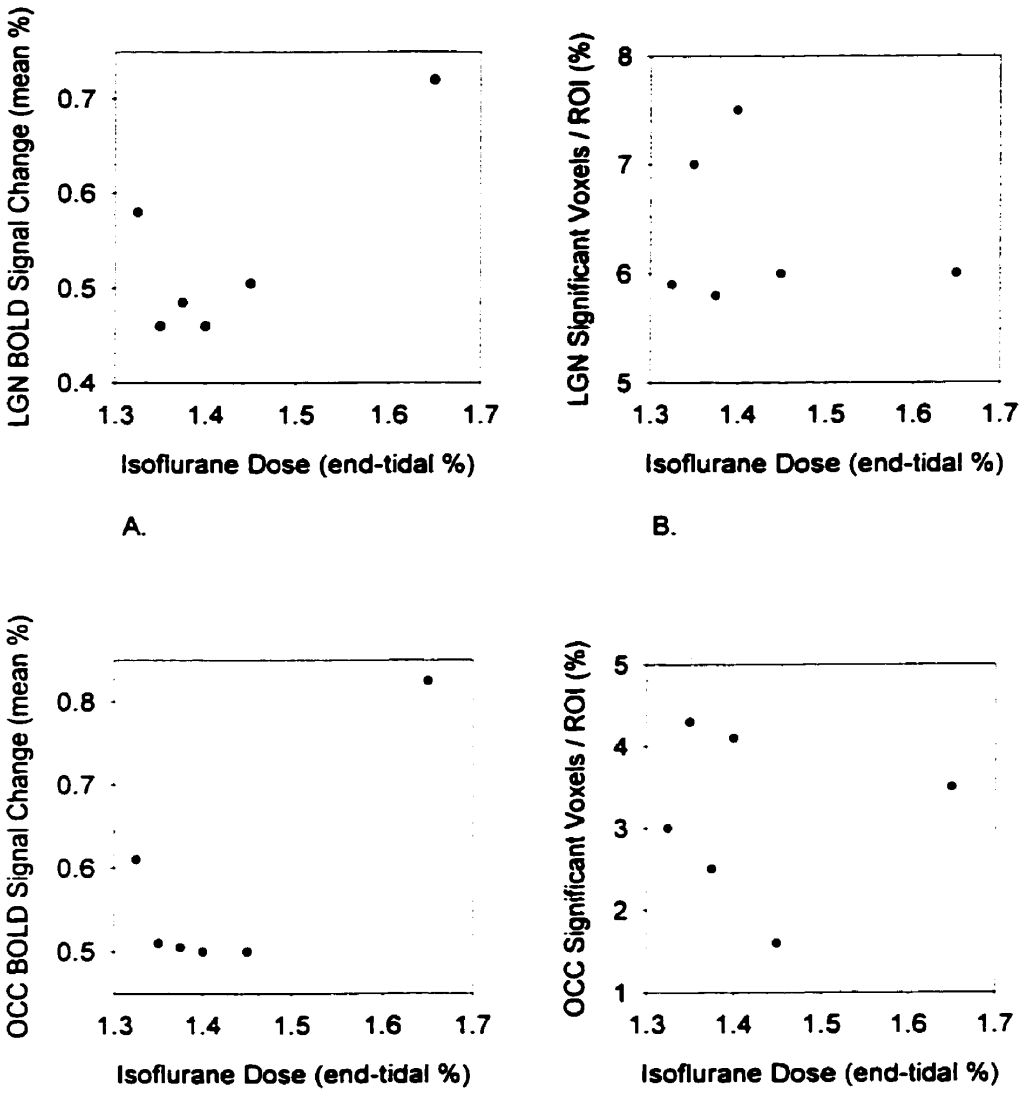
LGN BOLD Signal Change (mean %)
0.7
0.6
0.5
0.4
1.3
1.4
1.5
1.6
1.7
Isoflurane Dose (end-tidal %)
A.
LGN Significant Voxels / ROI (%)
8
7
6
5
1.3
1.4
1.5
1.6
1.7
Isoflurane Dose (end-tidal %)
B.
OCC BOLD Signal Change (mean %)
0.8
0.7
0.6
0.5
1.3
1.4
1.5
1.6
1.7
Isoflurane Dose (end-tidal %)
C.
OCC Significant Voxels / ROI (%)
5
4
3
2
1
1.3
1.4
1.5
1.6
1.7
Isoflurane Dose (end-tidal %)
D.

Figure 4.4. Scatter plots of two quantitative measures of blood oxygenation level dependant (BOLD) fMR image quality in 2 brain regions of interest (ROIs) against propofol dose, obtained during visual stimulation in propofol anesthetized dogs. Linear regression analyses were performed. There was no significant relationship in the lateral geniculate nucleus (LGN) ROI between dose and mean percentage BOLD signal change (A, $r^2 = 0.28$, $F = 1.56$, $p = 0.28$, $df = 5$) or number of significant voxels / ROI as a percentage of ROI size (B, $r^2 = 0.29$, $F = 1.63$, $p = 0.27$, $df = 5$), nor was there a significant difference in the occipital (OCC) ROI between dose and mean percentage BOLD signal change (C, $r^2 = 0.28$, $F = 1.61$, $p = 0.27$, $df = 5$) or number of significant voxels / ROI as a percentage of ROI size (D, $r^2 = 0.58$, $F = 4.2$, $p = 0.10$, $df = 5$). Each data point represents the mean of 2 experimental sessions for a single dog if data from both sessions were available.

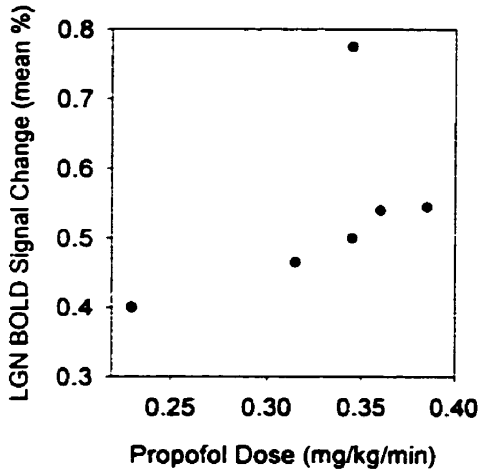
LGN BOLD Signal Change (mean %)
0.8
0.7
0.6
0.5
0.4
0.3
0.25
0.30
0.35
0.40
Propofol Dose (mg/kg/min)

A.

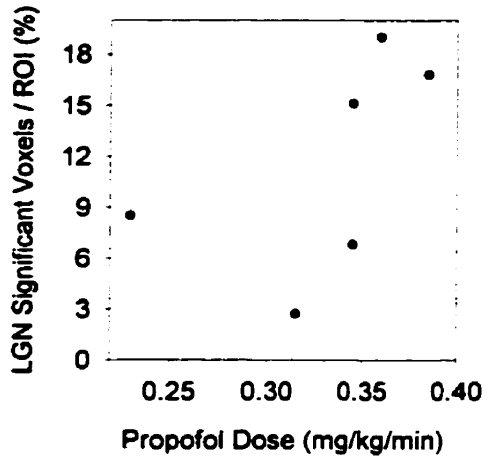
LGN Significant Voxels / ROI (%)
18
15
12
9
6
3
0
0.25
0.30
0.35
0.40
Propofol Dose (mg/kg/min)

B.

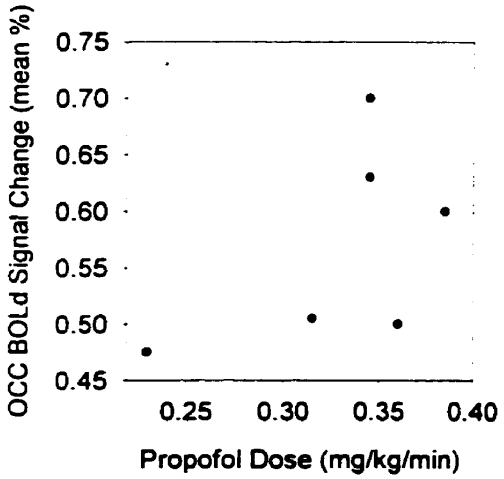
OCC BOLd Signal Change (mean %)
0.75
0.70
0.65
0.60
0.55
0.50
0.45
0.25
0.30
0.35
0.40
Propofol Dose (mg/kg/min)

C.

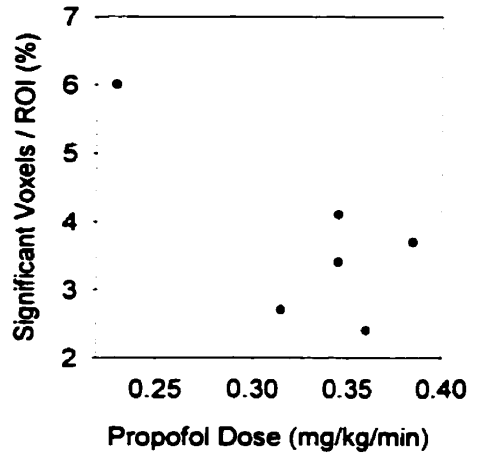
Significant Voxels / ROI (%)
7
6
5
4
3
2
0.25
0.30
0.35
0.40
Propofol Dose (mg/kg/min)

D.

Figure 4.5 Scatter plots of 2 quantitative measures of blood oxygenation level dependant (BOLD) fMR image quality in 2 brain regions of interest (ROIs) against fentanyl dose, obtained during visual stimulation in fentanyl / midazolam anesthetized dogs. Linear regression analyses were performed. There was no significant relationship in the lateral geniculate nucleus (LGN) ROI between dose and mean percentage BOLD signal change (A, $r = 0.24$, $F = 1.27$, $p = 0.32$, $df = 5$) or number of significant voxels / ROI as a percentage of ROI size (B., $r^2 = 0.47$, $F = 3.49$, $p = 0.14$, $df = 5$), nor was there a significant difference in the occipital (OCC) ROI between dose and mean percentage BOLD signal change (C, $r^2 = 0.17$, $F = 0.84$, $p = 0.41$, $df = 5$) or number of significant voxels / ROI as a percentage of ROI size (D, $r^2 = 0.005$, $F = 0.02$, $p = 0.89$, $df = 5$). Each data point represents the mean of 2 experimental sessions for a single dog if data from both sessions were available.

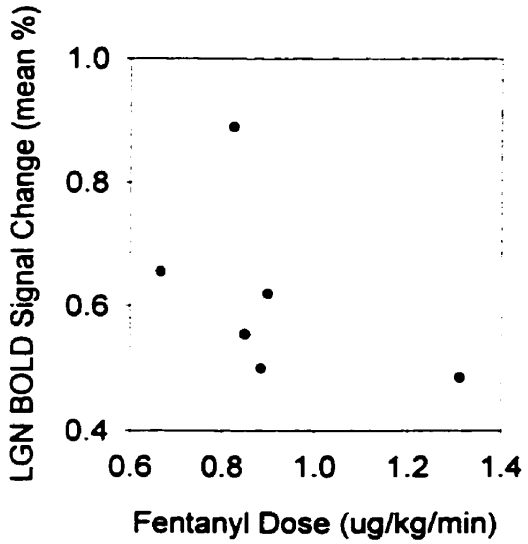
LGN BOLD Signal Change (mean %)
1.0
0.8
0.6
0.4
0.6
0.8
1.0
1.2
1.4
Fentanyl Dose (ug/kg/min)

A.

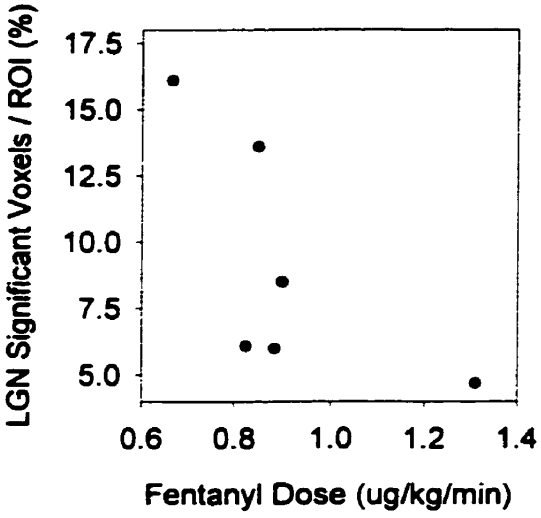
LGN Significant Voxels / ROI (%)
17.5
15.0
12.5
10.0
7.5
5.0
0.6
0.8
1.0
1.2
1.4
Fentanyl Dose (ug/kg/min)

B.

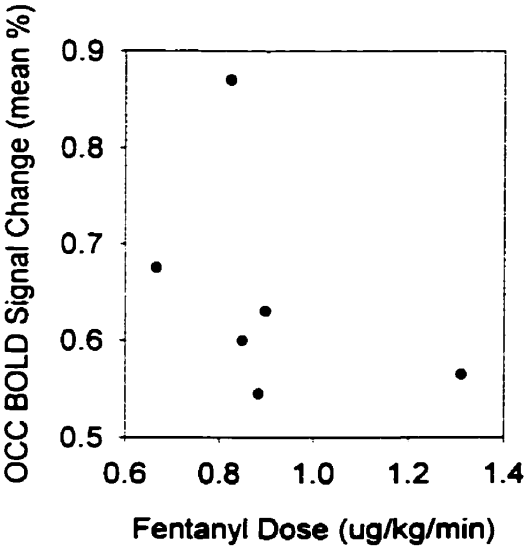
OCC BOLD Signal Change (mean %)
0.9
0.8
0.7
0.6
0.5
0.6
0.8
1.0
1.2
1.4
Fentanyl Dose (ug/kg/min)

C.

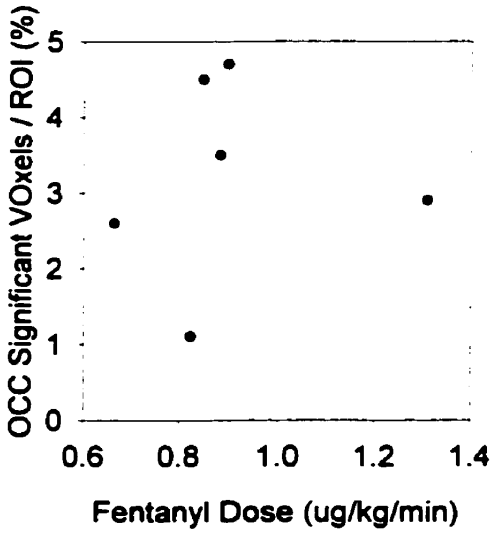
OCC Significant VOxels / ROI (%)
5
4
3
2
1
0
0.6
0.8
1.0
1.2
1.4
Fentanyl Dose (ug/kg/min)

D.

CHAPTER FIVE

GENERAL DISCUSSION AND CONCLUSIONS

This thesis is an investigation of visual evoked neural activity in the brains of anesthetized dogs using blood oxygenation level dependant (BOLD) functional magnetic resonance imaging (fMRI). The long term goal of this research is the development of an objective, reliable test of canine vision. Data from the present study suggest the following:

1. Neural activity, evoked by visual stimuli, can be recorded from the brains of anesthetized dogs using BOLD fMRI at 4T.
2. BOLD signal changes recorded were reproducible between dogs and, qualitatively, within dogs in repeated trials (Appendix I).
3. Signals evoked during isoflurane anesthesia were qualitatively less variable than those recorded during propofol or fentanyl / midazolam anesthesia, likely due to the fact that inhalant anesthetic dose can be more easily controlled than intravenous during high field fMRI.
4. Significant BOLD signal changes were reliably, but not exclusively, elicited in regions of interest (ROI) which included the lateral geniculate nucleus (LGN) of the thalamus and the cerebral cortex of the occipital lobe.
5. BOLD signal changes recorded from anesthetized dogs of between 0.3 and 1.1 % were considerably less than the 5 – 20% observed in awake humans with visual stimulation at 4T.[1]

These findings were predictable based on previous fMRI research, and our understanding of mammalian neuroanatomy. Reduced BOLD signal changes under anesthesia were expected given the results of studies addressing the effects of anesthesia on fMRI in cats,[2] and rats.[3] Jezzard et al. observed signal changes (0.7 – 2.0%) in anesthetized cats presented with visual stimuli, slightly larger than those observed in the present study.[2] This likely reflects the fact that the cats were scanned

using a higher field strength (4.7 T). The reduction in signal change compared to results from awake humans, in the current study and as reported by Jezzard et al., is almost certainly the result of anesthetic suppression of neural activity and vascular brain responses.[2] Inter-subject variability of percentage signal change in the present study (0.3 – 1.1%, slightly less than a factor of 4) is comparable to that observed by Jezzard et al. and slightly less than inter-subject variability normally observed in awake human studies (5 – 20%).[2] The comparable levels of inter-subject variability between anesthetized animal and awake human studies support the accuracy of fMR data obtained during anesthesia, despite the reduction in signal change.

Several unexpected observations were also made in this study. These include the following:

1. There was no significant difference in percentage BOLD signal change or the number of significant voxels as a percentage of ROI size in the lateral geniculate nucleus or occipital cortex under 3 anesthetic protocols (isoflurane, propofol, and fentanyl / midazolam). The impacts of different anesthetic agents on cerebral blood flow, cerebral metabolic rate and neural activity can differ.[4,5,6] Since these factors all play a role in fMRI, it was expected that there would be differences in the strength of BOLD signals under different anesthetics.

2. There were no significant correlations between anesthetic dose and either measure of BOLD activity, above, in either the LGN or occipital cortex for any of the 3 anesthetic protocols. As dose dependant effects on factors which mediate fMRI activity have been observed,[4,5,6] it was expected that a relationship would exist between anesthetic dose and cerebral activity as measured by fMRI. It is probable that dose dependant fMRI effects do exist, but that the range of anesthetic doses to which these dogs were exposed was too small to elucidate the effect.

3. The number of significant voxels as a percentage of ROI size in LGN was significantly greater during monocular stimulus presentations than during binocular

presentations. This result is unexpected, as well, because during monocular stimulus presentations, roughly 50% fewer neurons should propagate activity to the lateral geniculate nucleus than would during binocular stimulation.

4. There were no significant differences between either measure of BOLD activity in the left and right halves of either ROI during stimulus presentations to the right eye alone. It is estimated that approximately 75% of canine optic nerve axons decussate at the optic chiasm.[7] If this is the case, a stronger signal and a larger activated area should be observed contralateral to the stimulated eye. This unexpected result suggests that previous estimates of optic nerve decussation may by excessive.

One further explanation for all of these unexpected results involves difficulties encountered in administering a repeatable, consistent I.V. anesthetic dose. Unequal variances between anesthetic groups, combined with a relatively small sample size may have produced a vulnerability to statistical error. Other factors may also have resulted in variable results. For example, 4 of the 6 dogs had noticeably enlarged lateral ventricles (e.g. Figure 3.1, Figure 4.1). Although the effects of hydrocephalus on vision in dogs or other domestic animals are not addressed in the literature, and there were no differences in any of the dogs visual function based on the ophthalmic examination, removing this potential source of variation from future studies would be desirable.

SUGGESTIONS FOR FURTHER STUDY

Several areas for further study are suggested by the results above. Now that the reliability and reproducibility of fMRI in anesthetized dogs has been established, the next priority should be to address the dose dependence and anesthetic depth dependence of BOLD activity using a wide range of anesthetic doses both within and between dogs. This may be most practical using various inhalant agents because intravenous anesthetic dose is more difficult to control from the distances required by 4T fMRI. Developing means to better control intravenous anesthetic dose during fMRI would also be valuable to research investigating anesthetic action on cerebral activity. Humans are

the only candidates for within species, comparative study of anesthetic effects on fMRI. Another important priority, then, should be experiments comparing fMR signal within human subjects, awake and anesthetized. Results of the present study suggest that inhalant agents will be most appropriate for the majority of fMRI applications involving anesthesia.

Because of the variability of cerebral anatomy between subjects, anatomic comparisons of fMRI results between humans are facilitated through the use of the Talairach coordinate system.[8] The development of a canine brain coordinate system would be worthwhile for precise mapping of the functional architecture of visual processing and for comparisons of functional anatomy between dogs. This is an especially urgent consideration given the probable anatomic differences between breeds of dogs bred to excel at different functions, such as sight hunting or scent hunting.

Experiments addressing the functional anatomy of various aspects of visual processing would also be interesting, from both an evolutionary and neuroanatomic perspective. What differences and similarities can be found between dogs, cats and primates? How does visual processing differ in animals very sensitive to motion, like dogs, versus those more sensitive to colour and form, like humans? Using fMRI to evaluate canine brain activity in response to other stimulus modalities, such as touch or smell would be fascinating as well. Given the abundance of research addressing feline and primate brain function in the literature, the potential for comparative study with dogs is enormous.

Finally, from a clinical veterinary perspective comparing BOLD activity in dogs with obvious visual problems to clinically normal dogs would be extremely valuable, especially in light of the current absence of a reliable test for canine vision. If differences in BOLD fMRI correlate with apparent, subjective vision loss in dogs suffering visual disease, it would mean the technique could be used to evaluate treatments for visual problems, like glaucoma, more objectively.

REFERENCES

1. Menon RS, Ogawa S, Kim S, Ellerman JM, Merkle H, Tank DW, Ugurbil K. Functional brain mapping using magnetic resonance imaging: Signal changes accompanying visual stimulation. *Investigative Radiology* 1992; **27**: S47-S53.

2. Jezzard P, Rauschecker JP, Malonek D. An *in vivo* model of functional MRI in cat visual cortex. *Magnetic Resonance in Medicine* 1997; **38**: 699-705.

3. Lahti KM, Ferris CF, Li F, Sotak CH, King JA. Comparison of evoked cortical activity in concious and propofol anesthetized rats using functional MRI. *Magnetic Resonance in Medicine* 1998; **41**: 412-416.

4. Miller FL, Marshall BE.The inhaled anesthetics. In: *Dripps, Eckenhoff, Vandam: Introduction to Anesthesia* (ed. Longnecker DE, Murphy FL). WB Saunders: Philadelphia, 1992; 77-90.

5. Artu AA, Shapiro Y, Bowdle, TA. Electroencephalogram, cerebral metabolic and vascular responses to propofol anesthesia in dogs. *Journal of Neurosurgery and Anesthesia* 1992; **4**: 99-109.

6. Firestone LL, Gyulai F, Mintun M, Adler LJ, Urso K, Winter PM. Human brain activity response to fentanyl imaged by positron emission tomography. *Anesthesia and Analgesia* 1996; **82**: 1247-1251.

7. De Lahunta A. *Veterinary Neuroanatomy and Clinical Neurology* 2nd edn. WB Saunders: Philadelphia; 1983.

8. Talairach J, Tournoux P. *Co-Planar Sterotactic Atlas of the Human Brain*. Georg Thiem Verlag, Stuttgart, 1988.

Appendix I. Results of BOLD fMRI experiments of 6 dogs, anesthetized under isoflurane (I), propofol (P), and fentanyl / midazolam (F) and presented with a binocular visual stimulus. Data were obtained from regions of interest (ROIs) which focussed on the lateral geniculate nucleus of the thalamus (LGN) and the occipital cortex (OCC). The percentage signal change (PC) and number of significant voxels as a percentage of ROI size (V) were recorded.

Dog	Trial No.	Anesthetic	LGN/PC	LGN/V	OCC/PC	OCC/V
Bibi	2	I	0.46	7.5	0.50	4.1
Pakum	2	I	0.49	7	0.51	4.3
Bibi	1	P	0.4	8.3	0.51	8
Pakum	1	P	0.54	19	0.5	2.4
Bibi	1	F	0.82	26.5	0.86	3.2
Pakum	1	F	0.51	12.7	0.57	5.5
Bibi	2	F	0.49	5.7	0.49	2
Pakum	2	F	0.6	14.4	0.63	3.5
Bibi	2	P	0.45	8.6	0.44	3.9
Starr	1	P	0.51	1.9	0.58	4.8
Shadow	1	P	0.61	22.6	0.67	2.9
Starr	1	I	0.47	1.8	0.46	1.5
Shadow	1	I	0.6	4.1	0.6	3
Shadow	1	F	0.47	7.5	0.52	2.1
Starr	2	P	0.42	3.5	0.43	0.5
Shadow	2	P	0.48	11	0.53	4.5
Starr	2	F	0.62	8.5	0.63	4.7
Shadow	2	F	0.53	4.4	0.57	4.9
Starr	2	I	0.5	9.8	0.55	3.5
Shadow	2	I	0.56	7.7	0.62	2.5
Diosa	1	P	0.43	8.8	0.48	3.1
Broadway	1	P	0.75	3.1	0.63	1.9
Broadway	1	F	0.87	7.5	0.84	1.2
Diosa	1	I	0.48	5.1	0.46	1.6
Broadway	1	I	0.61	4.1	0.72	2.9
Diosa	2	I	0.53	6.9	0.54	1.6
Broadway	2	I	0.83	7.8	0.93	4.1
Diosa	2	P	0.57	21.4	0.78	3.7
Broadway	2	P	0.8	10.6	0.86	6.2
Diosa	2	F	0.5	2.8	0.58	3.8
Broadway	2	F	0.91	4.7	0.9	1.0

Appendix II. Results of BOLD fMRI experiments of 6 dogs anesthetized under isoflurane (I), propofol (P) and fentanyl / midazolam (F), and presented with a monocular visual stimulus to the right eye. Data were obtained from regions of interest (ROIs) which focussed on the lateral geniculate nuclei of the thalamus (LGN) and the occipital cortex (OCC). The percentage signal change (PC) and number of significant voxels as a percentage of ROI size (V) were recorded.

Dog	Trial No.	Anesthetic	LGN/PC	LGN/V	OCC/PC	OCC/V
Bibi	2	I	na	na	na	na
Pakum	2	I	na	na	na	na
Bibi	1	P	0.44	9.2	0.62	5.9
Pakum	1	P	0.51	8.4	0.64	2.7
Bibi	1	F	0.98	29.1	1.03	7.9
Pakum	1	F	0.44	4.0	0.48	2.5
Bibi	2	F	na	na	na	na
Pakum	2	F	0.65	5.9	0.64	2.4
Bibi	2	P	0.51	6.8	0.46	6.0
Starr	1	P	0.63	1.3	0.6	5.1
Shadow	1	P	0.59	15.7	0.65	2.1
Starr	1	I	0.53	3.8	0.52	3.1
Shadow	1	I	0.59	6.9	0.63	4.2
Starr	1	F	0.47	11.6	0.52	1.8
Shadow	1	F	0.44	4.2	0.43	1.7
Starr	2	P	0.47	5.5	0.47	2.5
Shadow	2	P	0.48	10.9	0.52	2.6
Starr	2	F	0.59	9.0	0.62	8.3
Shadow	2	F	0.56	7.2	0.55	2.9
Starr	2	I	0.49	8.2	0.49	1.7
Shadow	2	I	0.52	8.7	0.54	6.7
Diosa	1	P	0.43	6.0	0.5	3.1
Broadway	1	P	0.71	10.0	0.68	3.9
Broadway	1	F	na	na	na	na
Diosa	1	I	0.45	5.9	0.46	1.0
Broadway	1	I	0.67	5.4	0.66	1.5
Diosa	2	I	0.52	5.8	0.52	2.5
Broadway	2	I	0.88	4.3	0.93	0.9
Diosa	2	P	0.57	11.8	0.53	1.4
Broadway	2	P	0.82	7.4	0.8	4.1
Diosa	2	F	0.51	4.0	0.52	0.9
Broadway	2	F	0.87	7.4	0.86	4.8

Appendix III. Results of BOLD fMRI experiments of 6 dogs anesthetized under isoflurane (I), propofol (P) and fentnayl / midazolam (F), and presented with a monocular visual stimulus to the right eye. Data were obtained from regions of interest (ROIs) which focussed on the left and right lateral geniculate nuclei of the thalamus (LLGN and RLGN respectively) and left and rigt halves of the occipital cortex (LOCC and ROCC respectively). The percentage signal change (PC) and number of significant voxels as a percentage of ROI size (V) were recorded.

Dog	Anesthetic	LLGN PC	RLGN PC	LLGN V	RLGN V	LOCC PC	ROCC PC	LOCC V	ROCC V
Bibi	I	na	na	na	na	na	na	na	na
Pakum	I	na	na	na	na	na	na	na	na
Bibi	P	0.44	0.4	14	3.7	0.46	0.66	3.9	9.4
Pakum	P	0.46	0.51	11.9	4.2	0.58	0.64	1.1	4.4
Bibi	F	1.04	0.84	20.5	29.1	0.98	1.06	7.0	9.1
Pakum	F	0.42	0.44	4.9	2.7	0.51	0.42	3.2	1.5
Bibi	F	na	na	na	na	na	na	na	na
Pakum	F	0.58	0.61	7.8	5.6	0.61	0.63	1.7	3.1
Bibi	P	0.51	0.57	11.1	4.5	0.48	0.46	5.5	7.1
Starr	P	0.51	0.62	3.8	4.5	0.48	0.62	5.0	5.4
Shadow	P	0.59	0.62	8.0	24.5	0.65	0.65	1.6	2.4
Starr	I	0.52	0.51	4.9	2.9	0.5	0.52	3.2	3.0
Shadow	I	0.57	0.63	8.7	3.5	0.64	0.62	3.5	4.5
Starr	F	0.47	0.48	10.1	3.5	0.56	0.49	1.1	2.4
Shadow	F	0.47	0.47	4.3	4.9	0.44	0.42	0.4	1.6
Starr	P	0.49	0.46	9.0	4.2	0.47	0.47	2.0	0.4
Shadow	P	0.46	0.51	7.1	11.3	0.57	0.48	0.6	4.3
Starr	F	0.6	0.36	18.3	0.9	0.56	0.06	8.2	9.0
Shadow	F	0.57	0.51	8.2	5.2	0.62	0.52	1.3	3.9
Starr	I	0.48	0.5	10.1	6.2	0.48	0.47	1.6	1.8
Shadow	I	0.5	0.52	6.6	10.4	0.55	0.53	5.8	9.3
Diosa	P	0.46	0.43	13.1	1.3	0.47	0.51	2.3	4.1
Broadway	P	0.75	0.68	10.3	4.5	0.66	0.67	3.4	3.4
Broadway	F	na	na	na	na	na	na	na	na
Diosa	I	0.46	0.43	7.8	5.6	0.47	0.45	1.2	1.5
Broadway	I	0.76	0.59	4.4	7.4	0.68	0.57	2.3	0.5
Diosa	I	0.53	0.5	11.2	0.4	0.53	0.49	3.6	1.4
Broadway	I	0.83	1.01	8.0	2.3	0	0.95	0	1.9
Diosa	P	0.54	0.59	10.2	10.8	0.5	0.57	1.4	1.2
Broadway	P	0.83	0.79	8.3	6.1	0.82	0.78	3.1	4.4
Diosa	F	0.54	0.47	2.2	5.5	0.5	0.52	0.4	1.4
Broadway	F	0.85	0.91	3.3	8.1	0.82	0.9	5.2	4.4

Appendix IV. Anesthetic protocols, anesthetic doses, and end-tidal CO_2 values recorded during fMRI experiments using 3 anesthetic protocols: isoflurane (I); Propofol (P) and Fentanyl / Midazolam (F/M). Carbon dioxide values represent the mean of a pre-trial and a post-trial sample.

Dog	Trial No.	Anesthetic	Dose			CO_2
			I (%)	F/M (ug/kg/min)	P (mg/kg/min)	
Bibi	2	I	1.4			46
Pakum	2	I	1.35			44.5
Bibi	1	P			0.2	44
Pakum	1	P			0.36	45
Bibi	1	F/M		0.5 / 5		41.5
Pakum	1	F/M		1.3/ 13		45.5
Bibi	2	F/M		0.8 / 8		43.5
Pakum	2	F/M		0.4 / 4		54.5
Bibi	2	P			0.26	46.5
Starr	1	P			0.27	42
Shadow	1	P			0.44	45
Starr	1	I	1.3			48
Shadow	1	I	1.3			49
Starr	1	F/M		1.3 / 13		49
Shadow	1	F/M		0.9 / 9		54
Starr	2	P			0.36	46
Shadow	2	P			0.33	41.5
Starr	2	F/M		0.9 / 9		44.5
Shadow	2	F/M		0.9 / 9		48.5
Starr	2	I	1.45			45
Shadow	2	I	1.35			48
Diosa	1	P			0.33	43
Broadway	1	P			0.33	45.5
Diosa	1	F/M		1.7 / 17		39.5
Broadway	1	F/M		0.9 / 9		48.5
Diosa	1	I	1.6			44
Broadway	1	I	1.5			42.5
Diosa	2	I	1.3			40
Broadway	2	I	1.8			49
Diosa	2	P			0.36	39.5
Broadway	2	P			0.36	39.5
Diosa	2	F/M		0.9 / 9		49
Broadway	2	F/M		0.8 / 9		46

Appendix V. Oxygen saturation data based on pulse oximetry during fMRI scanning of 6 dogs anesthetized under isoflurane (I), propofol (P) and Fentanyl / Midazolam (F). Values were recorded 4 times (S1, S2, etc.) during each scanning session. The pulse oximeter had to be kept a minimum of 10 m from the MR unit during scanning resulting in some data loss. When the connection of the recording sensor to the dog's tongue was compromised it could not be re-attached until the session was complete. na = not available.

Dog	Trial No.	Anesthetic	S1	S2	S3	S4	Mean
Bibi	2	I	99	100	99	99	99.3
Pakum	2	I	98	98	98	98	98.0
Bibi	1	P	97	96	97	97	96.8
Pakum	1	P	98	98	100	98	98.5
Bibi	1	F	97	99	98	99	98.3
Pakum	1	F	na	na	na	na	na
Bibi	2	F	na	na	na	na	na
Pakum	2	F	99	99	98	100	99.0
Bibi	2	P	97	98	98	99	98.0
Starr	1	P	98	97	98	99	98.0
Shadow	1	P	98	98	na	na	98.0
Starr	1	I	98	99	98	98	98.3
Shadow	1	I	94	97	97	97	96.3
Starr	1	F	100	99	na	na	99.5
Shadow	1	F	98	100	na	na	99.0
Starr	2	P	98	98	100	100	99.0
Shadow	2	P	99	99	99	99	99.0
Starr	2	F	na	na	na	na	na
Shadow	2	F	na	na	na	na	na
Starr	2	I	96	97	97	96	96.5
Shadow	2	I	97	98	98	98	97.8
Diosa	1	P	98	97	97	96	97.0
Broadway	1	P	na	na	na	na	na
Diosa	1	F	98	98	100	99	98.8
Broadway	1	F	100	100	99	100	99.8
Diosa	1	I	98	98	99	99	98.5
Broadway	1	I	96	98	98	97	97.3
Diosa	2	I	100	100	98	99	99.3
Broadway	2	I	na	na	na	na	na
Diosa	2	P	97	99	98	99	98.3
Broadway	2	P	100	100	99	100	99.8
Diosa	2	F	96	na	na	na	96.0
Broadway	2	F	95	98	na	na	96.5

Appendix VI. Heart rate data based on pulse oximetry during fMRI scanning of 6 dogs anesthetized under isoflurane (I), propofol (P) and fentanyl / midazolam (F). If possible values were recorded 4 times (S1, S2, etc.) during each scanning session. The pulse oximeter had to be kept a minimum of 10 m from the MR unit during scanning resulting in some data loss because when the connection of the recording sensor to the dog's tongue was compromised it could not be re-attached until the end of the experiment. na = not available

Dog	Trial No.	Anesthetic	S1	S2	S3	S4	Mean
Bibi	2	I	115	119	115	117	116.5
Pakum	2	I	106	115	108	111	110.0
Bibi	1	P	114	118	120	119	117.8
Pakum	1	P	120	118	111	123	118.0
Bibi	1	F	123	125	119	122	122.3
Pakum	1	F	na	na	na	na	na
Bibi	2	F	na	na	na	na	na
Pakum	2	F	127	130	124	116	124.3
Bibi	2	P	108	118	120	117	115.8
Starr	1	P	118	127	119	121	121.3
Shadow	1	P	118	121	na	na	119.5
Starr	1	I	110	124	115	120	117.3
Shadow	1	I	127	121	121	119	122.0
Starr	1	F	129	123	na	na	126.0
Shadow	1	F	120	129	na	na	124.5
Starr	2	P	125	113	118	127	120.8
Shadow	2	P	128	130	122	122	125.5
Starr	2	F	na	na	na	na	na
Shadow	2	F	na	na	na	na	na
Starr	2	I	114	120	112	116	115.5
Shadow	2	I	118	125	127	119	122.3
Diosa	1	P	129	125	130	119	125.8
Broadway	1	P	na	na	na	na	na
Diosa	1	F	130	120	119	124	123.3
Broadway	1	F	140	134	133	137	136.0
Diosa	1	I	117	110	120	124	117.8
Broadway	1	I	116	107	120	121	116.0
Diosa	2	I	114	120	118	128	120.0
Broadway	2	I	na	na	na	na	na
Diosa	2	P	126	122	117	119	121.0
Broadway	2	P	129	135	130	127	130.3
Diosa	2	F	128	na	na	na	128.0
Broadway	2	F	140	136	na	na	138.0